AD_____

Award Number: W81XWH-04-1-0208

TITLE: Novel Gbeta Mimic Kelch Proteins (Gpb1 and Gpb2 Connect G-Protein Signaling to Ras via Yeast Neurofibromin Homologs Ira1 and Ira2: A Model for Human NF1

PRINCIPAL INVESTIGATOR: Joseph Heitman, M.D., Ph.D.

CONTRACTING ORGANIZATION: Duke University Medical Center
Durham, NC 27710

REPORT DATE: March 2008

TYPE OF REPORT: Final

PREPARED FOR: U.S. Army Medical Research and Materiel Command
Fort Detrick, Maryland 21702-5012

# REPORT DOCUMENTATION PAGE

*Form Approved*
*OMB No. 0704-0188*



| 1. REPORT DATE | 2. REPORT TYPE | 3. DATES COVERED |
|---|---|---|
| 31-03-2008 | Final | 1 MAR 2004 - 28 FEB 2008 |

**4. TITLE AND SUBTITLE**
Novel Gbeta Mimic Kelch Proteins Gpb1 and Gpb2 Connect G-Protein Signaling to Ras via Yeast Neurofibromin Homologs

Ira 1 and Ira 2: A Model for Human NF1

**5a. CONTRACT NUMBER**

**5b. GRANT NUMBER**
W81XWH-04-1-0208

**5c. PROGRAM ELEMENT NUMBER**

**6. AUTHOR(S)**
Joseph Heitman, Ph.D.

Email:

**5d. PROJECT NUMBER**

**5e. TASK NUMBER**

**5f. WORK UNIT NUMBER**

**7. PERFORMING ORGANIZATION NAME(S) AND ADDRESS(ES)**

Duke University Medical Center
Durham, NC 27710

**8. PERFORMING ORGANIZATION REPORT NUMBER**

**9. SPONSORING / MONITORING AGENCY NAME(S) AND ADDRESS(ES)**
U.S. Army Medical Research and Materiel Command
Fort Detrick, Maryland 21702-5012

**10. SPONSOR/MONITOR'S ACRONYM(S)**

**11. SPONSOR/MONITOR'S REPORT NUMBER(S)**

**12. DISTRIBUTION / AVAILABILITY STATEMENT**
Approved for Public Release; Distribution Unlimited

**13. SUPPLEMENTARY NOTES**

**14. ABSTRACT**

The Neurofibromatosis type 1 (NF1) gene encodes a large tumor suppressor protein, neurofibromin, which is a Ras GTPase-activating protein (RasGAP) activity. Although the NF1 gene was identified over a decade ago, the biological roles of neurofibromin in cellular processes remain unclear. Therefore it is crucial for therapy and developing new drugs for NF1 patients to elucidate how the RasGAP activity of neurofibromin is controlled. To achieve this goal, it is also important to identify regulatory elements for neurofibromin. We are investigating the molecular mechanisms by which the Ras GAP activity of the yeast neurofibromin homologs Ira1/2 is regulated as a model to understand human NF1. We have found that the kelch Gb subunit mimics Gpb1/2 interact with Ira1/2 and control the Ras GAP activity of Ira1/2. Here, we found that the Gpb1/2 proteins are localized to the cell membrane in a Gpa2 dependent manner and function at the cell membrane. Gpb1/2 bind to the C-terminus of Ira1/2 and stabilize the Ira1/2 proteins. Moreover we also identified a Gpb1/2 binding domain near the C-terminus of Ira1/2 (GBD) that is significantly conserved in neurofibromin homologs, including a human counterpart. Therefore, similar regulatory mechanisms might be conserved in evolution.

**15. SUBJECT TERMS**
GTPase activating protein (GAP); Ras: yeast; signal transduction; adenylyl cyclase; protein kinase A

| 16. SECURITY CLASSIFICATION OF: | | | 17. LIMITATION OF ABSTRACT | 18. NUMBER OF PAGES | 19a. NAME OF RESPONSIBLE PERSON |
|---|---|---|---|---|---|
| a. REPORT | b. ABSTRACT | c. THIS PAGE | | | USAMRMC |
| U | U | U | UU | 87 | 19b. TELEPHONE NUMBER *(include area code)* |

**Introduction**

Neurofibromatosis type 1 (NF1) is one of the most common genetic disorders in humans and the Ras GTPase-activating protein (RasGAP) neurofibromin is intimately associated with NF1 (For reviews, see Dasgupta and Gutmann, 2003; Parada, 2000; Zhu and Parada, 2002). It is therefore critical to elucidate the molecular mechanisms by which the RasGAP activity of neurofibromin are regulated, as well as the biological roles of neurofibromin, which are as yet incompletely understood. We employ the budding yeast *Saccharomyces cerevisiae* as a model to understand how the GAP activity of the yeast neurofibromin homologs, Ira1 and Ira2, is governed. The biochemical and biological roles of these yeast homologs are well conserved in evolution (Ballester et al., 1990; Ballester et al., 1989; Buchberg et al., 1990; Martin et al., 1990; Tanaka et al., 1991; Tanaka et al., 1989; Tanaka et al., 1990a; Tanaka et al., 1990b; Xu et al., 1990a; Xu et al., 1990b).

Recently, we identified the kelch Gβ mimic proteins Gpb1 and Gpb2, which are structurally and functionally related to Gβ subunits yet share no primary sequence identity with known Gβ subunits (Harashima and Heitman, 2002, 2005). We discovered that Gpb1/2 bind to Ira1/2 in vivo and regulate cAMP signaling by inhibiting the Gα subunit Gpa2 and concomitantly activating the Ira1/2 RasGAPs. In the approved Statement Of Work (See appendices), we proposed to elucidate the roles of the Gβ mimic kelch proteins Gpb1/2 in regulating the yeast neurofibromin homologs Ira1/2 for the first years of this project. We have found that Gpb1/2 are localized to the cell membrane in a Gpa2-dependent manner (Harashima and Heitman, 2005) and function at the cell membrane where Gpb1/2 bind to the C-terminus of Ira1/2 and stabilize the Ira1/2 proteins.

These studies were published in *Molecular Cell* (Harashima et al, 2006). These findings set the stage for studies to examine NF1 and possible mammalian kelch protein homologs of Gpb1/2, and extension of these studies to homologs in other fungi, and to other components of the Gpb1/2-protein kinase A signaling cascade. We summarize here the findings for the entire period of support.

**Body**

**A carboxy terminal domain of Ira1 spanning from amino acids 2715 to 2925 was identified as the Gpb1/2 binding domain (GBD).** To understand how Gpb1/2 control Ira1/2 RasGAP activity, the Gpb1/2 binding domain on Ira1/2 was identified. In this study, the Ira1 protein was deleted for N-terminal and C-terminal regions and fused to the 3HA protein tag. Using these deletion constructs and FLAG-Gpb1/2 constructs, physical protein interactions were examined in vivo by FLAG tag based affinity purification methods, and a Gpb1/2 binding domain (GBD) was identified and mapped to a carboxy-terminal segment spanning amino acid residues 2715-2925 (Figures 2 and 5 in Supporting Data). The GBD in the Ira2 protein was also identified in the corresponding region of Ira2 (Supplemental Figure 1 in Supporting Data).

**The GBD is significantly conserved in evolution.** To examine whether the GBD is conserved in evolution, psi-BLAST searches in the NCBI database were performed using the amino acid sequence of the GBD derived from the yeast Ira1 neurofibromin homolog, revealing identity with neurofibromin homologs including one in Drosophila, mouse, and human. Therefore, the GBD that is the binding target of the Gpb1/2 kelch proteins is conserved in evolution. Importantly many mutations (including nonsense mutations, deletions, and mutations in splice sites) have been identified in the corresponding domain of human neurofibromin from NF1 patients (Ars et al., 2003; De Luca et al., 2003; Fahsold et al., 2000; Origone et al., 2002; Rasmussen and Friedman, 2000; Upadhyaya et al., 1997).

**Binding of Gpb1/2 to the GBD stabilizes the Ira1/2 proteins.** In parallel with the experiments described above, protein stability of the deletion derivatives was also assessed by western blot using anti-HA antibodies. Remarkably, the deletion of the C-terminus resulted in instability of Ira1/2 (Figure 5 in Supporting Data). Furthermore, the protein levels of Ira1/2 were dramatically reduced in *gpb1,2* double mutant cells compared to wild-type cells (Figure 2 in Supporting Data). RT-PCR analysis of *IRA1*/2 expression revealed comparable transcript levels between *gpb1,2* mutant and wild-type cells. Reintroduction of the *GPB1/2* genes into *gpb1,2* double mutant cells restored Ira1/2 protein levels to the wild-type level (Figure 2 in Supporting Data). Therefore, Gpb1/2 stabilize the Ira1/2 proteins by binding to the GBD.

An extensive series of studies were conducted supporting the conclusion that Gpb1/2 bind to the conserved C-terminal domain of Ira1/2 and stabilize Ira1/2 to control their RasGAP activity. These studies shed light on how RasGAP activity of the mammalian counterpart neurofibromin is controlled, which largely remains unknown. We summarize here the major points. **First**, we conducted key biochemical experiments that reveal the involvement of Gpb1/2 in stabilizing Ira1/2. As shown in Figures 4C and D, the half-lives of Ira1 (panel C) and Ira2 (panel D) in *gpb1,2* double mutant cells are much shorter than in wild-type cells. In these key experiments, the half-lives of the Ira1 and Ira2 proteins were measured by pulse-chase after cycloheximide addition and IP-Western blot. In contrast to the control protein Fpr1, the half-lives for both Ira proteins were substantially reduced in the absence of Gpb1/2. These findings substantiate and extend the biochemical and genetic data shown in Figures 4A and B, 5, and 6. **Second**,

we have constructed a 3HA tagged Gpb1/2 binding domain (GBD) of Ira1 that spans amino acids 2715-2925 and the corresponding Ira2 GBD to test for protein-protein interactions with Gpb1/2. **Third**, we show that the 3HA tagged GBDs from Ira1 and Ira2 indeed bind to Gpb1/2, as shown in Figure 5D and Supplemental Figure 1D. **Fourth**, we have substantially improved Figures 4A and B by repeating experiments and including new data. We have measured Ras2-GTP levels in *ira2* single and *ira1,2* double mutant cells expressing wild-type Ras2. We show in Figure 4A that the Ras2-GTP level in *ira2* mutant cells is almost equivalent to that in *ira1* single and *gpb1,2* double mutant cells that express the wild-type Ras2 protein, and the Ras2-GTP level in *ira1,2* mutant cells is largely equivalent to that in wild-type and *gpb1,2* single mutant cells expressing a dominant form of Ras2 ($Ras2^{G19V}$). We have measured Ras2-GTP levels in *ira2* single and *ira1,2* double mutant cells. *ira2* mutant cells expressing the wild-type Ras2 protein exhibited a 5-fold increase in Ras2-GTP, similar to *ira1* single mutant cells. On the other hand, an approximately 25-fold increase was observed in *ira1,2* mutant cells that express the wild-type Ras2 protein, which is comparable to wild-type cells expressing the dominant active $Ras2^{G19V}$ protein (Figure 4A). These results are consistent with previous findings by Tanaka *et al.* (Cell, 1990). Therefore, Ira1 and Ira2 are largely functionally redundant.

We addressed the issue as to why there is a difference between *gpb1,2* double mutant cells expressing the wild-type Ras2 protein (5-fold increase) and those expressing the dominant active $Ras2^{G19V}$ protein (25-fold increase) with respect to the Ras2-GTP level. Our biochemical data provide evidence that the Ira1/2 RasGAP proteins are both still present in *gpb1,2* mutant cells, although their levels are significantly decreased.

Furthermore, Ira1 and Ira2 are functionally redundant. Therefore, the reduced but not abolished level of Ira1/2 contributes to the observed difference in Ras2-GTP.

We also measured the Ras2-GTP levels when Gpb1/2 were overexpressed in wild-type cells. Our data provide evidence that Gpb1/2 overexpression elicits little if any effect on Ras2-GTP level in wild-type cells (data not shown). This is consistent with the finding that Gpb1/2 overexpression is unable to inhibit pseudohyphal differentiation in wild-type cells.

We have conducted additional co-immunoprecipitation studies (see Figure 5 and Supplemental Figure 1) to further support the conclusion that the Gpb1/2 binding domain (GBD) is present in the conserved C-terminal region in Ira1/2. Furthermore, the GBD (2715~2925 aa) in Ira1 was deleted and tested for an impact on stability, and we found that this Ira1 deletion variant was destabilized (Figure 5). This observation supports the hypothesis that Gpb1/2 stabilize Ira1/2 by binding to the GBD. We also expressed the Ira1/2 isolated GBD to test for association with Gpb1/2. As shown in Figure 5D and Supplemental Figure 1D, the GBD from Ira1/2 binds to Gpb1/2, further assigning the GBD to the conserved C-terminal region.

We examined whether Gpb1/2 could affect a protein-protein interaction between Ira1 and adenylyl cyclase. Because a physical interaction between Ira1 and Cyr1 has not been demonstrated directly, we constructed a functionally FLAG tagged Cyr1 protein and tested for interaction with the 3HA tagged Ira1 in vivo. We were unable to detect interaction between the FLAG tagged Cyr1 protein and the Ira1-3HA fusion protein under our standard conditions (data not shown). This result raises the possibility that Cyr1 is indirectly associated with Ira1. This is consistent with our hypothesis that Cyr1

regulatory elements including Gpr1, Gpa2, Gpb1/2, Ras, Cdc25, and Ira1/2 form a supramolecular complex and control Cyr1 activity in response to extracellular stimuli (Figure 7 and Discussion). Further studies will be required to understand in detail these aspects of the mechanisms by which cAMP is produced and signals.

We have tested whether Ras is required for the observed interaction of Gpb1/2 with Ira1/2 and whether Gpa2 might compete with Ira1/2 for binding to Gpb1/2. To answer these questions, Gpb2-Ira1 interactions were examined in the presence and absence of Ras2 or Gpa2. We found that Ras2 is dispensable for this interaction, and the data are presented in Figure 2D. We also found that loss of Gpa2 elicits little effect on Gpb2-Ira1 interaction, if any (data not shown). This finding indicates that there is no competition between Gpa2 and Ira1/2 for Gbp1/2 interaction.

Invasive growth, nitrogen starvation sensitivity, glycogen accumulation, and cAMP levels have been examined as independent corroboration of our findings and model (Figure 7) and are included as panels in Figures 2 and 6.

To determine whether the functions of the kelch proteins are evolutionarily conserved, we have extended our studies to another genetically tractable fungal model system, *Cryptococcus neoformans*, and identified two kelch repeat homologs that are involved in mating (Kem1 and Kem2). To find kelch-repeat proteins involved in G protein signaling, *Cryptococcus* homologues of Gpb1/2, which interacts with and negatively regulates the G protein alpha subunit, Gpa2, in *S. cerevisiae*, were searched by BLAST (tblastn) in *Cryptococcus* genome database of serotype A (Duke University Medical Center (center for genome technology, http://cneo.genetics.duke.edu/) or the Whitehead Institute Center for Genome Research, http://www-

genome.wi.mit.edu/annotation/fungi/cryptococcus_neoformans/index.html) or serotype D (TIGR (http://www.tigr.org/tdb/e2k1/cna1/) or Stanford Genome Technology Center (SGTC, http://www-sequence.stanford.edu/group/C.neoformans/) database). However, Gpb1 and Gbp2 homologues were not found in serotype A or D *Cryptococcus neoformans* genome. Therefore, kelch-repeat proteins involved in mating of other fungi were investigated. In fission yeast *Schizosaccharomyces pombe*, a kelch-repeat protein, Ral2 (Ras-like), is involved in cell morphology, conjugation and sporulation upstream of Ras1. A BLAST search of the *Cryptococcus* genome database showed that both serotype A and D *Cryptococcus neoformans* contain Ral2 homologues (Figure 8). Interestingly, *S. cerevisiae* seems not appear to have any Ral2 homologues. Instead, the kelch-repeat containing amino terminal half of Kel1 (Kelch-repeat protein 1) is homologous to *S. pombe* or *C. neoformans* Ral2. *S. cerevisiae* Kel1 is involved in cell morphology and mating. Based on BLAST searches, *C. neoformans* has genes encoding hypothetical proteins homologous to the kelch-repeat containing amino terminus of Kel1. Here we name the genes encoding these kelch repeat containing proteins *KEM1* and *KEM2* (Kelch repeat proteins involved in mating), respectively. Therefore, Kem1 and Kem2 are homologuous to *S. pombe* Ral2 and the amino terminal half of *S. cerevisiae* Kel1.

We disrupted all three genes (*KEM1*(*RAL2*), *KEM2*(*KEL1*), *KEL2*) in the *C. neoformans* H99 strain background and found that Kem1 (Ral2) and Kem2 (Kel1), but not Kel2, are in part involved in mating (Figures 9, 10, and 13). Otherwise we have not found any other phenotypes associated with these mutations. Capsule and melanin production seem to be normal in these strains (Figures 11, 12), although more detailed

analysis might be required. Currently, we are constructing *kem1 kem2* double mutant strains for further analysis.

Recent studies by other groups have implicated the kelch proteins Gpb1/2 in exerting an additional level of regulatory control, possibly via direct interactions with PKA. Our hypothesis is that the signaling components exist as components of a larger macromolecular complex, and this likely will provide insights into the functions of the human NF1 homolog. Our ongoing studies address the physical interaction binding partners for the protein kinase A catalytic subunits Tpk1 and Tpk2, and reveal that protein kinase A is physically associated with RNA polymerase II in the nucleus. Taken together with recent studies from Rick Young's lab (Pokholok et al, 2006) that provide evidence that PKA occupies chromatin at the promoters for regulatory target genes, these studies forge a link between signaling pathway components and direct nuclear control of gene expression. The role that the kelch proteins play in this novel aspect of PKA signaling is under current investigation and a manuscript describing these studies is in preparation to be submitted.

**Key Research accomplishments for years one, two, and three.**

1. The kelch Gβ mimic Gpb1/2 proteins are recruited to the plasma membrane in a Gα Gpa2-dependent manner.
2. The kelch proteins Gpb1/2 were shown to function at the cell membrane.
3. The yeast neurofibromin homologs Ira1 and Ira2 were identified as physical and functional binding partners for the kelch proteins Gpb1/2.

4. Genetic and physical data support Ira1/2 as physiological targets of the kelch proteins Gpb1/2.
5. Regions of Ira1 and Ira2 that interact with Gpb1/2 were identified and found to be conserved in evolution.
6. Pulse-chase studies were conducted to establish that Gpb1/2 bind to and stabilize the yeast neurofibromin homologs Ira1/2 via the conserved interaction domain.
7. Homologs of the kelch proteins were identified in a divergent fungal species, enabling further molecular and genetic analysis of their roles in governing signaling via the cAMP pathway.
8. Mass spectrometric analysis was applied to identify and study proteins directly interacting with protein kinase A. A prominent interaction with RNA polymerase II was uncovered, providing key insights into how the kelch protein regulated protein kinase A pathway may participate in more direct control of transcription than previously appreciated.

**Reportable outcomes**

1. Toshiaki Harashima and Joseph Heitman. Gαsubunit Gpa2 recruits kelch repeat subunits that inhibit receptor-G protein coupling during cAMP induced dimorphic transitions in *Saccharomyces cerevisiae*, *Molecular Biology of the Cell*, 16, 4557-4571, 2005.
2. Toshiaki Harashima, Scott Anderson, John R. Yates, and **Joseph Heitman**. The kelch proteins Gpb1 and Gpb2 inhibit Ras activity via assocation with the yeast RasGAP neurofibromin homologs Ira1 and Ira2, *Molecular Cell*, 22, 819-830, 2006.

3. Julian Rutherford, Gordon Chua, Timothy Hughes, Maria E. Cardenas, and **Joseph** Heitman. A Mep2-dependent transcriptional profile links permease function to gene expression during pseudohyphal growth in *Saccharomyces cerevisiae*, *Molecular Biology of the Cell*, published online April 23, 2008.
4. We were invited to present our findings at the annual Neurofibromatis Conference sponsored by the Children's Tumor Foundation, which was held in Canyons Resort near Park City, Utah from June 10-12, 2007. My colleague and collaborator Toshiaki Harashima attended this meeting to present our studies on the role of Gpa2 in a talk entitled: "The kelch proteins Gpb1 and Gpb2 inhibit Ras activity via association with the yeast RasGAP neurofibromin homologs Ira1 and Ira2." The submitted abstract and letter of invitation are included with the submitted materials.

**Conclusions**

These studies have identified the Gpb1/2 binding domain (GBD) near the C-terminus of the neurofibromin homologs Ira1/2 and function to stabilize Ira1/2 enabling control of Ras signaling. Loss of Gpb1/2 results in a decrease in the RasGAP Ira1/2 proteins and consequently to an increase in the GTP bound form of Ras, which is the active form of Ras and ultimately associated with NF1. Importantly the GBD is significantly conserved in neurofibromin homologs, including the human counterpart, and mutations that lead to loss of the GBD have been identified from NF1 patients. Therefore the same regulatory mechanisms may be conserved in evolution, and this study should provide information as to how the RasGAP activity of neurofibromin is regulated and ultimately provide therapeutic clues for NF1 patients and possible avenues for novel drug development.

**References**

Ars, E., Kruyer, H., Morell, M., Pros, E., Serra, E., Ravella, A., Estivill, X., and Lázaro, C. (2003). Recurrent mutations in the *NF1* gene are common among neurofibromatosis type 1 patients. J Med Genet *40*, e82.

Ballester, R., Marchuk, D., Boguski, M., Saulino, A., Letcher, R., Wigler, M., and Collins, F. (1990). The *NF1* locus encodes a protein functionally related to mammalian GAP and yeast *IRA* proteins. Cell *63*, 851-859.

Ballester, R., Michaeli, T., Ferguson, K., Xu, H. P., McCormick, F., and Wigler, M. (1989). Genetic analysis of mammalian GAP expressed in yeast. Cell *59*, 681-686.

Buchberg, A. M., Cleveland, L. S., Jenkins, N. A., and Copeland, N. G. (1990). Sequence homology shared by neurofibromatosis type-1 gene and *IRA-1* and *IRA-2* negative regulators of the *RAS* cyclic AMP pathway. Nature *347*, 291-294.

Dasgupta, B., and Gutmann, D. H. (2003). Neurofibromatosis 1: closing the GAP between mice and men. Curr Opin Genet Dev *13*, 20-27.

De Luca, A., Buccino, A., Gianni, D., Mangino, M., Giustini, S., Richetta, A., Divona, L., Calvieri, S., Mingarelli, R., and Dallapiccola, B. (2003). NF1 gene analysis based on DHPLC. Hum Mutat *21*, 171-172.

Fahsold, R., Hoffmeyer, S., Mischung, C., Gille, C., Ehlers, C., Kücükceylan, N., Abdel-Nour, M., Gewies, A., Peters, H., Kaufmann, D., *et al.* (2000). Minor lesion mutational spectrum of the entire *NF1* gene does not explain its high mutability but points to a functional domain upstream of the GAP-related domain. Am J Hum Genet *66*, 790-818.

Harashima, T., and Heitman, J. (2002). The Gα protein Gpa2 controls yeast differentiation by interacting with kelch repeat proteins that mimic Gβ subunits. Mol Cell *10*, 163-173.

Harashima, T., and Heitman, J. (2005). Gα subunit Gpa2 recruits kelch repeat subunits that inhibit receptor-G protein coupling during cAMP induced dimorphic transitions in *Saccharomyces cerevisiae*. Mol Biol Cell *16*, 4557-4571.

Harashima, T., Anderson, S., Yates, J. R., and Heitman, J. (2006). The kelch proteins Gpb1 and Gpb2 inhibit Ras activity via assocation with the yeast RasGAP neurofibromin homologs Ira1 and Ira2, *Molecular Cell*, 22, 819-830.

Martin, G. A., Viskochil, D., Bollag, G., McCabe, P. C., Crosier, W. J., Haubruck, H., Conroy, L., Clark, R., O'Connell, P., Cawthon, R. M., and et al. (1990). The GAP-related domain of the neurofibromatosis type 1 gene product interacts with *ras* p21. Cell *63*, 843-849.

Origone, P., De Luca, A., Bellini, C., Buccino, A., Mingarelli, R., Costabel, S., La Rosa, C., Garrè, C., Coviello, D. A., Ajmar, F., *et al.* (2002). Ten novel mutations in the human neurofibromatosis type 1 (NF1) gene in Italian patients. Hum Mutat *20*, 74-75.

Parada, L. F. (2000). Neurofibromatosis type 1. Biochim Biophys Acta *1471*, M13-19.

Pokholok DK, Zeitlinger J, Hannett NM, Reynolds DB, Young RA (2006). Activated signal transduction kinases frequently occupy target genes. Science. 313, 533-536.

Rasmussen, S. A., and Friedman, J. M. (2000). *NF1* gene and neurofibromatosis 1. Am J Epidemiol *151*, 33-40.

Tanaka, K., Lin, B. K., Wood, D. R., and Tamanoi, F. (1991). *IRA2*, an upstream negative regulator of RAS in yeast, is a RAS GTPase-activating protein. Proc Natl Acad Sci U S A *88*, 468-472.

Tanaka, K., Matsumoto, K., and Toh-e, A. (1989). *IRA1*, an inhibitory regulator of the *RAS*-cyclic AMP pathway in *Saccharomyces cerevisiae*. Mol Cell Biol *9*, 757-768.

Tanaka, K., Nakafuku, M., Satoh, T., Marshall, M. S., Gibbs, J. B., Matsumoto, K., Kaziro, Y., and Toh-e, A. (1990a). *S. cerevisiae* genes *IRA1* and *IRA2* encode proteins that may be functionally equivalent to mammalian *ras* GTPase activating protein. Cell *60*, 803-807.

Tanaka, K., Nakafuku, M., Tamanoi, F., Kaziro, Y., Matsumoto, K., and Toh-e, A. (1990b). *IRA2*, a second gene of *Saccharomyces cerevisiae* that encodes a protein with a domain homologous to mammalian *ras* GTPase-activating protein. Mol Cell Biol *10*, 4303-4313.

Upadhyaya, M., Osborn, M. J., Maynard, J., Kim, M. R., Tamanoi, F., and Cooper, D. N. (1997). Mutational and functional analysis of the neurofibromatosis type 1 (*NF1*) gene. Hum Genet *99*, 88-92.

Xu, G. F., Lin, B., Tanaka, K., Dunn, D., Wood, D., Gesteland, R., White, R., Weiss, R., and Tamanoi, F. (1990a). The catalytic domain of the neurofibromatosis type 1 gene product stimulates *ras* GTPase and complements *ira* mutants of *S. cerevisiae*. Cell *63*, 835-841.

Xu, G. F., O'Connell, P., Viskochil, D., Cawthon, R., Robertson, M., Culver, M., Dunn, D., Stevens, J., Gesteland, R., White, R., and et al. (1990b). The

neurofibromatosis type 1 gene encodes a protein related to GAP. Cell *62*, 599-608.

Zhu, Y., and Parada, L. F. (2002). The molecular and genetic basis of neurological tumours. Nat Rev Cancer *2*, 616-626.

## Appendices

### Statement of Work

*Task 1.* To characterize the roles of the Gβ mimic kelch proteins Gpb1 and Gpb2 in regulating the yeast neurofibromin homologs Ira1 and Ira2 (Months 1-12):

a. Determine the role of Gpb1/2 on Ira1/2 (Months 1-4.5)
    I. Construct and develop materials required for GAP assay of Ira1/2 (Months 1-3).
    II. Perform GAP assay to examine the roles of Gpb1/2 on Ira1/2 RasGAP activity (Months 3-4.5).

b. Identify the Gpb1/2-binding domain on Ira1/2 (Months 1-6):
    I. Construct Ira1/2 derivatives carrying various deletions in the N-terminal, central, and C-terminal regions (Months 1-4.5).
    II. Test protein-protein interactions and identify the Gpb1/2-binding domain (Months 4.5-6).

c. Identify amino acid residues in Ira1/2 required for protein-protein interactions with Gpb1/2 (Months 6-12):
    I. Mutagenize the Gpb1/2-interacting domain in Ira1/2 and clone into the yeast two-hybrid vector (Months 6-7).
    II. Test protein-protein interactions and identify amino acids required for physical interactions with Gpb1/2 (Months 7-9).

III. Introduce mutations in the *IRA1/2* genes that abolish physical interactions with Gpb1/2 in vivo (Months 9-11).

IV. Test for pseudohyphal differentiation to characterize the role of the mutated amino acids in vivo (Months 11-12).

*Task 2*. To identify amino acid residues important for function of neurofibromin and Ira1/2 (Months 12-24):

a. Construct and express the *NF1* gene in yeast *ira1,2* mutants to examine whether the full length neurofibromin is functional when heterologously expressed in yeast cells (Months 12-13).

b. To identify putative Gpb1/2 binding sites in neurofibromin (Months 13-24):

   I. Introduce mutations in those ones of neurofibromin and clone these novel *NF1* alleles into yeast and mammalian expression vectors (Months 13-17).

   II. Express these *NF1* alleles in the yeast *ira1,2* mutant and mouse $NF1^{-/-}$ cells and characterize the roles of the mutated amino acids in vivo (Months 17-24).

c. To characterize the roles of the consensus PKA phosphorylation sites in neurofibromin and Ira1/2 (Months 13-24):

   I. Introduce mutations in candidate PKA phosphorylation sites in neurofibromin and Ira1/2 (Months 13-17).

II. Express these *NF1* mutant alleles in the yeast *ira1,2* mutant and mouse *NF1*$^{-/-}$ cells and the *IRA1/2* mutant alleles in the *ira1,2* mutant cells and test for phenotypes to examine the roles of those putative PKA phosphorylation sites (Months 17-24).

*Task 3*. To identify a human Gpb1/2 counterpart (Months 24-36):

a. To examine whether yeast Gpb1/2 interact with neurofibromin (Months 24-27):
    I. Construct FLAG-Gpb1/2 to be expressed and transfected into murine cells (Months 24-25).
    II. Examine protein-protein interactions by FLAG tag based immunopurification methods and western blots using anti-neurofibromin and anti-FLAG antibodies (Months 25-27).
b. To isolate a human Gpb1/2 counterpart (Months 27-36):
    I. Perform psi-BLAST searches against human sequence databases (Month 27).
    II. Make constructs for analysis in the yeast two-hybrid system and test protein-protein interactions between neurofibromin and putative Gpb1/2 counterparts (Months 27-31).

III. Also generate yeast two-hybrid constructs of the candidate Gpb1/2 binding domain in neurofibromin and screen human two-hybrid libraries to identify putative Gpb1/2 counterparts (Months 31-36).

**Supporting Data**

***Figure legends***

**Figure 1. Genetic interactions between *gpb1,2* and *ras2* mutations.** (A) *gpb1,2* mutations are unable to suppress the synthetic growth defect of *gpa2 ras2* mutant cells. Diploid *gpa2::G418/gpa2::hph ras2::nat/RAS2* (left, THY388a/α) and *gpb1,2::loxP/gpb1,2::loxP gpa2::loxP-G418/GPA2 ras2::nat/ras2::nat* (right, see "Materials and Discussion") cells were sporulated and dissected. Progeny genotypes were determined based on segregation of the dominant drug resistant markers (*G418*, *hph*, and *nat*). (B-F) *ras2* mutations alleviate increased PKA phenotypes associated with *gpb1,2* mutations, including enhanced pseudohyphal growth (B), hyperinvasive growth (C), increased *FLO11* expression (D), sensitivity to nitrogen starvation (E), and reduced glycogen accumulation (F). Diploid strains, MLY61a/α (WT), THY170a/α (*gpa2*), XPY5a/α (*tpk2*), MLY187a/α (*ras2*), THY212a/α (*gpb1,2*), THY242a/α (*gpb1,2 gpa2*), THY245a/α (*gpb1,2 tpk2*), and THY247a/α (*gpb1,2 ras2*) were employed to assay pseudohyphal growth, and isogenic haploid strains, MLY40α (WT), THY170α, XPY5α, MLY187α, THY212α, THY242α, THY245α, and THY247α to study invasive growth, *FLO11* expression, sensitivity to nitrogen starvation, and glycogen accumulation. (G) Glucose-induced cAMP production in WT (MLY40α), *ras2* (MLY187α), *gpb1,2* (THY212α), and *gpb1,2 ras2* (THY247α) mutant cells. Glucose was added to glucose starved cells, and at the indicated time points, cells were collected and cAMP levels were determined. The values shown are the mean of two independent experiments.

**Figure 2. Kelch Gβ mimic subunits interact with RasGAP Ira1/2.** (A and B) Ira1 (A) and Ira2 (B) physically bind to Gpb1/2 in vivo. The N-terminally FLAG-tagged Gpb1 (pTH111) and Gpb2 (pTH88) proteins were expressed in yeast cells that also express C-terminally 3HA tagged Ira1 (THY355a, panel A) or Ira2 (THY356a, panel B). (C) Gpb2 requires both the unique N-terminal and the C-terminal kelch domains to interact with Ira1. The N-terminally FLAG tagged Gpb2 N-terminal region (FLAG-Gpb2N, pTH190), C-terminal kelch domains (FLAG-Gpb2C, pTH188), or full length Gpb2 (FLAG-Gpb2, pTH88) were co-expressed with the Ira1-3HA protein in vivo (THY381a). Positions of molecular marker (128, 85, 41.7, and 32.1 k) are indicated to the right of the panel. (D) Ras2 is dispensable for the Gpb2-Ira1 interaction. Protein-protein interactions between Gpb2 and Ira1 were examined in the presence (THY355a) and absence (THY479α) of Ras2 using cells that express the FLAG tagged Gpb2 (pTH88). Crude cell extracts were prepared from exponentially growing cells and subjected to immunoprecipitations using anti-FLAG affinity gel. To verify expression levels of the 3HA tagged Ira1/2 proteins and because of low expression levels of Ira1/2, the Ira1/2-3HA proteins were immunoprecipitated using anti-HA agarose beads, eluted, and then analyzed by western analysis and indicated as "Input". Cells expressing both Ira1-3HA and Trp1-FLAG fusion proteins (THY450a) served as the control. Fpr1 was used as the loading control.

**Figure 3. Genetic interactions between *gpb1,2* and *ira1,2* mutations.** (A) Wild-type (MLY61a/α), *gpb1,2* (THY212a/α), *ira1,2* (THY345a/α), *ira1* (THY337a/α), *ira2* (THY336a/α), and *gpb1,2 ira1,2* (THY346a/α) mutant strains were assayed

for pseudohyphal growth. (B) The dominant active *GPA2*$^{Q300L}$ (pTH48) and *RAS2*$^{G19V}$ (pMW2) alleles were introduced into wild-type (MLY61a/α) and *gpb1,2* mutant cells (THY212a/α) and tested for effects on filamentous growth. (C) The *IRA2* gene (pKF56) suppressed the increased filamentous phenotype of *gpb1,2* mutant cells (THY212a/α). pTH27 (*GPB2*) and an empty vector pTH19 were introduced into wild-type (MLY61a/α) or *gpb1,2* mutant cells (THY212a/α) as controls. Cells were grown on SLAD agar medium at 30ºC for 5 days and photographed in panels A, B, and C. Haploid cells indicated were tested for invasive growth (D), nitrogen starvation sensitivity (E), glycogen accumulation (F), and glucose-induced cAMP production (G). (D) Cells were grown on YPD at 30ºC for 5 days and photographed after weak (W), mild (M) or strong (S) washing. (E) Cells were grown on YPD at 30ºC for 2 days, replica-plated onto nitrogen replete (+$NH_4$) and no nitrogen (-$NH_4$) media. After 6 (left panel) or 10 (right panel) days at 30 ºC, cells were replica-plated onto YPD again and incubated under the same conditions. (F) Glycogen levels of cells grown on YPD at 30ºC for 2 days were determined using iodine vapor. (G) cAMP levels were determined in response to glucose readdition as described in the legend of Figure 1.

**Figure 4. Kelch subunits Gpb1/2 stabilize the RasGAP proteins Ira1/2.** (A) The relative increase in Ras2-GTP was examined in isogenic wild-type (MLY41a) and *ras2* (MLY187α), *ira1* (THY337a), *ira2* (THY336a), *ira1,2* (THY345a), and *gpb1,2* (THY212a) mutant cells, expressing the wild-type (pMW1) or dominant active (G19V, pMW2) *RAS2* gene. Representative data are shown in the upper panel.

Note that purified Ras2-GTP from *ira1,2* double mutant cells expressing the wild-type Ras2 protein and wild-type and *gpb1,2* mutant cells that express the dominant active Ras2 ($Ras2^{G19V}$) protein was 5-fold diluted prior to western analysis, as the levels of Ras2-GTP in these cells were higher than those in the other cells. This permitted accurate measurement of the levels of Ras2-GTP by densitometry. After detection of levels of the GTP bound Ras2 and total cellular Ras protein ("Input") by western blot, signals were densitometrically quantified. Levels of Ras2-GTP were normalized to "Input" Ras2 levels and shown as a relative level to Ras2-GTP in wild-type cells in the lower panel. The values shown in the lower panel are the means of two or three independent experiments with the standard error of the mean. (B) The *GPB1* (pTH26) and *GPB2* (pTH114) genes were introduced into wild-type strains THY427a (*IRA1-3HA*) and THY428a *(IRA2-3HA*) and *gpb1,2* double mutant strains THY425a (*gpb1,2 IRA1-3HA*) and THY426a (*gpb1,2 IRA2-3HA*) to examine protein stability of Ira1/2 and the interactions between Ras2 and Ira1/2. The Ira1/2-Ras2 protein complex was co-immunoprecipitated using anti-HA conjugated agarose gels and eluted by the addition of HA peptide (shown as "Co-IP (HA)" in upper panel). A yeast strain THY475 (Trp1-3HA) carrying the empty vector pTH19 was employed as a control. Fpr1 served as a loading control. "NT" indicates the non-tagged, wild-type Ira1 or Ira2 protein. Based on densitometric analysis the steady state protein levels of Ira1 and Ira2 were reduced in *gpb1,2* double mutant cells by at least 2- to 10-fold compared to wild-type cells. Cells expressing a 3HA tagged Trp1 fusion protein served as a control. Note that the Ira1/2 proteins were undetectable in western blot using crude extracts because of low expression levels. (C and D) Gpb1/2 stabilize Ira1/2. Protein stability of Ira1 (C) and Ira2

(D) was investigated by cycloheximide-chase assay in the presence and absence of Gpb1/2. Cycloheximide (CHX) was added to exponentially growing cells at a final concentration of 50 μg/ml. At the indicated time points after CHX addition, cells expressing the 3HA tagged Ira1 protein (THY425 and THY427, panel C) or the 3HA tagged Ira2 protein (THY426 and THY428, panel D) were collected, washed, and cell extracts were prepared. The 3HA tagged Ira1/2 proteins were analyzed as above. After western blot (upper panel), signals were densitometorically quantified, and % protein abundance of Ira1 and Fpr1 at "Time 0" is shown in the lower panel.

**Figure 5. Kelch Gpb1/2 subunits bind to the C-terminus of Ira1.** The FLAG-Gpb1 (pTH111) and FLAG-Gpb2 (pTH88) fusion proteins were expressed in yeast cells that also express the 3HA tagged wild type Ira1 or Ira1 deletion variants, and protein complexes were immunoprecipitated. (A) Schematic of Ira1 deletion proteins created and summary of results obtained from assays of protein abundance (western blots) and Gpb1/2 binding (immunoprecipitation) as below. Positions of deletions created in Ira1 are shown and numbered. A conserved region between Ira1/2 and the human neurofibromin protein is shaded in grey. The RasGAP related domain (GRD) and the Gpb1/2 binding domain (GBD) are shown as a hatched and dark grey rectangle, respectively. (B) Protein interactions were investigated using crude cell extracts from cells expressing the 3HA tagged full length Ira1 (1~3092, THY355a) or Ira1 deletion variants (1~2925 (THY424a), 1~2714 (THY402a), 1~2432 (THY401a), and 1~1257 (THY404a)). Positions of full length wild-type Ira1 (1~3092 aa) and deletion variants (1~2925 and 1~1257 aa) are indicated to the left of the panel. Positions at which

molecular weight markers (250, 210, and 148 k) migrated are indicated to the right of the panels. The deletion of 167 amino acids from the Ira1 C-terminus leads to reduced protein levels of Ira1 from 3- to 7 fold in comparison of the full length Ira1 protein level and the further deletion (378 amino acids) results in undetectable levels ("Input" panel). Note that some smaller Ira1-3HA species were also detected via the C-terminal HA tag, indicating that these are proteolysis products lacking N-terminal regions. This further supports the assignment of the GBD to the C-terminal region of Ira1. (C) N-terminal deletion Ira1 variants (2433~3092 aa (THY438a) and 2715~3092 aa (THY440a)) were tested for interaction with Gpb1/2. Positions of the N-terminal deletion Ira1 variants (2432~3092 and 2715~3092 aa) are indicated to the left of the panel. (D) A putative GBD of Ira1 spanning amino acids 2715~2925 (THY468a) was examined for Gpb1/2 interactions. Note that a deletion Ira1 variant that lacks this domain (Ira1 Δ2715~2925 aa variant in panel A) was undetectable because of protein instability, consistent with the role of Gpb1/2 in Ira1 protein stability. Crude extracts were prepared from cells grown to mid-log phase in synthetic dropout medium. Protein complexes were immunoprecipitated using anti-FLAG affinity gel. Because the levels of the full length Ira1 and these Ira1 N- and C-terminal deletion variant proteins in crude extracts were too low to detect by western blot, the full length and deletion Ira1 proteins were immunoprecipitated using anti-HA agarose beads, eluted, subject to western analysis, and examined for protein stability and indicated as "Input" in panels B, C, and D. Yeast strains (THY450a, THY464a, and THY467a) that carry the empty vector pTH19 were used as a control. Fpr1 in crude cell extracts served as loading controls and were also shown as "Input".

**Figure 6. The C-terminus of Ira1/2 is necessary for function.** (A) Isogenic homozygous diploid cells were tested for filamentous growth: WT (MLY61a/α), *gpb1,2* (THY212a/α), *ira1* (THY337a/α), *IRA1-3HA* (1~3092 aa, THY355a/α), *IRA1-3HA* (1~2925 aa, THY424a/α), *IRA1-3HA* (1~2714 aa, THY402a/α), *IRA1-3HA* (ΔGBD (Δ2715~2925 aa), THY471a/α). Cells were grown at 30°C for 5 days on SLAD medium and photographed. Invasive growth (B), nitrogen starvation sensitivity (C), and glycogen accumulation (D) were examined using isogenic haploid cells. (B) Cells were grown on YPD 30°C for 5 days and washed off under a current of water. (C) After 7 days on nitrogen replete or depleted medium, cells were replica-plated onto YPD. (D) Glycogen accumulation was assessed using iodine vapor. Details were as described in the figure legend to Figure 1.

**Figure 7. A dual role of the kelch proteins Gpb1/2 as molecular brakes on cAMP signaling.** (A) A schematic of the yeast neurofibromin homolog Ira1 and human neurofibromin proteins. A conserved region including the GRD and the GBD is shown in grey. GRD; hatched rectangle, GBD; bold rectangle. (B) A model for how the kelch Gβ mimic proteins Gpb1/2 control cAMP signaling. See details in the text.

**Figure 8. Structure of the *KEM1* and *KEM2* genes encoding kelch repeat homologs in *Cryptococcus neoformans*.**

**Figure 9. Gene disruption allele for the kelch repeat homolog Ral2 of *Cryptococcus neoformans*.**

**Figure 10. Southern blot analysis demonstrating that the *RAL2* gene has been successfully disrupted by biolistic transformation and homologous recombination.**

**Figure 11. The *RAL2* is not required to produce melanin.** *ral2* mutants in both mating types were grown on niger seed medium with low or high levels of glucose and the level of pigmentation produced following 2 or 4 days incubation compared to the isogenic wild type strains and mutants with defects in the enzyme laccase (*lac1*) or the protein kinase A signaling pathway.

**Figure 12. RAL2 is not required for capsule production.** Strains were growth in DMEM medium and the capsule was detected by staining with India Ink particles.

**Figure 13. *ral2* mutants exhibit a mating defect.** Strains were crossed on V8 mating media pH 5 or 7 and mated for five or ten days at room temperature in the dark, and filaments produced by mating photographed.

**Supplemental Figure 1. The GBD in Ira2 maps to the equivalent C-terminal region of Ira1.** (A) The protein structure of the Ira1/2 proteins is depicted schematically. Positions of deletions created in Ira1/2 are shown and numbered. The Gpb1/2 biding domain (GBD) on Ira2 was also determined by assessing

protein interactions between Gpb1/2 and C-terminal (1~2922 aa (THY 456a) and 1~2702 aa (THY 457a), panel B) and N-terminal ( 2703~3079 aa (THY 466a), panel C) Ira2 deletion variants and an Ira2 C-terminal domain (2703~2922 aa (THY473), panel B). The migration positions of full length wild-type Ira2 (3079 aa) and Ira2 deletion variants (1~2922 aa) are indicated to the left of the panel. Positions at which molecular weight markers (250, 210, and 148 k) migrated are also indicated to the right of the panels in B. Yeast strains (THY451a, THY466a,and THY474a) carrying the empty plasmid pTH19 were employed as a control. Details are essentially as described in the legend to Figure 5, unless otherwise specifically noted.

Figure 1. Harashima et al.

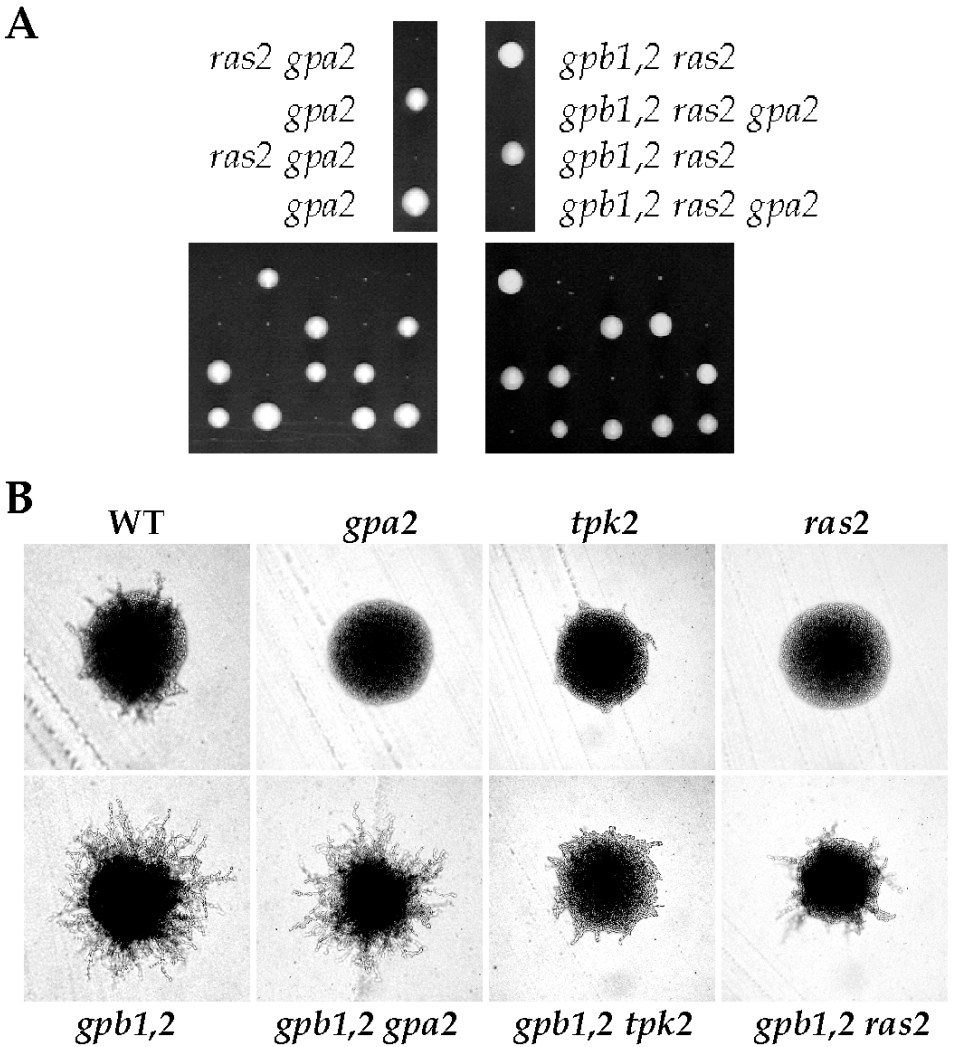


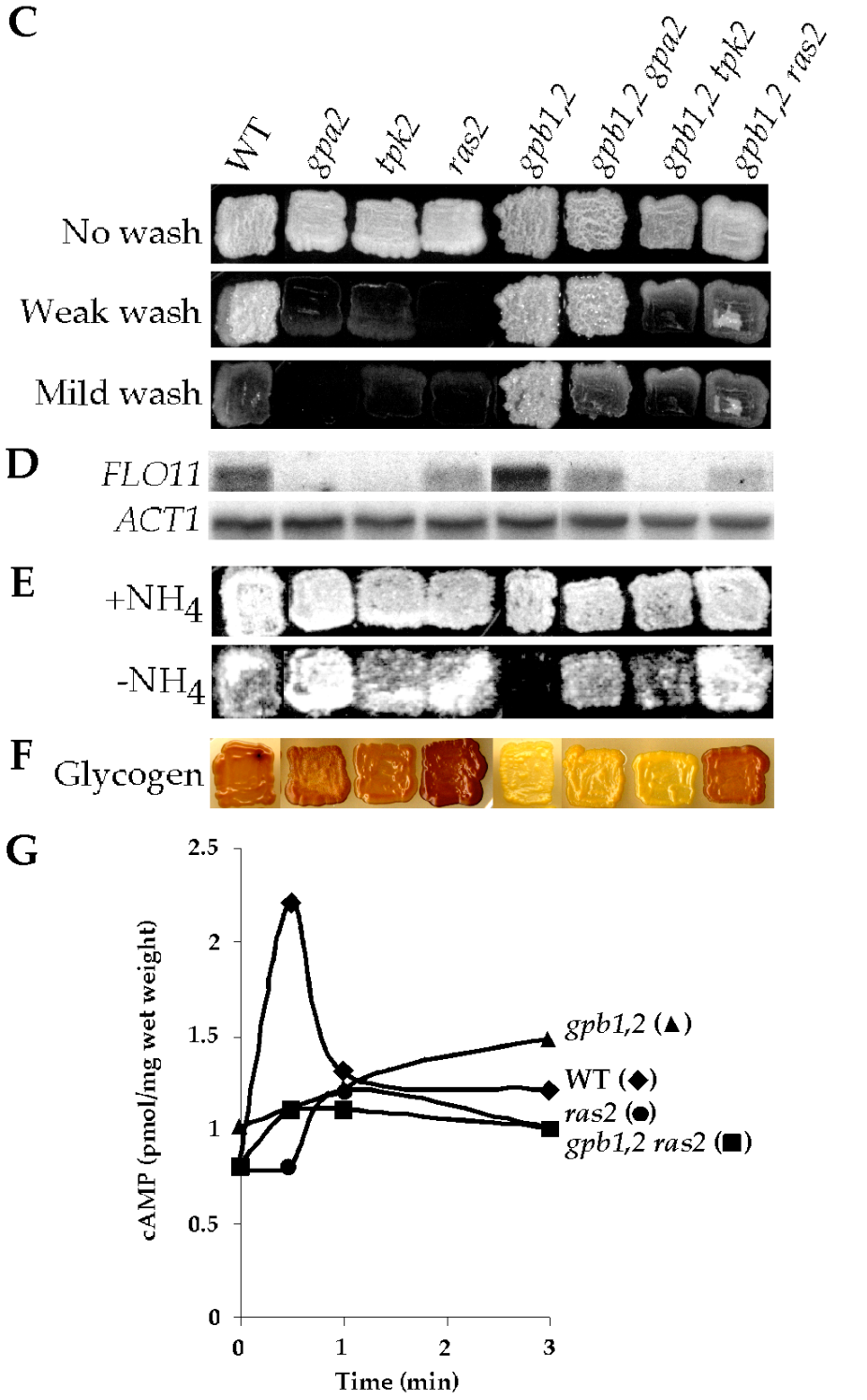

Figure 2. Harashima et al.

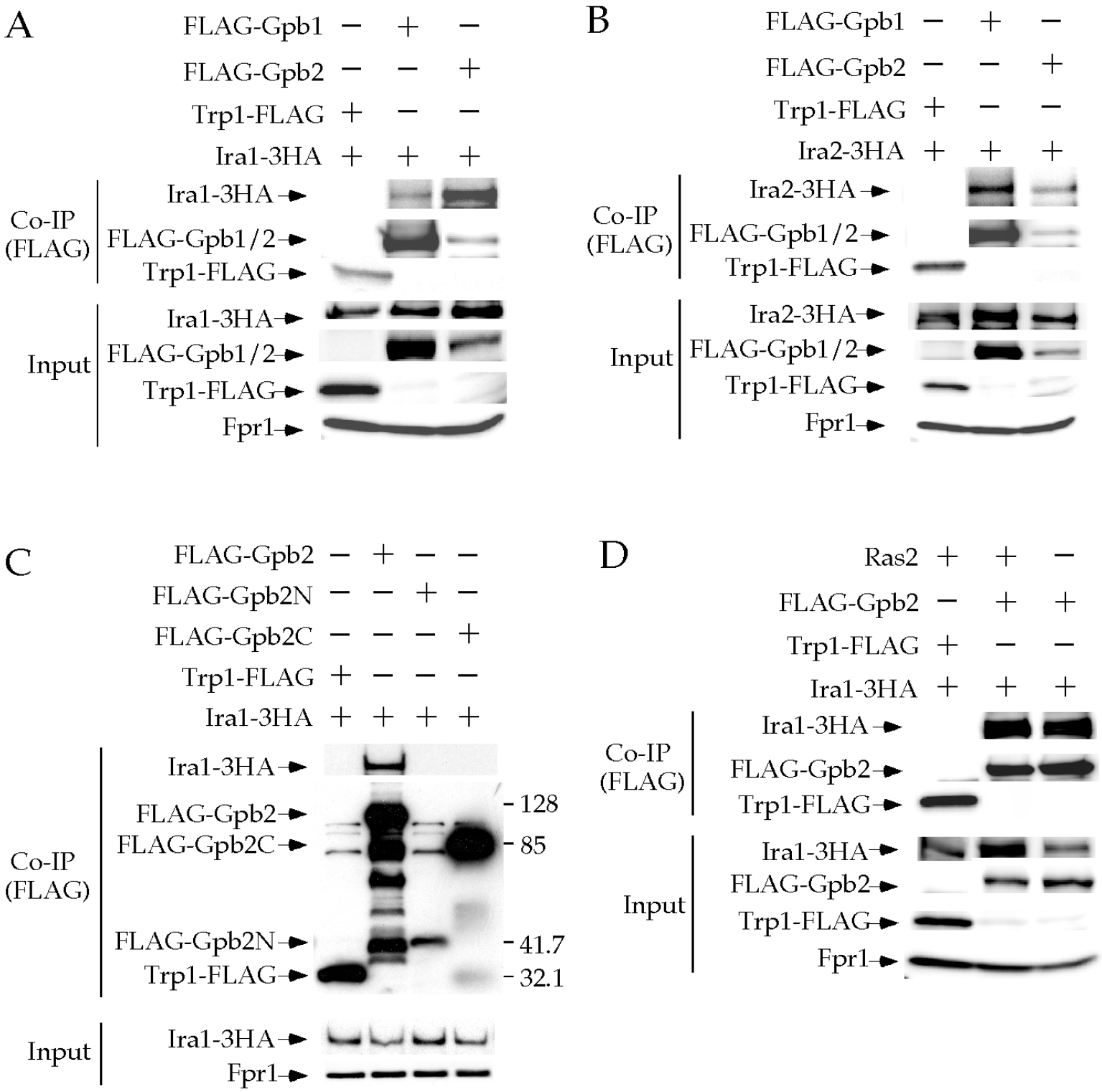

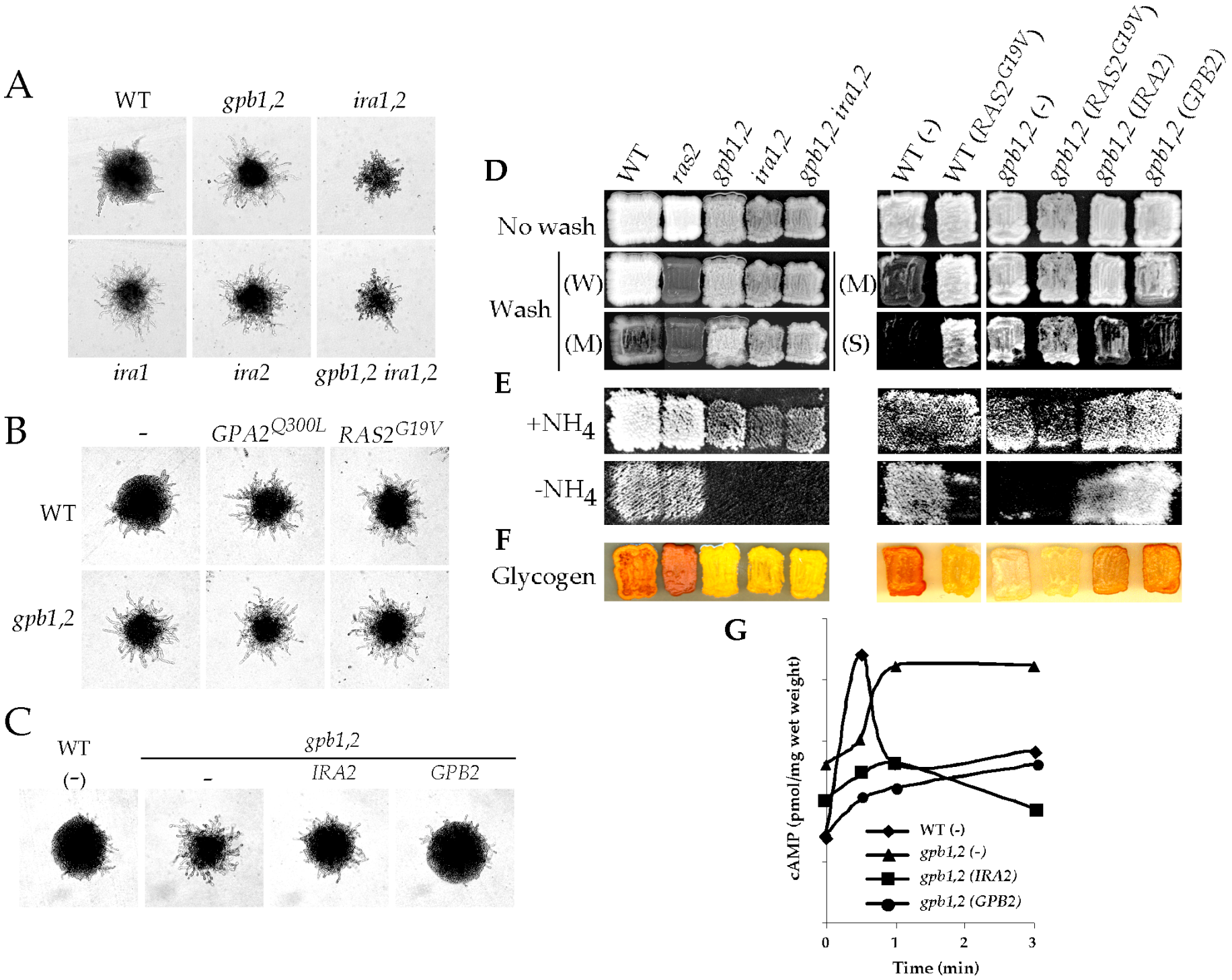
A
WT
gpb1,2
ira1,2
ira1
ira2
gpb1,2 ira1,2
B
-
GPA2Q300L
RAS2G19V
WT
gpb1,2
C
WT
(-)
gpb1,2
-
IRA2
GPB2
D
WT
ras2
gpb1,2
ira1,2
gpb1,2 ira1,2
WT (-)
WT (RAS2G19V)
gpb1,2 (-)
gpb1,2 (RAS2G19V)
gpb1,2 (IRA2)
gpb1,2 (GPB2)
No wash
Wash
(W)
(M)
(M)
(S)
E
+NH4
-NH4
F
Glycogen
G
cAMP (pmol/mg wet weight)
WT (-)
gpb1,2 (-)
gpb1,2 (IRA2)
gpb1,2 (GPB2)
0
1
2
3
Time (min)

Figure 4. Harashima et al.

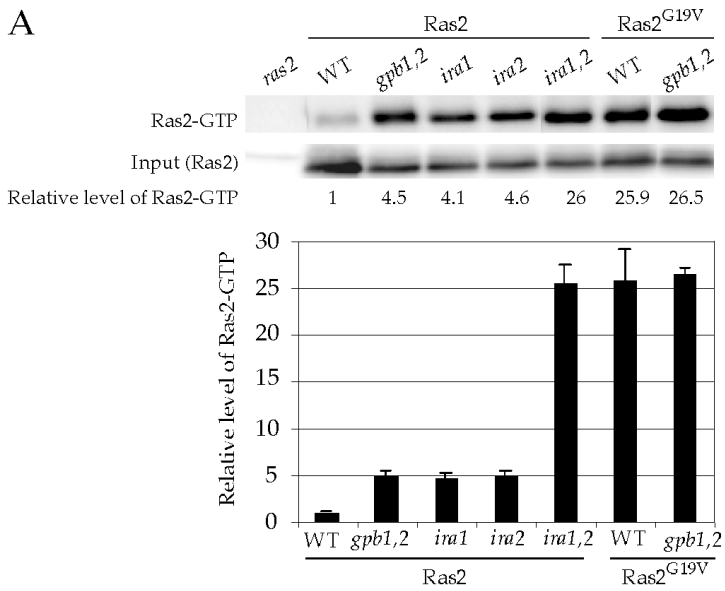


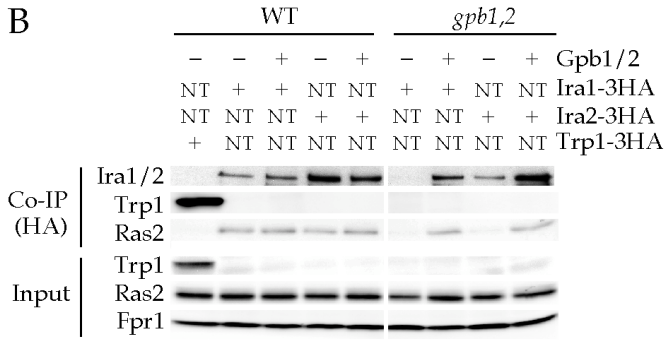


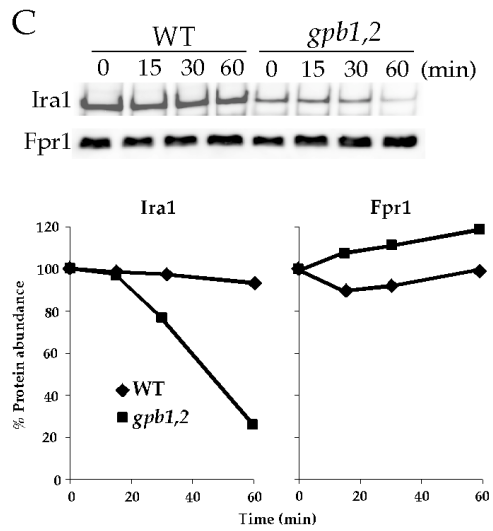


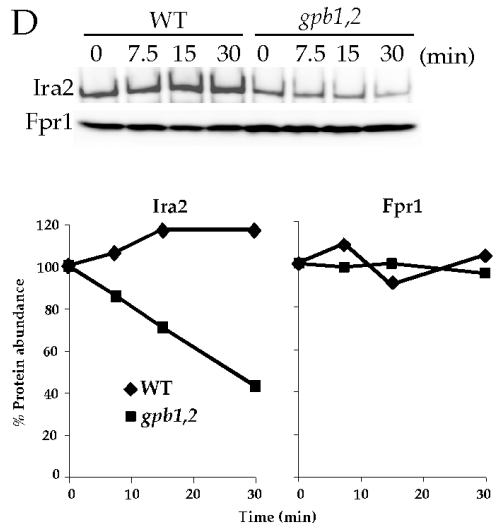

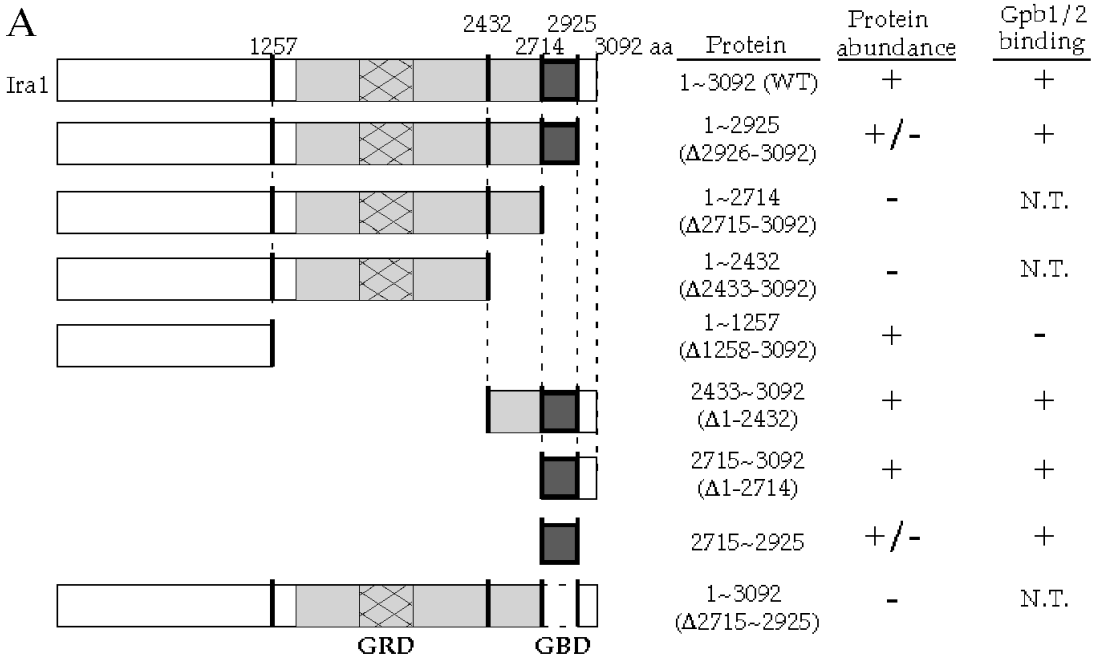
A
1257
2432
2714
2925
3092 aa
Ira1
GRD
GBD
Protein
Protein abundance
Gpb1/2 binding
1~3092 (WT) + +
1~2925 (Δ2926-3092) +/- +
1~2714 (Δ2715-3092) - N.T.
1~2432 (Δ2433-3092) - N.T.
1~1257 (Δ1258-3092) + -
2433~3092 (Δ1-2432) + +
2715~3092 (Δ1-2714) + +
2715~2925 +/- +
1~3092 (Δ2715~2925) - N.T.

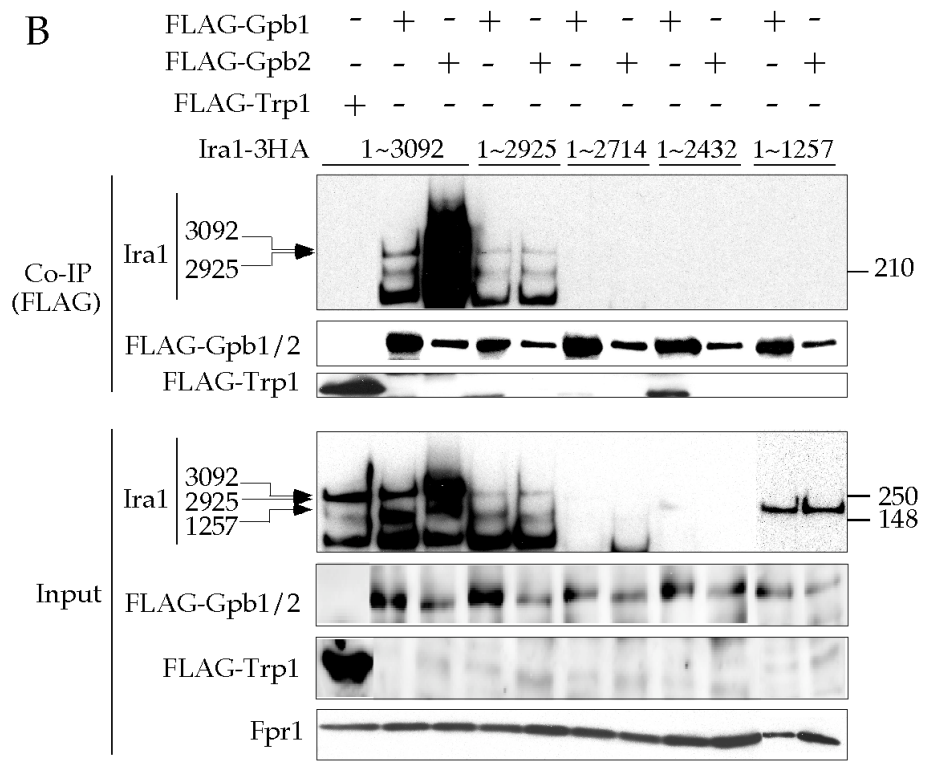
B
FLAG-Gpb1
FLAG-Gpb2
FLAG-Trp1
Ira1-3HA
1~3092
1~2925
1~2714
1~2432
1~1257
Co-IP (FLAG)
Ira1
3092
2925
210
FLAG-Gpb1/2
FLAG-Trp1
Input
Ira1
3092
2925
1257
250
148
FLAG-Gpb1/2
FLAG-Trp1
Fpr1

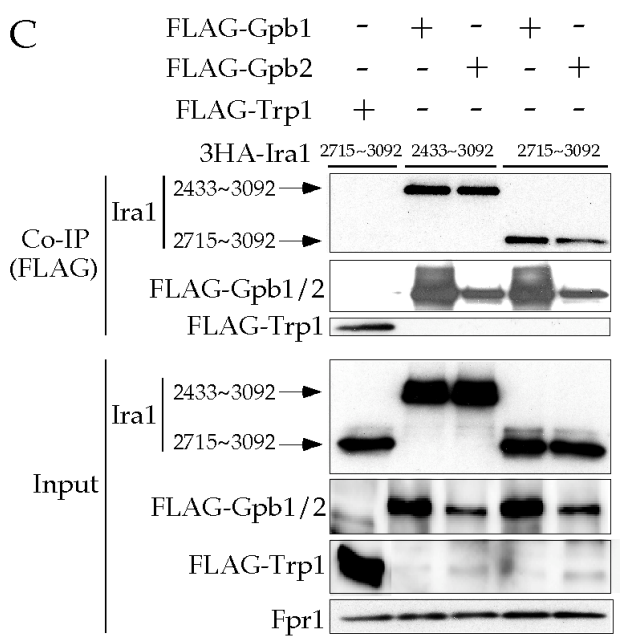
C
FLAG-Gpb1
FLAG-Gpb2
FLAG-Trp1
3HA-Ira1
2715~3092
2433~3092
2715~3092
Co-IP (FLAG)
Ira1
2433~3092
2715~3092
FLAG-Gpb1/2
FLAG-Trp1
Input
Ira1
2433~3092
2715~3092
FLAG-Gpb1/2
FLAG-Trp1
Fpr1

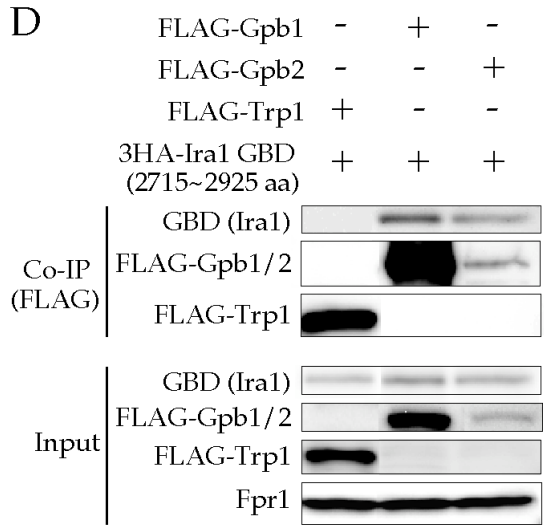
D
FLAG-Gpb1
FLAG-Gpb2
FLAG-Trp1
3HA-Ira1 GBD (2715~2925 aa)
Co-IP (FLAG)
GBD (Ira1)
FLAG-Gpb1/2
FLAG-Trp1
Input
GBD (Ira1)
FLAG-Gpb1/2
FLAG-Trp1
Fpr1

Figure 6. Harashima et al.

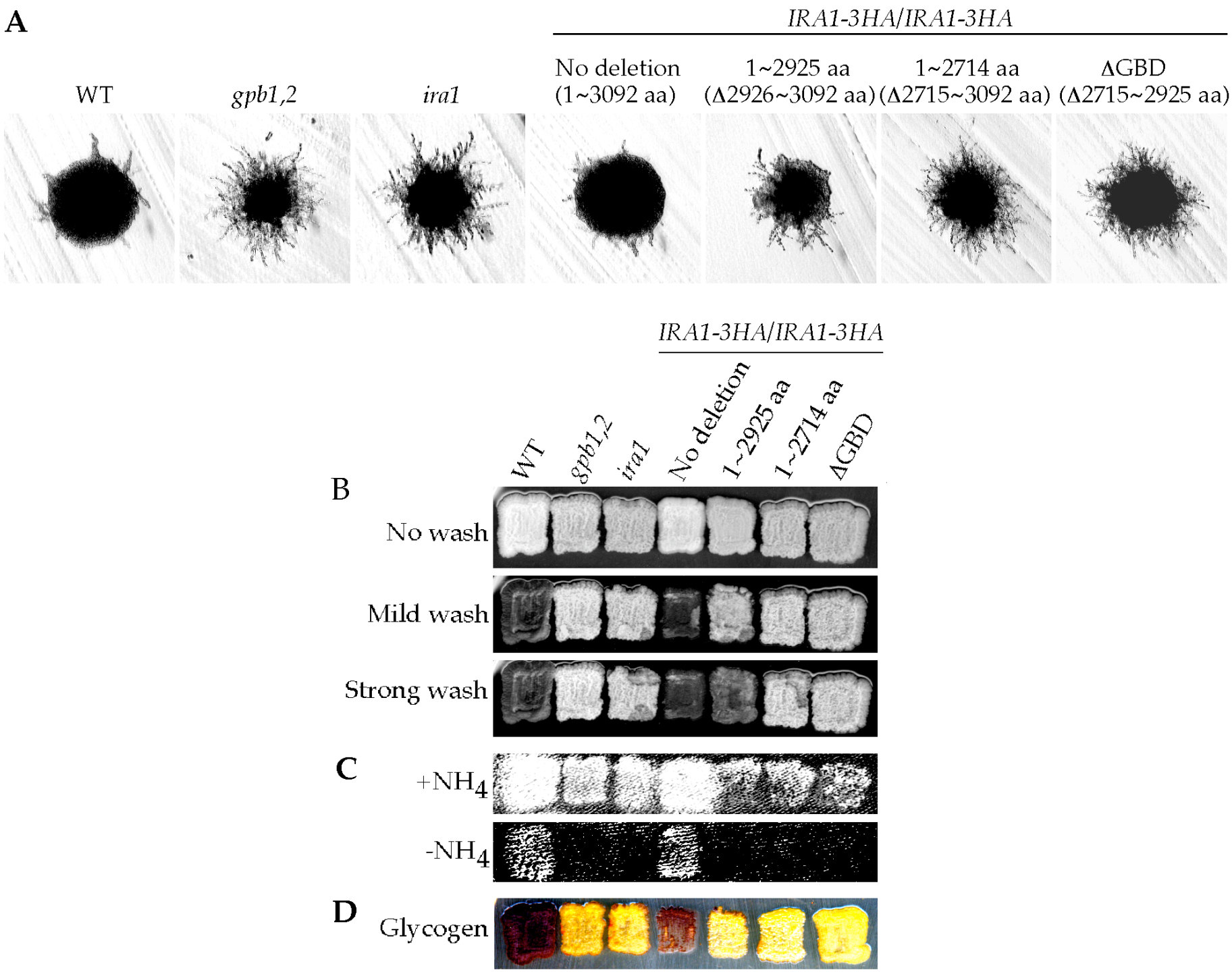

Figure 7. Harashima et al

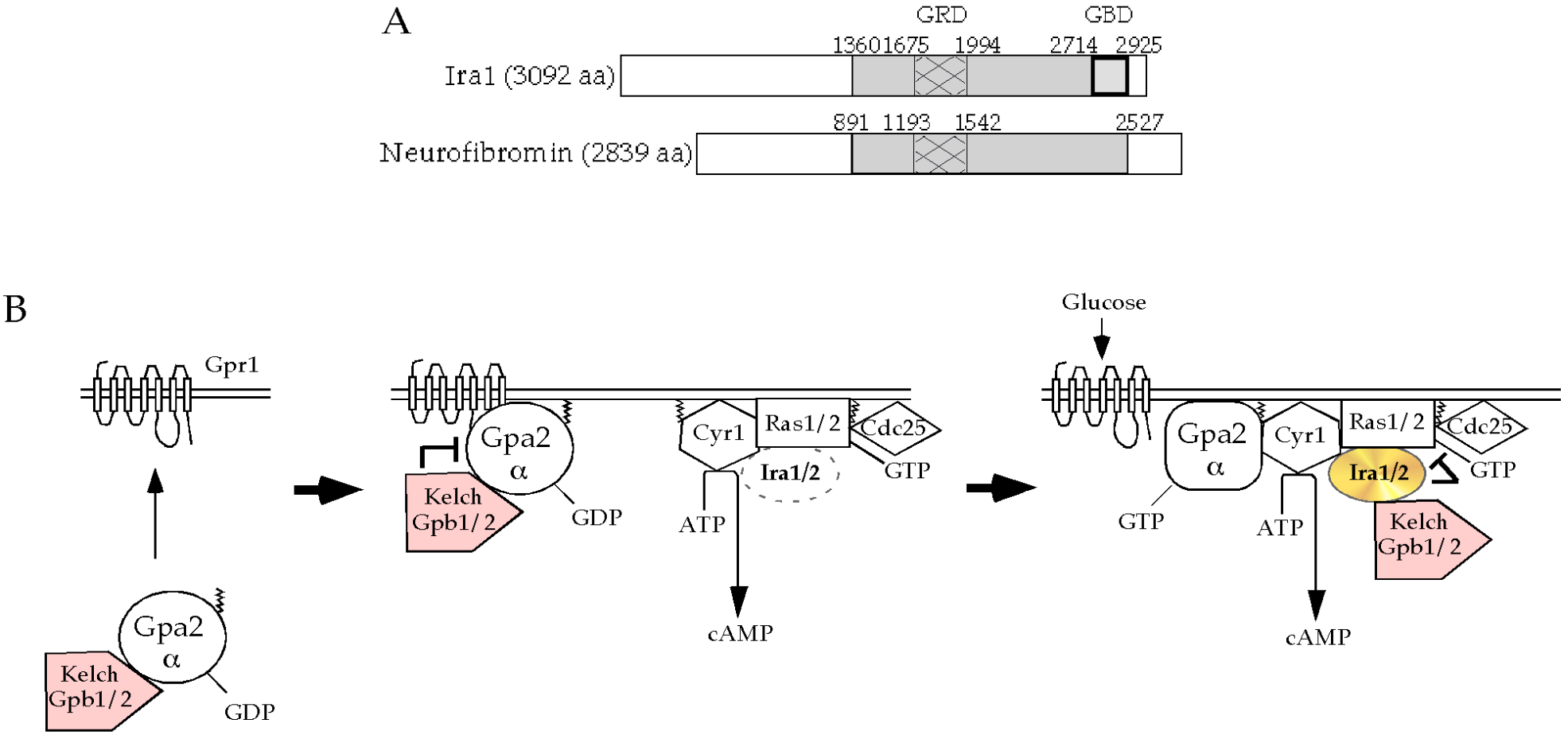


- Gpa2-dependent membrane localization
- Gpb1/2-dependent inhibition of Gpr1-Gpa2 coupling
- Ras-dependent adenylyl cyclase activation
- Gpa2-dependent adenylyl cyclase activation
- Gpb1/2-dependent Ira1/2 stabilization

Figure 8

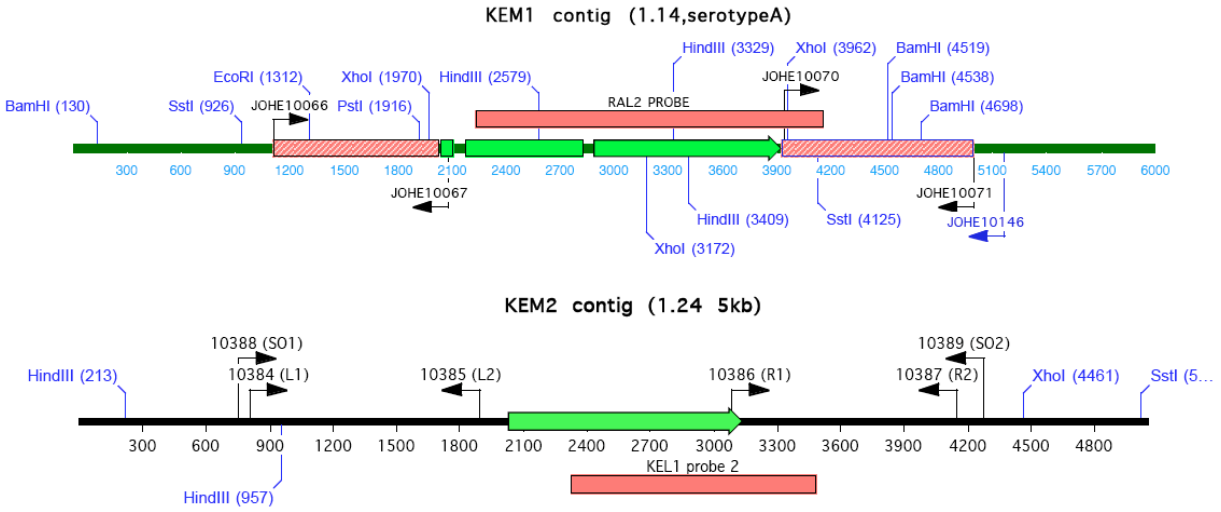
KEM1 contig (1.14,serotypeA)
HindIII (3329)
XhoI (3962)
BamHI (4519)
EcoRI (1312)
XhoI (1970)
HindIII (2579)
JOHE10070
BamHI (4538)
BamHI (130)
SstI (926)
JOHE10066
PstI (1916)
RAL2 PROBE
BamHI (4698)
300 600 900 1200 1500 1800 2100 2400 2700 3000 3300 3600 3900 4200 4500 4800 5100 5400 5700 6000
JOHE10067
JOHE10071
HindIII (3409)
SstI (4125)
JOHE10146
XhoI (3172)
KEM2 contig (1.24 5kb)
10388 (SO1)
10389 (SO2)
HindIII (213)
10384 (L1)
10385 (L2)
10386 (R1)
10387 (R2)
XhoI (4461)
SstI (5...
300 600 900 1200 1500 1800 2100 2400 2700 3000 3300 3600 3900 4200 4500 4800
KEL1 probe 2
HindIII (957)

Figure 9

# *RAL2* disruption

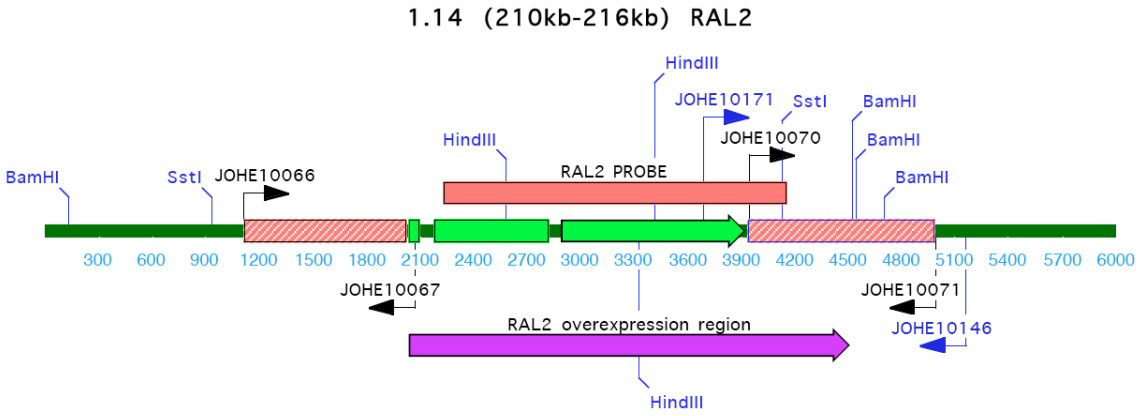

Figure 10

## Southern blot analysis of *RAL2* mutants

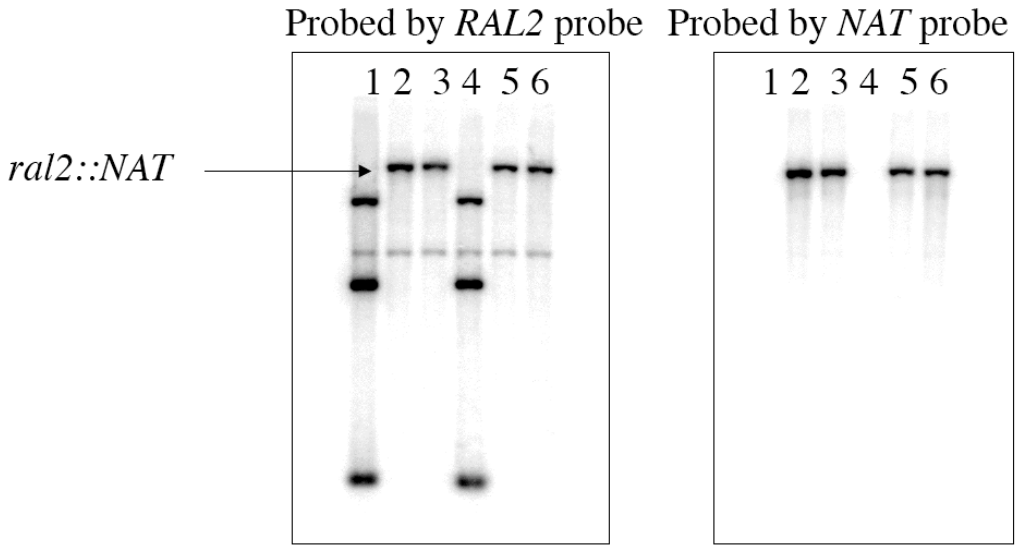


1: WT (H99)
2, 3: *ral2* mutant (H99 background)
4: WT (KN99)
5, 6: *ral2* mutant
(KN99 background

Figure 11

## *RAL2* is not required for melanin production

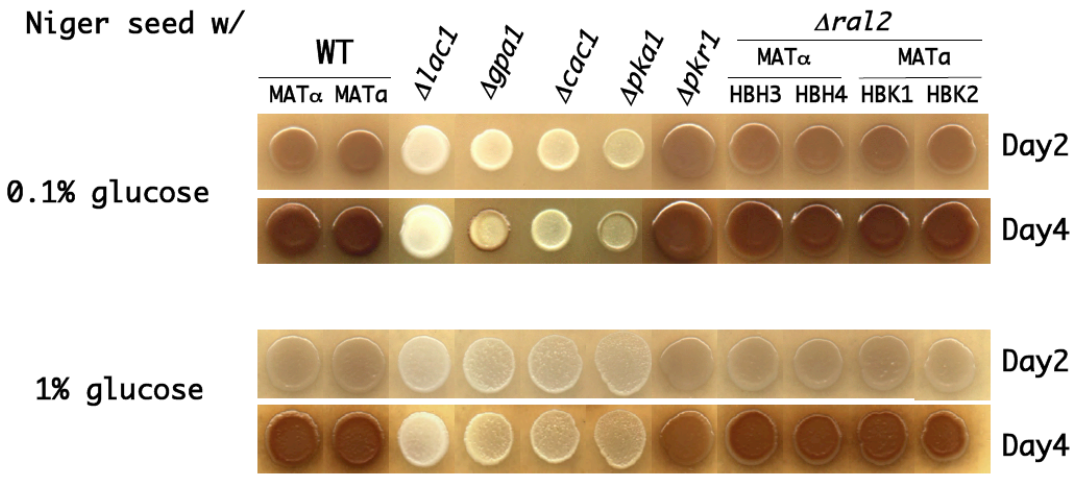


WT MATα; H99 Serotype A
WT MATa; KN99 Serotype A

Figure 12

## *RAL2* is not required for capsule production

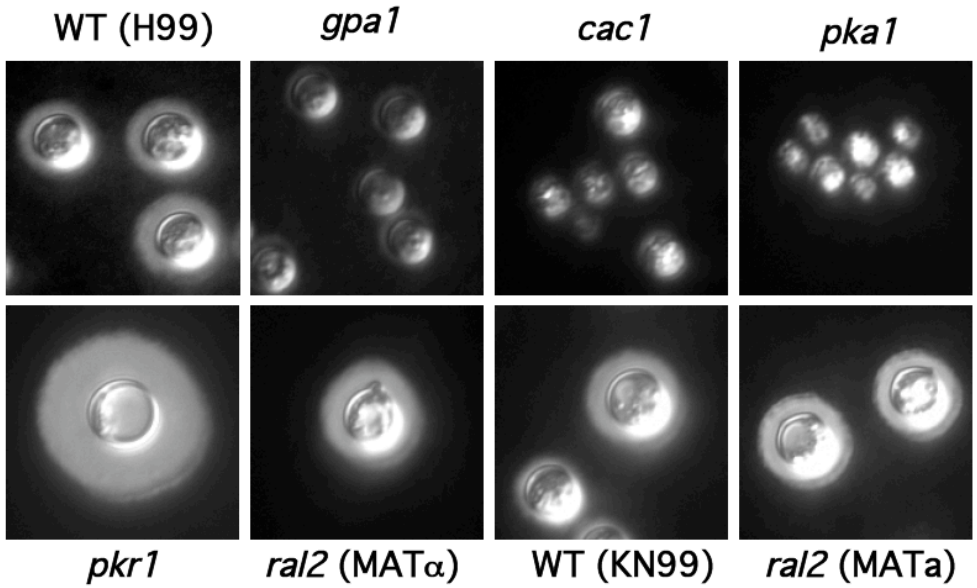

Figure 13

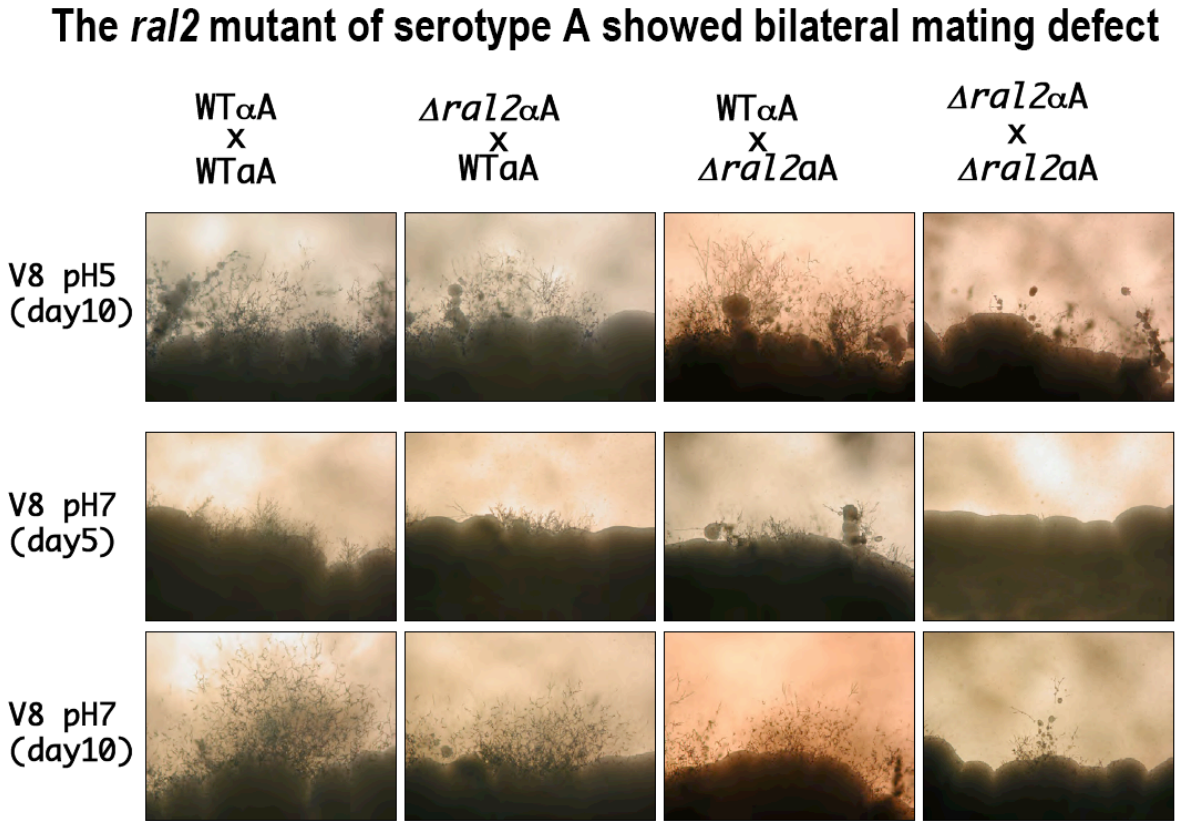
The ral2 mutant of serotype A showed bilateral mating defect
WTαA x WTaA
Δral2αA x WTaA
WTαA x Δral2aA
Δral2αA x Δral2aA
V8 pH5 (day10)
V8 pH7 (day5)
V8 pH7 (day10)

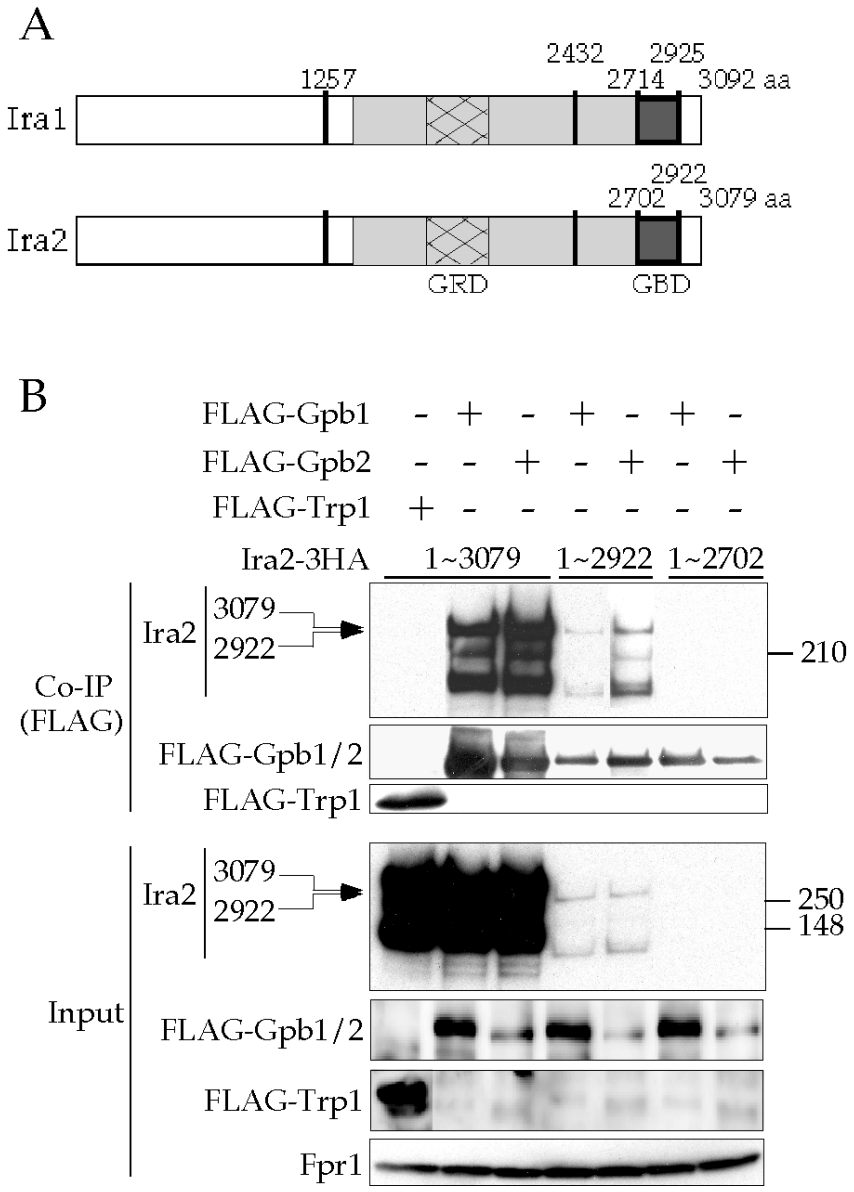
A
Ira1
1257
2432
2925
2714
3092 aa
Ira2
2922
2702
3079 aa
GRD
GBD
B
FLAG-Gpb1 - + - + - + -
FLAG-Gpb2 - - + - + - +
FLAG-Trp1 + - - - - - -
Ira2-3HA 1~3079 1~2922 1~2702
Co-IP (FLAG)
Ira2
3079
2922
210
FLAG-Gpb1/2
FLAG-Trp1
Input
Ira2
3079
2922
250
148
FLAG-Gpb1/2
FLAG-Trp1
Fpr1
C
FLAG-Gpb1 - + -
FLAG-Gpb2 - - +
FLAG-Trp1 + - -
Ira2-3HA 2703~3079
Co-IP (FLAG)
Ira2 (2703~3079)
FLAG-Gpb1/2
FLAG-Trp1
Input
Ira2 (2703~3079)
FLAG-Gpb1/2
FLAG-Trp1
Fpr1
D
FLAG-Gpb1 - + -
FLAG-Gpb2 - - +
FLAG-Trp1 + - -
Ira2-3HA 2703~2922
Co-IP (FLAG)
Ira2 (2703~2922)
FLAG-Gpb1/2
FLAG-Trp1
Input
Ira2 (2703~2922)
FLAG-Gpb1/2
FLAG-Trp1
Fpr1

Molecular Biology of the Cell
Vol. 16, 4557–4571, October 2005

# Gα Subunit Gpa2 Recruits Kelch Repeat Subunits That Inhibit Receptor-G Protein Coupling during cAMP-induced Dimorphic Transitions in *Saccharomyces cerevisiae*

**Toshiaki Harashima* and Joseph Heitman*†**

*Department of Molecular Genetics and Microbiology and †Howard Hughes Medical Institute, Duke University Medical Center, Durham, NC 27710

Submitted May 9, 2005; Revised June 23, 2005; Accepted July 12, 2005
Monitoring Editor: Charles Boone

**All eukaryotic cells sense extracellular stimuli and activate intracellular signaling cascades via G protein-coupled receptors (GPCR) and associated heterotrimeric G proteins. The *Saccharomyces cerevisiae* GPCR Gpr1 and associated Gα subunit Gpa2 sense extracellular carbon sources (including glucose) to govern filamentous growth. In contrast to conventional Gα subunits, Gpa2 forms an atypical G protein complex with the kelch repeat Gβ mimic proteins Gpb1 and Gpb2. Gpb1/2 negatively regulate cAMP signaling by inhibiting Gpa2 and an as yet unidentified target. Here we show that Gpa2 requires lipid modifications of its N-terminus for membrane localization but association with the Gpr1 receptor or Gpb1/2 subunits is dispensable for membrane targeting. Instead, Gpa2 promotes membrane localization of its associated Gβ mimic subunit Gpb2. We also show that the Gpa2 N-terminus binds both to Gpb2 and to the C-terminal tail of the Gpr1 receptor and that Gpb1/2 binding interferes with Gpr1 receptor coupling to Gpa2. Our studies invoke novel mechanisms involving GPCR-G protein modules that may be conserved in multicellular eukaryotes.**

## INTRODUCTION

All eukaryotic cells deploy on their surface signaling modules composed of G protein-coupled receptors (GPCR) and heterotrimeric G proteins to sense extracellular cues. GPCRs are conserved from yeasts to humans and constitute a family of cell surface receptors that contain seven transmembrane domains and sense myriad extracellular ligands including nutrients, odorants, hormones and pheromones, and photons (Gilman, 1987; Strader *et al.*, 1994; Lefkowitz, 2000; Mombaerts, 2004). Heterotrimeric G proteins consist of α, β, and γ subunits, in which the Gα subunits are guanine nucleotide binding proteins and the Gβγ subunits form a membrane-tethered heterodimer (Bourne, 1997; Sprang, 1997; Gautam *et al.*, 1998; Schwindinger and Robishaw, 2001; Cabrera-Vera *et al.*, 2003). Ligand binding triggers conformational changes in the GPCR that stimulate GDP-GTP exchange on Gα and release of the Gβγ dimer. Released Gα-GTP, Gβγ, or both signal downstream effectors. GTP-to-GDP hydrolysis (either intrinsic or RGS protein-stimulated) induces reassociation of the Gα-GDP subunit with Gβγ, extinguishing the signal (De Vries and Gist Farquhar, 1999; Guan and Han, 1999; Ross and Wilkie, 2000).

The yeast *Saccharomyces cerevisiae* expresses 3 GPCRs (Ste2, Ste3, and Gpr1) and 2 Gα subunits (Gpa1 and Gpa2), comprising two signaling modules: one that senses pheromones during mating and the other that senses nutrients and controls filamentous growth (Lengeler *et al.*, 2000; Harashima and Heitman, 2004). *S. cerevisiae* exists in two haploid mating types, **a** and α, which communicate via mating pheromones. **a** haploid cells express **a** pheromone and the GPCR Ste2 to sense extracellular α pheromone. α haploid cells express α pheromone and the GPCR Ste3 that senses **a** pheromone. In both cell types, Ste2 and Ste3 are coupled to the Gα subunit Gpa1, which forms a conventional heterotrimeric G protein with the Gβγ subunits Ste4/18. On pheromone binding to either receptor, GDP-GTP exchange occurs on Gpa1 and the Ste4/18 Gβγ complex dissociates. The liberated Ste4/18 dimer activates the pheromone responsive MAP kinase cascade culminating in mating (for reviews, see Dohlman and Thorner, 2001; Dohlman, 2002; Schwartz and Madhani, 2004).

In contrast to the pheromone GPCRs that are haploid- and mating-type-specific, a distinct GPCR, Gpr1, is expressed in both diploid and haploid cells. The Gpr1 receptor activates cAMP-PKA signaling and governs diploid pseudohyphal differentiation and haploid invasive growth via the coupled Gα subunit Gpa2 (for reviews, see Lengeler *et al.*, 2000; Pan *et al.*, 2000; Gancedo, 2001; Harashima and Heitman 2004). *gpr1* and *gpa2* mutants are defective in both pseudohyphal growth and transient cAMP production in response to glucose (Kübler *et al.*, 1997; Lorenz and Heitman, 1997; Colombo *et al.*, 1998; Yun *et al.*, 1998; Kraakman *et al.*, 1999; Lorenz *et al.*, 2000; Rolland *et al.*, 2000; Tamaki *et al.*, 2000; Lemaire *et al.*, 2004). Recent studies provide evidence that glucose and structurally related sugars serve as ligands for the GPCR Gpr1 (Kraakman *et al.*, 1999; Lorenz *et al.*, 2000; Rolland *et al.*, 2000; Lemaire *et al.*, 2004).

The yeast Gα subunit Gpa2 shares 35–55% identity with other fungal and mammalian Gα subunits, and the predicted secondary structures are highly conserved between Gpa2 and canonical Gα subunits (Harashima and Heitman,

This article was published online ahead of print in *MBC in Press* (http://www.molbiolcell.org/cgi/doi/10.1091/mbc.E05–05–0403) on July 19, 2005.

Address correspondence to: Joseph Heitman (heitm001@duke.edu).

2004). Amino acid residues that confer dominant phenotypes when mutated are also conserved. For instance, a mutation of $Gln^{300}$ to Leu (Q300L) in Gpa2 is analogous to the Gi$\alpha$1 Q204L mutation that abolishes the intrinsic GTPase activity and functions as an activated form of Gpa2 (Harashima and Heitman, 2002). A mutation of $Gly^{299}$ to Ala (Gpa2 G299A) is analogous to Gi$\alpha$1 G203A and G$\alpha$s G226A that fail to undergo the GTP-induced conformational change and thereby serves as a dominant negative allele and interacts with Gpb1/2 and Gpr1 more strongly compared with the wild-type Gpa2 (Lorenz and Heitman 1997; Harashima and Heitman, 2002).

Nevertheless, Gpa2 does not form a heterotrimeric complex with the known yeast G$\beta\gamma$ subunits Ste4/18 (Lorenz *et al.,* 2000; Harashima and Heitman, 2002, 2004). Recent studies identified two novel Gpa2 associated proteins, the kelch proteins Gpb1 and Gpb2, which are functionally redundant and share ~35% identity (Harashima and Heitman, 2002; Batlle *et al.,* 2003). The kelch motif is known to mediate protein-protein interactions (Adams *et al.,* 2000). Gpb1 and Gpb2 each contain seven kelch repeats, which share no sequence homology with the seven WD40 repeats of canonical G$\beta$ subunits. The crystal structure of the kelch repeat enzyme galactose oxidase reveals that the seven kelch repeats can adopt a seven-bladed $\beta$-propeller structure strikingly similar to G$\beta$ subunits (Ito *et al.,* 1991, 1994; Wall *et al.,* 1995; Lambright *et al.,* 1996; Sondek *et al.,* 1996; Adams *et al.,* 2000; Harashima and Heitman, 2002).

*gpb1,2* mutants exhibit enhanced PKA phenotypes, including increased filamentous growth, sensitivity to nitrogen starvation and heat shock, reduced glycogen accumulation, and reduced sporulation (Harashima and Heitman, 2002; Batlle *et al.,* 2003). The *gpb1,2* mutant phenotypes are partially alleviated by *gpa2* mutations and abolished by mutation of the *TPK2* gene that encodes one of the three PKA catalytic subunits. These genetic findings support a model in which the kelch proteins Gpb1/2 negatively regulate the cAMP signaling pathway by inhibiting Gpa2 and an unidentified target that may be an upstream element of the PKA pathway including adenylyl cyclase or its regulator Ras or regulatory proteins of Ras (Harashima and Heitman, 2002).

In contrast to canonical G$\alpha$ subunits, G$\alpha$ Gpa2 has an extended N-terminus (Figure 1). This region shares no homology with known G$\alpha$ subunits, whereas the remainder of Gpa2 shares >60% identity with G$\alpha$ subunits in closely related yeasts and >40% identity with mammalian G$\alpha$ subunits. The N-terminal regions of G$\alpha$ subunits are known to mediate membrane localization and physical interactions with the cognate GPCR and G$\beta\gamma$ dimer (Navon and Fung, 1987; Hamm *et al.,* 1988; Journot *et al.,* 1991; Lambright *et al.,* 1996; Wall *et al.,* 1998; Yamaguchi *et al.,* 2003; Herrmann *et al.,* 2004).

All G$\alpha$ subunits of heterotrimeric G proteins bear N-terminal lipid modifications (myristoylation and palmitoylation) necessary for membrane targeting (for reviews, see Chen and Manning, 2001; Cabrera-Vera *et al.,* 2003). Myristoylation involves the irreversible cotranslational addition of a 14-carbon myristoyl group on glycine at the second position in the consensus sequence MGXXXS and this occurs via an amide linkage after proteolytic removal of the initiating methionine (Johnson *et al.,* 1994; Ashrafi *et al.,* 1998; Farazi *et al.,* 2001). Palmitoylation occurs on all G$\alpha$ subunits with the exception of G$\alpha$t (transducin) and involves posttranslational attachment of a saturated 16-carbon fatty acid, palmitate, via thioester linkage to cysteine residue(s) near the N-terminus. There is no palmitoylation consensus sequence, and palmitoylation is reversible and may be regulated. Both palmitoylation and myristoylation may play roles in addition to membrane localization (Linder *et al.,* 1991; Gallego *et al.,* 1992; Wedegaertner *et al.,* 1993; Wilson and Bourne, 1995; Wise *et al.,* 1997; Morales *et al.,* 1998; Evanko *et al.,* 2000; Fishburn *et al.,* 2000).

*S. cerevisiae* serves as a powerful model to study GPCR-G protein signaling (for reviews, see Jeansonne, 1994; Lengeler *et al.,* 2000; Dohlman and Thorner, 2001; Dohlman, 2002; Harashima and Heitman, 2004). The G$\alpha$ subunit Gpa1 is myristoylated at the $Gly^2$ residue and palmitoylated at the $Cys^3$ residue (Song and Dohlman, 1996; Song *et al.,* 1996). Myristoylation is required for Gpa1 membrane targeting and palmitoylation, yet not for interaction with G$\beta\gamma$ (Song *et al.,* 1996). On the other hand, a Gpa1 palmitoylation-site mutant protein ($Gpa1^{C3A}$) is still partially localized to the plasma membrane, partially functional, and bound to G$\beta\gamma$ (Song and Dohlman, 1996). The G$\beta\gamma$ dimer, the associated GPCR Ste2/3, or components of the Gpa1 mediated MAP kinase cascade are not required for Gpa1 membrane localization (Song and Dohlman, 1996), but the Ste4/18 G$\beta\gamma$ dimer does promote receptor-Gpa1 coupling (Blumer and Thorner, 1990).

The distinct G$\alpha$ subunit Gpa2 forms an unusual protein complex with the atypical binding partner kelch G$\beta$ mimics Gpb1/2 and contains an extended N-terminus. Thus novel regulatory mechanisms may direct Gpa2 to the plasma membrane and enable Gpa2 to function as a molecular switch. Here we show that Gpa2 shares similar characteristics with Gpa1 involving lipid modifications and their function. Gpa2 interacting proteins are dispensable for Gpa2 membrane localization. However, unexpectedly, Gpa2 is required for membrane targeting of the kelch G$\beta$ mimic Gpb2, in striking contrast to conventional heterotrimeric G proteins. Furthermore, the kelch G$\beta$ mimic proteins Gpb1/2 were found to interfere with Gpr1 receptor-G$\alpha$ Gpa2 coupling.

## MATERIALS AND METHODS

### *Strains, Media, and Plasmids*

Media and standard yeast experimental procedures were as described (Sherman, 1991). To express genes heterologously in yeast cells, an attenuated *ADH1* promoter and an *ADH1* terminator from the yeast two-hybrid vector pGBT9 were amplified by fusion PCR using primers, GCTTGCATGCAACTTCTTTT/CGACGGATCCCCGGGAATTCCATCTTTCAGGAGGCTTGCT and AGCAAGCCTCCTGAAAGATGGAATTCCCGGGGATCCGTCG/CGGCATGCCGGTAGAGGTGT, for the 1st round PCR and primers, GCTTGCATGCAACTTCTTTT/CGGCATGCCGGTAGAGGTGT for the second round PCR. The resulting PCR products were blunted with T4 DNA polymerase and cloned into the 2$\mu$ plasmid YEplac195 that was digested with *Hin*dIII and *Eco*RI and then blunted with T4 DNA polymerase to create a yeast expression vector pTH19 (*URA3* 2$\mu$). pTH171 (*LEU2* 2$\mu$), pTH172 (*TRP1* 2$\mu$), and pTH173 (*LYS5* 2$\mu$) are pTH19 derivatives. The nuclear localization signal (NLS) derived from the SV40 T antigen (PPKKKRKVA) was used to direct fusion proteins into the nucleus (Arévalo-Rodríguez and Heitman, 2005). pFA6a-GFP(S65T)-kanMX6 was used as the substrate for PCR to amplify GFP (Longtine *et al.,* 1998). Plasmids and yeast strains used in this study are listed in Tables 1 and 2. Details of plasmids and strains are available upon request.

### *Pseudohyphal and Invasive Growth*

Pseudohyphal and invasive growth assays were investigated as described previously (Harashima and Heitman, 2002).

### *Microscopic Studies*

If not specifically described in figure legends, growth conditions were as follows. For protein localization study, cells were grown in synthetic minimal media to stationary phase and examined for protein localization under a fluorescent microscope (Zeiss Axioskop2 plus, Thornwood, NY) or a confocal microscope (Zeiss LSM 410).

**Table 1.** *S. cerevisiae* strains

| Strain | Genotype | Source/Reference |
|---|---|---|
| Σ1278b congenic strains | | |
| MLY40α | *MATα ura3-52* | Lorenz and Heitman (1997) |
| MLY61a/α | *MAT***a**/α *ura3-52/ura3-52* | Lorenz and Heitman (1997) |
| MLY97a/α | *MAT***a**/α *ura3-52/ura3-52 leu2Δ::hisG/leu2Δ::hisG* | Lorenz and Heitman (1997) |
| MLY132α | *MATα gpa2Δ::G418 ura3-52* | Lorenz and Heitman (1997) |
| MLY132a/α | *MAT***a**/α *gpa2Δ::G418/gpa2Δ::G418 ura3-52/ura3-52* | Lorenz and Heitman (1997) |
| MLY212a/α | *MAT***a**/α *gpa2Δ::G418/gpa2Δ::G418 ura3-52/ura3-52 leu2Δ::hisG/leu2Δ::hisG* | Lorenz and Heitman (1997) |
| MLY232a/α | *MAT***a**/α *gpr1Δ::G418/gpr1Δ::G418 ura3-52/ura3-52* | Lorenz *et al.* (2000) |
| MLY277a/α | *MAT***a**/α *gpa2Δ::G418/gpa2Δ::G418 gpr1Δ::G418/gpr1Δ::G418 ura3-52/ura3-52* | Laboratory stock |
| THY212a/α | *MAT***a**/α *gpb1Δ::hph/gpb1Δ::hph gpb2Δ::G418/gpb2Δ::G418 ura3-52/ura3-52* | Harashima and Heitman (2002) |
| THY224a/α | *MAT***a**/α *gpg1Δ::hph/gpg1Δ::hph ura3-52/ura3-52* | This study |
| THY243a/α | *MAT***a**/α *gpb1Δ::hph/gpb1Δ::hph gpb2Δ::G418/gpb2Δ::G418 gpr1Δ::hph/gpr1Δ::hph ura3-52/ura3-52* | Harashima and Heitman (2002) |
| THY246a/α | *MAT***a**/α *gpb1Δ::hph/gpb1Δ::hph gpb2Δ::G418/gpb2Δ::G418 gpg1Δ::nat/gpg1Δ::nat ura3-52/ura3-52* | Harashima and Heitman (2002) |
| S288C background strains | | |
| S1338 | *MAT***a** *ura3Δ::loxP leu2Δ::loxP trp1Δ::loxP gal2* | Ito-Harashima |
| THY452 | *MAT***a** *ura3Δ::loxP leu2Δ::loxP trp1Δ::loxP lys5Δ::loxP gal2* | This study |

### *Preparation of Crude Cell Extracts and Immunoprecipitation*

Total cell extracts from yeast cells that were grown to midlog phase ($OD_{600} \cong 0.8$) in synthetic dropout media were prepared in lysis buffer (50 mM HEPES, pH 7.6, 120 mM NaCl, 0.3% CHAPS, 1 mM EDTA, 20 mM NaF, 20 mM β-glycerophosphate, 0.1 mM Na-orthovanadate, 0.5 mM dithiothreitol, protease inhibitors (Calbiochem, La Jolla, CA; cocktail IV), and 0.5 mM phenylmethylsulfonyl fluoride) using a bead-beater. After centrifugation (25,000 × *g*, 20 min), crude extracts (2 mg) were mixed with anti-FLAG M2 affinity gel (Sigma, St. Louis, MO) to precipitate FLAG tagged proteins.

### *In Vivo Lipid Modifications*

Cells were grown in 10 ml of SD-Ura medium to $OD_{600}$ = 0.6–0.7, collected, and resuspended into 5 ml of fresh SD-Ura medium. After 10 min, cerulenin was added at a final concentration of 2 μg/ml, and cells were incubated for an additional 15 min under the same conditions. Subsequently, [$^3$H]myristic acid or [$^3$H]palmitic acid was added to the cultures at a final concentration of 50 μCi/ml for myristoylation analysis or 500 μCi/ml for palmitoylation analysis. After 3 h, cells were collected and washed once with $H_2O$ and twice with phosphate-buffered saline. Preparation of crude cell extracts and immunoprecipitation of FLAG tagged proteins were performed as above. The bound FLAG tagged proteins were eluted by boiling for 5 min in SDS-PAGE sample buffer in the presence of β-mercaptoethanol for the myristoylation analysis and in the absence of β-mercaptoethanol for the palmitoylation analysis (Song and Dohlman, 1996). After SDS-PAGE, gels were fixed in $H_2O$/2-propanol/acetic acid (65:25:10 vol/vol/vol) for 30 min and then soaked at room temperature for 18 h either in 1 M hydroxylamine (pH 7.0) to cleave thioester-linked fatty acids or 1 M Tris-HCl (pH 7.0) as a control. The gels were fixed again, treated with Amplify (Amersham, Piscataway, NJ) for 30 min, dried, and then exposed to an x-ray film (BioMax MS film, Eastman Kodak, Rochester, NY) with an intensifying screen (BioMax Transcreen LE, Kodak) at −80°C for 1–2 mo. Expression of the FLAG-tagged proteins was verified by Western blot analysis using anti-FLAG M2 antibody (Sigma).

### *cAMP Assay*

cAMP assay was as described in Lorenz *et al.* (2000) with some modifications. Briefly, at the time points indicated, 0.5 ml of cell suspension was transferred into a microfuge tube containing 0.5 ml of 10% ice-cold trichloroacetic acid and was immediately frozen in liquid nitrogen. To prepare intracellular cAMP, cells were permeabilized by defrosting at 4°C overnight. Cell extracts were neutralized by ether extraction and lyophilized. Intracellular cAMP levels were determined by using a cAMP enzyme immunoassay kit (Amersham).

## RESULTS

### *Gα Subunit Gpa2 Is Myristoylated and Palmitoylated*

The Gα protein Gpa2 is coupled to the GPCR Gpr1 and signals to activate the downstream effector adenylyl cyclase in response to glucose. Based on analogy to other GPCR-Gα systems, we hypothesized that Gpa2 would be localized to the cell membrane for function. To address this, Gpa2 was fused to green fluorescent protein (GFP). To avoid perturbing protein localization or receptor coupling sequences typically linked to the amino and carboxy terminal regions of Gα proteins (Figure 1A), GFP was fused between the first 10 amino acids (1–10) of Gpa2 and the remainder of the protein (amino acids 4–449) to produce a Gpa2$^{1-10}$-GFP-Gpa2$^{4-449}$ internal fusion protein. This Gpa2-GFP fusion protein was functional based on its ability to complement the pseudohyphal defect of *gpa2* mutant cells (unpublished data). As shown in Figure 2A, the Gpa2-GFP fusion protein was localized to the cell membrane. A C-terminally GFP tagged Gpa2 protein was nonfunctional (unpublished data), in accord with the known role of the Gα C-terminal domain in receptor coupling (Slessareva *et al.*, 2003; Herrmann *et al.*, 2004).

To establish the minimal Gpa2 domain required for membrane localization, the first 10 (Gpa2$^{1-10}$), 20 (Gpa2$^{1-20}$), or 30 (Gpa2$^{1-30}$) amino acids of Gpa2 were fused to a GFP cassette and expressed in vivo. All three C-terminally tagged Gpa2-GFP proteins were localized to the plasma membrane (Figure 2A). Therefore, as few as the first 10 amino acids of Gpa2 suffice for plasma membrane targeting.

In conventional Gα subunits, lipid modifications of the N-terminus mediate membrane localization (Chen and Manning, 2001). Myristoylation occurs at Gly$^2$ in the myristoylation consensus sequence G$^2$XXXS$^6$ (Johnson *et al.*, 1994). Palmitoylation can occur at any cysteine residue near the N-terminus. Gpa2 contains glycine and serine in the second and sixth positions for myristoylation and cysteine at the fourth position from the N-terminus. To examine whether these sites are lipid modified, a Gpa2$^{1-20}$-GFP-FLAG protein in which the first 20 amino acids of Gpa2 were fused to a GFP-FLAG cassette was expressed in yeast cells and assessed for lipid modifications. Gpa2$^{1-20}$-GFP-FLAG variants containing mutations in the potential lipid modification sites (G2A, C4A, or S6Y) were also analyzed.

As a positive control for lipid modification experiments, an equivalent Gpa1$^{1-20}$-GFP-FLAG protein was constructed,

**Table 2.** Plasmids

| Plasmid | Description | Source/Reference |
|---|---|---|
| pTH19 | $P_{ADH1}$ *URA3* 2μ | This study |
| pTH26 | $P_{ADH1}$-*GPB1 URA3* 2μ (pTH19) | This study |
| pTH27 | $P_{ADH1}$-*GPB2 URA3* 2μ (pTH19) | This study |
| pTH47 | $P_{ADH1}$-*GPA2 URA3* 2μ (pTH19) | This study |
| pTH48 | $P_{ADH1}$-$GPA2^{Q300L}$ *URA3* 2μ (pTH19) | This study |
| pTH49 | $P_{ADH1}$-$GPA2^{G299A}$ *URA3* 2μ (pTH19) | This study |
| pTH62 | $P_{ADH1}$-$GPA2^{G2A}$ *URA3* 2μ (pTH19) | This study |
| pTH65 | $P_{ADH1}$-$GPA2^{1–30\ aa}$::*GFP URA3* 2μ (pTH19) | This study |
| pTH68 | $P_{ADH1}$-$GPA2^{C4A}$ *URA3* 2μ (pTH19) | This study |
| pTH69 | $P_{ADH1}$-$GPA2^{S6Y}$ *URA3* 2μ (pTH19) | This study |
| pTH71 | $P_{ADH1}$-$GPA2^{1–10\ aa}$::*GFP URA3* 2μ (pTH19) | This study |
| pTH73 | $P_{ADH1}$-*GFP URA3* 2μ (pTH19) | This study |
| pTH75 | $P_{ADH1}$-*GFP-GPB2 URA3* 2μ (pTH19) | This study |
| pTH80 | $P_{ADH1}$-$GPA2^{1–10}$::*GFP*::$GPA2^{4–449}$ *URA3* 2μ (pTH19) | This study |
| pTH81 | $P_{ADH1}$-$GPA2^{1–20\ aa}$::*GFP-FLAG URA3* 2μ (pTH19) | This study |
| pTH84 | $P_{ADH1}$-*GFP-GPB2 LEU2* 2μ (pTH171) | This study |
| pTH91 | $P_{ADH1}$-$GPA2^{1–20\ aa\ G2A}$::*GFP-FLAG URA3* 2μ (pTH19) | This study |
| pTH92 | $P_{ADH1}$-$GPA2^{1–20\ aa\ C4A}$::*GFP-FLAG URA3* 2μ (pTH19) | This study |
| pTH93 | $P_{ADH1}$-$GPA2^{1–20\ aa\ S6Y}$::*GFP-FLAG URA3* 2μ (pTH19) | This study |
| pTH100 | $P_{ADH1}$- *GFP-FLAG URA3* 2μ (pTH19) | This study |
| pTH103 | $P_{ADH1}$-$GPA1^{1–20\ aa}$::*GFP-FLAG URA3* 2μ (pTH19) | This study |
| pTH106 | $P_{ADH1}$-*GFP-GPB1 URA3* 2μ (pTH19) | This study |
| pTH114 | $P_{ADH1}$-*GPB2 LEU2* 2μ (pTH171) | This study |
| pTH127 | $P_{ADH1}$-$GPA1^{1–10}$-$GPA2^{\Delta 1–100}$ *URA3* 2μ (pTH19) | This study |
| pTH128 | $P_{ADH1}$-$GPA1^{1–10}$-$GPA2^{\Delta 1–100\ G299A}$ *URA3* 2μ (pTH19) | This study |
| pTH130 | $P_{ADH1}$-$GPA2^{\Delta\alpha\ (51–57)\ G299A}$ *URA3* 2μ (pTH19) | This study |
| pTH133 | $P_{ADH1}$-$GPA2^{\Delta\alpha\ (51–57)}$ *URA3* 2μ (pTH19) | This study |
| pTH134 | $P_{ADH1}$-$GPA1^{1–10}$-$GPA2^{\Delta 1–29\ G299A}$ *URA3* 2μ (pTH19) | This study |
| pTH136 | $P_{ADH1}$-$GPA2^{\Delta 16–84\ G299A}$ *URA3* 2μ (pTH19) | This study |
| pTH144 | $P_{ADH1}$-$GPA1^{1–10}$-$GPA2^{\Delta 1–14\ G299A}$ *URA3* 2μ (pTH19) | This study |
| pTH145 | $P_{ADH1}$-$GPA2^{\Delta 46–84\ G299A}$ *URA3* 2μ (pTH19) | This study |
| pTH149 | $P_{ADH1}$-$GPA2^{G2A}$-*NLS URA3* 2μ (pTH19) | This study |
| pTH155 | $P_{ADH1}$-$GPA2^{\Delta 46–100}$ *URA3* 2μ (pTH19) | This study |
| pTH157 | $P_{ADH1}$-$GPA1^{1–10}$-$GPA2^{\Delta 1–29}$ *URA3* 2μ (pTH19) | This study |
| pTH158 | $P_{ADH1}$-$GPA2^{\Delta 46–84}$ *URA3* 2μ (pTH19) | This study |
| pTH159 | $P_{ADH1}$-$GPA2^{\Delta 31–84\ G299A}$ *URA3* 2μ (pTH19) | This study |
| pTH160 | $P_{ADH1}$-$GPA2^{\Delta 31–84}$ *URA3* 2μ (pTH19) | This study |
| pTH161 | $P_{ADH1}$-$GPA2^{\Delta 16–84}$ *URA3* 2μ (pTH19) | This study |
| pTH163 | $P_{ADH1}$-*MLS-GFP-GPB2 URA3* 2μ (pTH19) | This study |
| pTH164 | $P_{ADH1}$-*MLS-GFP-GPB1 URA3* 2μ (pTH19) | This study |
| pTH166 | $P_{ADH1}$-*NLS-GFP-GPB2 URA3* 2μ (pTH19) | This study |
| pTH167 | $P_{ADH1}$-*NLS-GFP-GPB1 URA3* 2μ (pTH19) | This study |
| pTH168 | $P_{ADH1}$-$GPA2^{\Delta 46–100\ G299A}$ *URA3* 2μ (pTH19) | This study |
| pTH169 | $P_{ADH1}$-$GPA1^{1–10}$-$GPA2^{\Delta 1–14}$ *URA3* 2μ (pTH19) | This study |
| pTH170 | $P_{ADH1}$-*GFP-GPR1C TRP1* 2μ (pTH172) | This study |
| pTH171 | $P_{ADH1}$ *LEU2* 2μ | This study |
| pTH172 | $P_{ADH1}$ *TRP1* 2μ | This study |
| pTH173 | $P_{ADH1}$ *LYS5* 2μ | This study |
| pTH174 | $P_{ADH1}$-*GPB1 LYS5* 2μ (pTH173) | This study |
| pTH178 | $P_{ADH1}$-$GPA2^{\Delta 46–449}$ *URA3* 2μ (pTH19) | This study |
| pTH191 | $P_{ADH1}$-$GPA1^{1–10}$-$GPA2^{\Delta 1–44}$ *URA3* 2μ (pTH19) | This study |
| pTH192 | $P_{ADH1}$-$GPA1^{1–10}$-$GPA2^{\Delta 1–44\ G299A}$ *URA3* 2μ (pTH19) | This study |

which was derived from the Gpa1 Gα subunit coupled to the Ste2/3 pheromone receptors (Figure 2B). Gpa1 is known to be myristoylated at the second position on glycine ($Gly^2$) and palmitoylated on cysteine in the third position ($Cys^3$) (Song and Dohlman, 1996; Song *et al.*, 1996). Gpa1 myristoylation is essential for membrane localization and function and required for palmitoylation, and palmitoylation also promotes membrane localization and function. In addition, the first 9 amino acids of Gpa1 suffice for membrane localization of a Gpa1-GST fusion protein (Gillen *et al.*, 1998).

As shown in Figure 2B, the wild-type Gpa2 fusion protein was myristoylated and the myristoylation site and myristoylation consensus sequence mutant proteins, $Gpa2^{G2A}$ and $Gpa2^{S6Y}$, were not, suggesting that Gpa2 is subject to myristoylation at $Gly^2$. Gpa2 was also palmitoylated and a mutation in the putative palmitoylation site ($Gpa2^{C4A}$) abolished this modification (Figure 2C). Therefore, Gpa2 is also subject to palmitoylation at $Cys^4$. We note that the $Gpa2^{C4A}$ fusion protein exhibited a decreased level of myristoylation compared with the wild-type protein. Interestingly, reduced myristoylation was also observed with the $Gpa1^{C3S}$ mutant (Song and Dohlman, 1996). These results are indicative of either a sequence preference in the myristoylation consensus sequence ($G^2XXXS^6$) or a role for palmitoylation in promoting myristoylation or its maintenance.

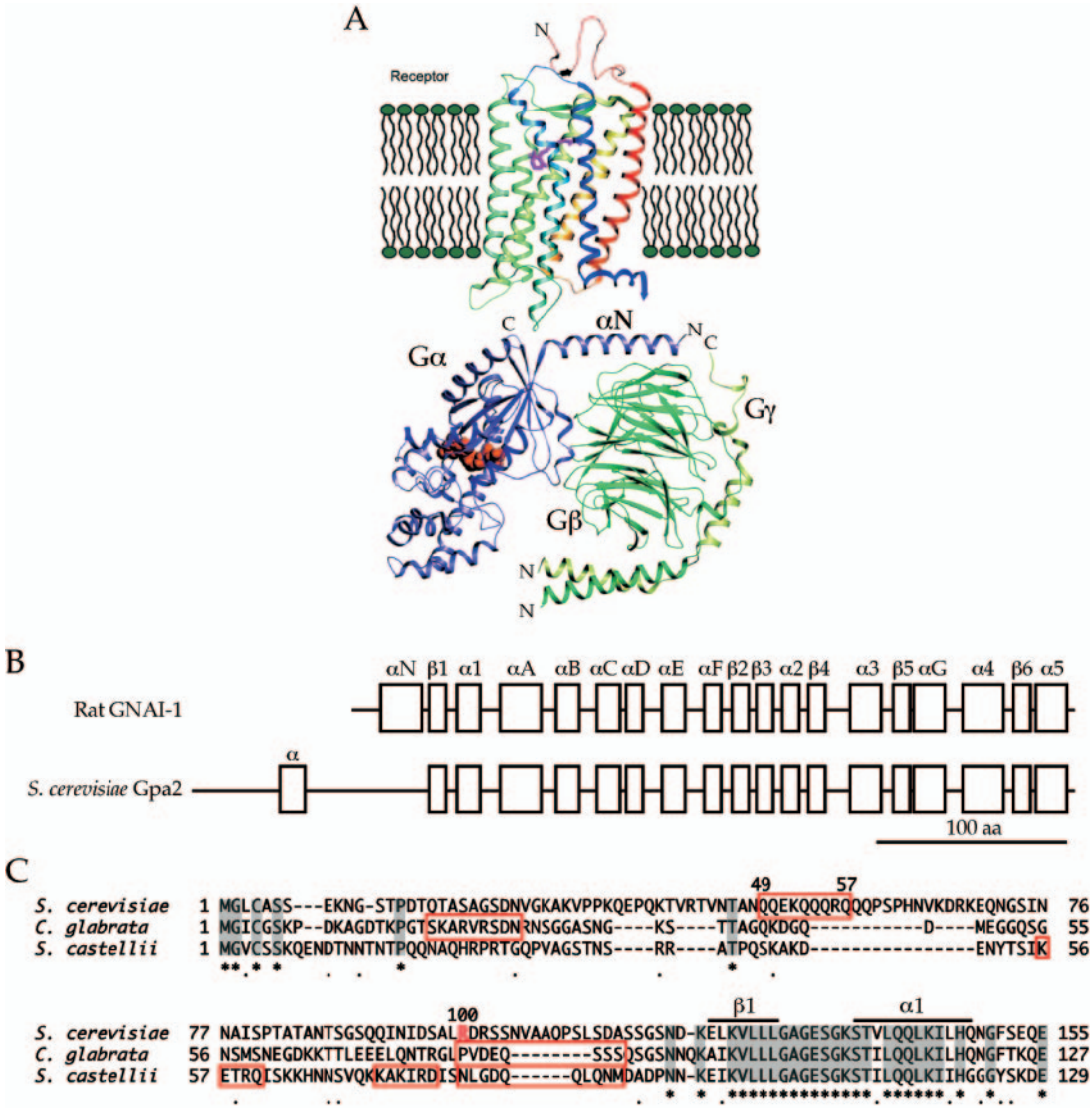


**Figure 1.** N-terminal alpha helix of Gα subunits (αN domain) is involved in receptor and Gβγ dimer coupling. (A) The αN domain provides one of the binding interfaces between Gα and Gβ and the receptor. This image shows a hypothetical model (PDB file 1BOK) for a GPCR-G protein module (GPCR; Rhodopsin, PDB file 1F88, G protein; PDB file 1GOT). The αN domain of the Gα subunit that is required for Gβ subunit and receptor coupling is shown (modified from Cabrera-Vera *et al.*, 2003). (B) The predicted secondary structures of the conventional rat Gαi subunit and the yeast Gα Gpa2 protein based on PHD (Rost *et al.*, 1993). Gpa2 shares 34% identity with the rat Gαi subunit and the predicted secondary structure is highly conserved between the two, except for the extended Gpa2 N-terminus. Secondary structure assignments were based on those of $G_{\alpha t/\alpha I}$ (Lambright *et al.*, 1996). (C) An alignment of the amino acid sequence of the N-terminus of Gpa2 homologues from *S. cerevisiae* and the related yeasts *C. glabrata* and *S. castellii*. *C. glabrata* and *S. castellii* express homologues of the *S. cerevisiae* GPCR Gpr1 and Gβ mimic Gpb1/2 proteins as well as a Gpa2 homologue, yet the N-termini of their Gpa2 homologues share no significant homology. Amino acids forming a potential alpha helix in the N-termini are indicated by red rectangles. Identical amino acids are marked (*) and shaded in gray, and conserved amino acids are also indicated (●). The 100th amino acid (R) of Gpa2 is shown in red. The β1 and α1 domains assigned in Figure 1B are shown. Alignments were obtained using Clustal W (Thompson *et al.*, 1994).

Similar to Gpa1, Gpa2 requires myristoylation for palmitoylation because the G2A and S6Y mutations, which abolish myristoylation, also blocked palmitoylation. Consistent with these results, the Gpa2-GFP-FLAG proteins bearing the G2A, C4A, or S6Y mutations failed to localize to the plasma membrane, and thus myristoylation and palmitoylation are required for Gpa2 plasma membrane localization (Figure 2A).

To address the physiological roles of these lipid modifications, the G2A, C4A, and S6Y mutations were introduced into the *GPA2* gene and expressed in a Σ1278b *gpa2/gpa2* diploid or *gpa2* haploid mutant strain. As shown in Figure 2, D and E, the $GPA2^{G2A}$ myristoylation site mutant failed to complement either the pseudohyphal or the invasive growth defects. The $GPA2^{S6Y}$ and $GPA2^{C4A}$ myristoylation consensus sequence or palmitoylation site mutants showed severe defects in both assays. Furthermore, introduction of a dominant active mutation (Q300L) that abolishes Gpa2 GTPase activity failed to restore activity of the $GPA2^{G2A}$ mutant protein ($Gpa2^{G2A,\ Q300L}$, unpublished data). Thus, myristoylation and palmitoylation both play critical roles in Gpa2 membrane localization and signaling. Importantly, the unusual Gα subunit Gpa2 shares common features with the

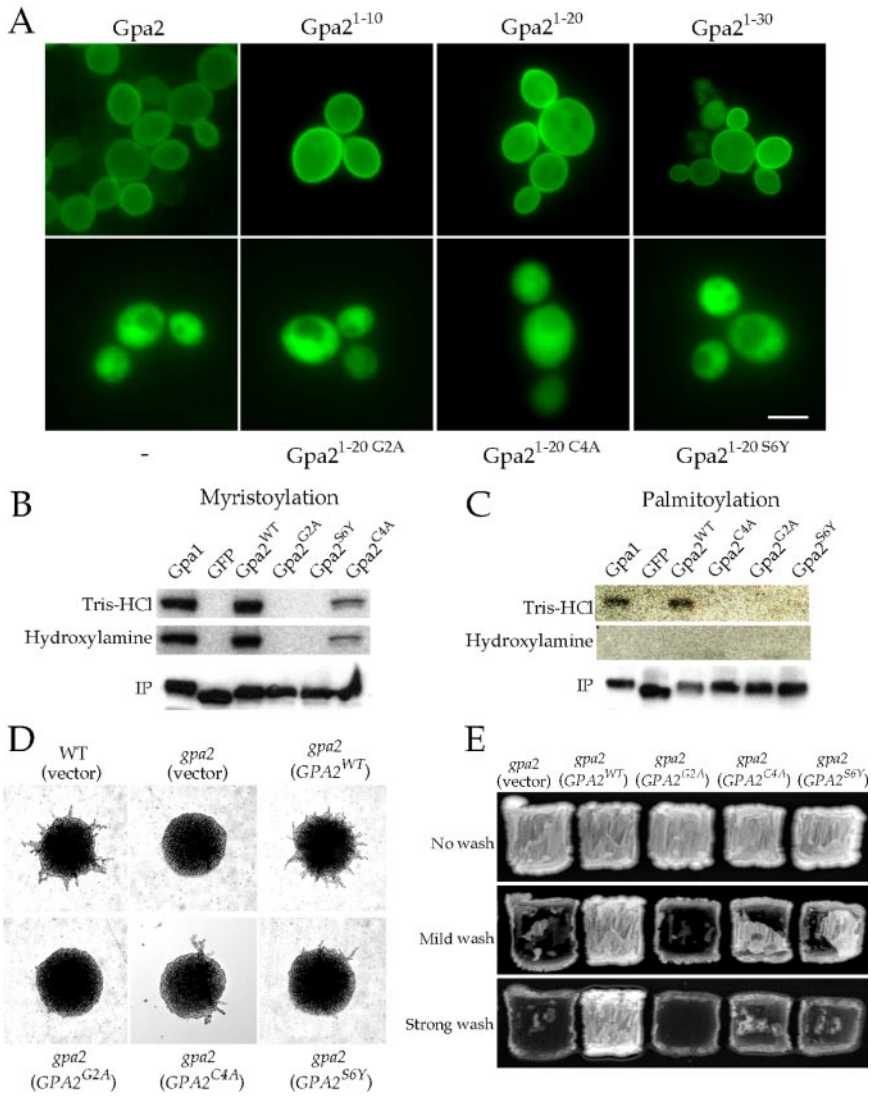


**Figure 2.** Myristoylation and palmitoylation are required for membrane localization and function of the Gα subunit Gpa2. (A) The first 10 amino acids from Gpa2 are sufficient for membrane localization. A functionally, internally GFP-tagged Gpa2 (Gpa2, pTH80), truncated GFP-tagged Gpa2 proteins, $Gpa2^{1–10}$-GFP ($Gpa2^{1–10}$, pTH71), $Gpa2^{1–20}$-GFP-FLAG ($Gpa2^{1–20}$, pTH81), and $Gpa2^{1–30}$-GFP ($Gpa2^{1–30}$, pTH65), or mutant truncated GFP-tagged Gpa2 proteins, $Gpa2^{1–20\ G2A}$-GFP-FLAG ($Gpa2^{1–20\ G2A}$, pTH91), $Gpa2^{1–20\ C4A}$-GFP-FLAG ($Gpa2^{1–20\ C4A}$, pTH92), and $Gpa2^{1–20\ S6Y}$-GFP-FLAG ($Gpa2^{1–20\ S6Y}$, pTH93), were expressed from a 2μ plasmid in wild-type yeast cells (MLY61a/α) to test for protein localization. The GFP cassette alone (−, pTH73) was also expressed as a control. Scale bar, 5 μm. (B and C) Gpa2 is myristoylated (B) and palmitoylated (C). *gpa2* mutant cells (MLY132a/α) expressing the $Gpa2^{1–20}$-GFP-FLAG ($Gpa2^{WT}$, pTH81), $Gpa2^{1–20\ G2A}$-GFP-FLAG ($Gpa2^{G2A}$, pTH91), $Gpa2^{1–20\ S6Y}$-GFP-FLAG ($Gpa2^{S6Y}$, pTH93), $Gpa2^{1–20\ C4A}$-GFP-FLAG ($Gpa2^{C4A}$, pTH92), GFP-FLAG (GFP, pTH100), or $Gpa1^{1–20}$-GFP-FLAG (Gpa1, pTH103) proteins were metabolically labeled with [$^3$H]myristic acid or [$^3$H]palmitic acid. FLAG-tagged proteins were purified using anti-FLAG affinity gel and subjected to SDS-PAGE. Gels were treated with 1 M Tris-HCl, 1 M hydroxylamine that cleaves the palmitoyl moiety of fatty acids, or subjected to Western blot using an anti-FLAG antibody to verify purified protein levels. Radiolabeled purified proteins were visualized by autoradiography. (D and E) Myristoylation and palmitoylation are required for Gpa2 function. Full-length wild-type ($Gpa2^{WT}$, pTH47) or mutant Gpa2 proteins ($Gpa2^{G2A}$ (pTH62), $Gpa2^{C4A}$ (pTH68), and $Gpa2^{S6Y}$ (pTH69)) were expressed in *gpa2* mutant cells (MLY132a/α or MLY132α) to test for diploid filamentous growth (D) and haploid invasive growth (E). *gpa2* mutant cells containing an empty plasmid (pTH19) served as control.

conventional Gα subunit Gpa1 with respect to lipid modifications and their physiological roles.

### *Gpa2 Binding Partners Are Not Required for Gpa2 Membrane Localization*

In heterotrimeric G proteins, Gβγ subunits can promote membrane localization of their associated Gα subunits. Therefore, the localization of Gpa2 was examined in the absence of Gpb1/2 or when Gpb1/2 were overexpressed. As shown in Figure 3, A and B, Gpa2 membrane localization was unchanged under both conditions. Furthermore, deletion of other known Gpa2 associated proteins, namely the GPCR Gpr1 or the Gγ subunit mimic Gpg1, or even the elimination of multiple binding partners (Gpb1/2 and Gpr1 or Gpb1/2 and Gpg1), did not perturb Gpa2 plasma membrane localization, suggesting these binding partners are not required for membrane targeting (Figure 3A).

Because Gpa2 is a component of the glucose sensing cAMP signaling pathway and the agonist induced redistribution of Gαs has been reported in mammalian cells (Wedegaertner *et al.*, 1996; Thiyagarajan *et al.*, 2002), we examined if carbon source affects Gpa2 protein localization (Figure 3C). Glucose serves as a ligand for Gpr1 (Yun *et al.*, 1998; Kraakman *et al.*, 1999; Lorenz *et al.*, 2000; Rolland *et al.*, 2000; Lemaire *et al.*, 2004). Glucose, fructose, and galactose are structurally related hexoses, yet galactose is not a ligand for Gpr1 (Lorenz *et al.*, 2000; Lemaire *et al.*, 2004). Fructose is controversial, although fructose can induce cAMP production when added to glucose-starved cells (Yun *et al.*, 1998; Lemaire *et al.*, 2004). Maltose and galactose induce filamentous growth in a Gpr1-Gpa2-independent manner (Lorenz *et al.*, 2000). Ethanol and glycerol are structurally unrelated nonfermentable carbon sources. As shown in Figure 3C, Gpa2 was localized to the plasma membrane to the same extent under all conditions tested. Therefore, the carbon sources examined do not influence Gpa2 protein localization and Gpa2 is localized to the cell membrane irrespective of activity of the Gpr1-Gpa2 signaling pathway.

### *Kelch Gβ Mimic Gpb2 Is Recruited to the Plasma Membrane by Gpa2*

If the kelch proteins Gpb1/2 function as Gβ mimics, we hypothesized that Gpb1/2 should also be membrane localized. To examine protein localization, a functional GFP-Gpb2 protein was expressed in *gpa2*Δ cells (Figure 4). When GFP-Gpb2 was expressed alone, Gpb2 was found to be

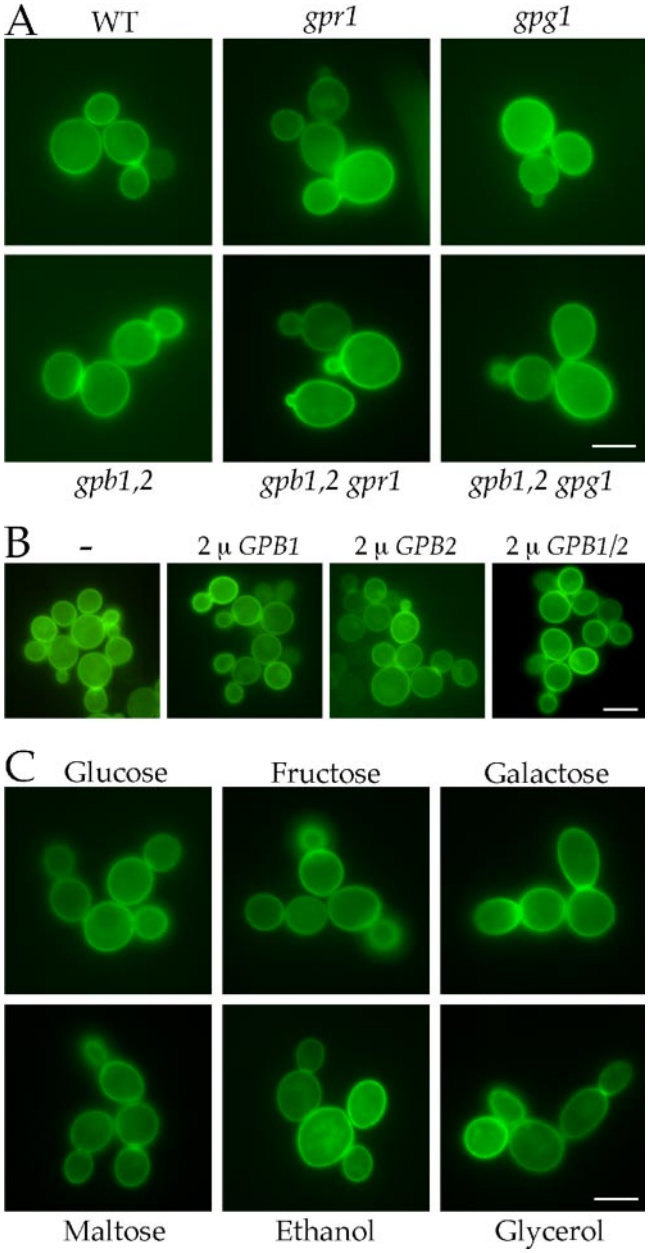


**Figure 3.** The Gα subunit Gpa2 is localized to the plasma membrane independent of its known binding partners. (A) Gpa2-GFP protein (pTH80) was expressed in *gpr1* (MLY232a/α), *gpg1* (THY224a/α), *gpb1,2* (THY212a/α), *gpb1,2 gpr1* (THY243a/α), and *gpb1,2 gpg1* (THY246a/α) mutant cells and protein localization was analyzed. (B) Overexpression of the kelch Gβ mimic proteins Gpb1/2 has no effect on Gpa2 membrane localization. The Gpa2-GFP protein was coexpressed with Gpb1 (pTH26), Gpb2 (pTH27), or both (pTH26 and pTH114) in wild-type cells (MLY97a/α). (C) Membrane localization of Gpa2 was not altered by carbon sources. *gpa2* mutant cells (MLY132a/α) expressing the Gpa2-GFP protein were grown in synthetic media containing different carbon sources and Gpa2 protein localization was assessed. Scale bars, 5 μm.

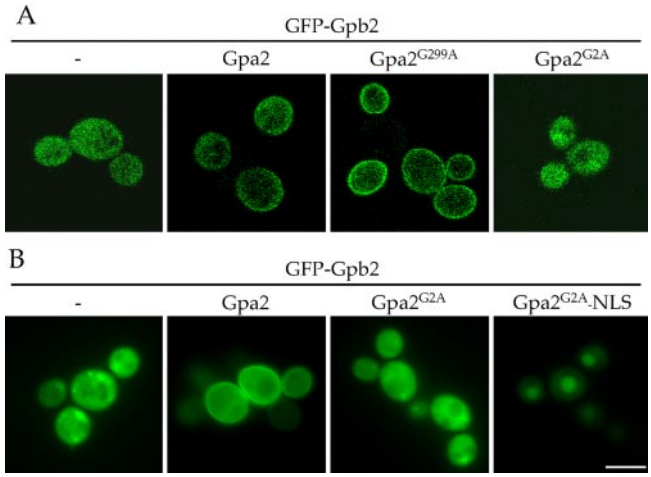


**Figure 4.** Gα subunit Gpa2 recruits the kelch Gβ subunit mimic Gpb2 to the plasma membrane. (A) A functional GFP-Gpb2 protein (pTH84) was coexpressed with Gpa2 (pTH47), $Gpa2^{G299A}$ (pTH49), $Gpa2^{G2A}$ (pTH62), or $Gpa2^{G2A}$-NLS (pTH149) proteins in *gpa2*Δ mutant cells (MLY212a/α), and protein localization was investigated by confocal (A) or direct fluorescence microscopy (B). The empty vector pTH19 (−) served as control. Nuclear localization was confirmed by DAPI staining (unpublished data). Scale bar, 5 μm.

cytoplasmic. However, when GFP-Gpb2 was coexpressed with either wild-type Gpa2 or a dominant negative Gpa2 ($Gpa2^{G299A}$), GFP-Gpb2 was directed to the plasma membrane (Figure 4). Confocal microscopic analysis revealed that Gpb2 was localized to the plasma membrane more extensively when coexpressed with the $Gpa2^{G299A}$ mutant protein that is unable to undergo the GTP-induced conformational change when compared with wild-type Gpa2 (Figure 4A). This finding is in accord with previous data showing that Gpb2 binds to Gpa2 in vivo and preferentially associates with Gpa2-GDP (Harashima and Heitman, 2002).

When GFP-Gpb2 was coexpressed with the nonfunctional $Gpa2^{G2A}$ mutant that is no longer directed to the plasma membrane, GFP-Gpb2 was no longer localized to the plasma membrane (Figure 4). To exclude the possibility that the observed Gpb2 membrane localization is an indirect secondary consequence due to overexpression of the functional wild-type Gpa2 protein, GFP-Gpb2 was coexpressed with a nuclear localization signal (NLS) containing $Gpa2^{G2A}$ mutant protein ($Gpa2^{G2A}$-NLS). Strikingly, $Gpa2^{G2A}$-NLS now misdirected Gpb2 to the nucleus (Figure 4B). Therefore, the Gα protein Gpa2 forms a stable complex with the kelch Gβ mimic protein Gpb2 and serves to recruit Gpb2 to the plasma membrane. That $Gpa2^{G2A}$-NLS directs Gpb2 to the nucleus also demonstrates that lipid modifications are not required for the Gpa2-Gpb2 interaction. This is consistent with findings regarding interaction of the yeast Gα subunit Gpa1 and the mammalian Gα subunit Gαi with their respective Gβ subunits (Jones *et al.*, 1990; Song *et al.*, 1996).

### *Kelch Gβ Mimic Gpb2 and the C-terminal Tail of the Gpr1 Receptor Bind to the N-terminal Region of Gpa2*

In canonical Gα subunits, an N-terminal alpha helix called the αN domain provides a binding surface for the Gβ subunit and the coupled receptor (Lambright *et al.*, 1996; Wall *et al.*, 1998). Because the αN domain is less conserved among Gα subunits, we searched for any related alpha helical domain in the extended N-terminus of Gpa2 using the PHD secondary structure prediction method (Rost and Sander, 1993). A sequence spanning amino acid residues 49–57 was identified that is predicted to form an alpha helix, although this region does not share any significant identity with known αN domains (Figure 1).

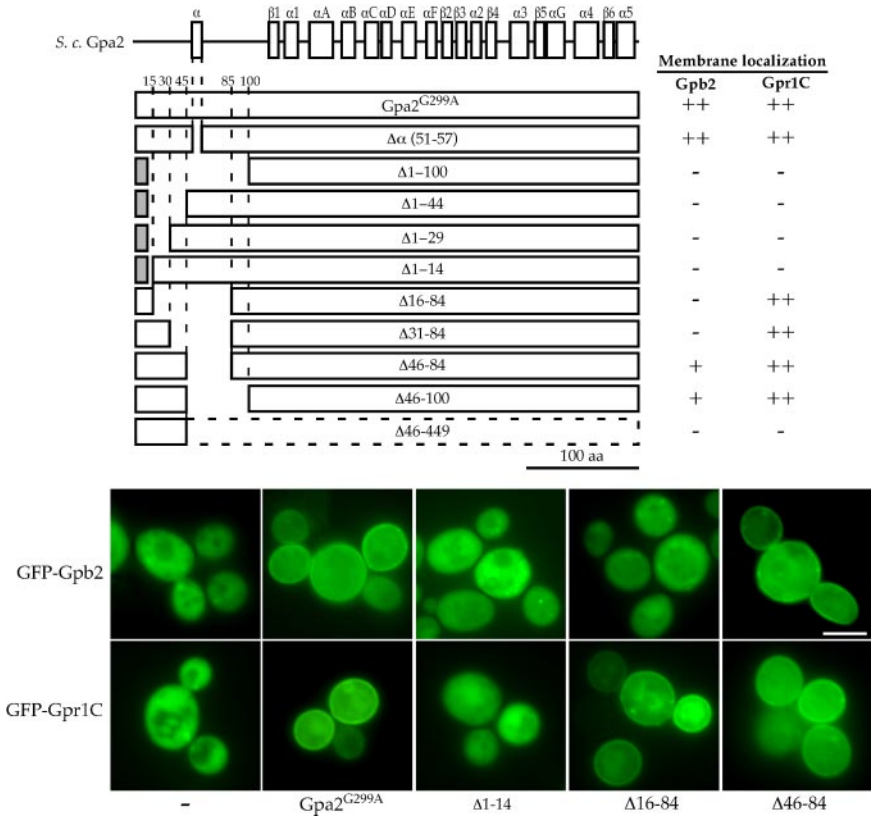


**Figure 5.** N-terminus of Gα Gpa2 is required for binding to the kelch protein Gpb2 and the GPCR Gpr1. A series of deletions was created in the N-terminal region of $Gpa2^{G299A}$, and these deletion constructs were coexpressed with the GFP-Gpb2 protein (pTH84) in *gpa2*Δ cells (MLY212a/α) or with GFP-Gpr1C (pTH170) in wild-type cells (S1338) to determine roles of the N-terminal region of Gpa2 on interaction with Gpb2 and the C-terminal tail of Gpr1. Deletion mutant $Gpa2^{G299A}$ proteins constructed and results are shown schematically. Δ1–14, Δ1–29, Δ1–44, and Δ1–100 mutant proteins were fused to the first 10 amino acids from the yeast Gα subunit Gpa1 to restore targeting to the plasma membrane and Gpa1 residues are depicted as a gray box. Scale bar, 5 μm.

To examine if this candidate alpha helical domain of Gpa2 is involved in the interaction with Gpb2, the domain was deleted in the dominant negative $Gpa2^{G299A}$ mutant ($Gpa2^{\Delta\alpha\ (51-57)}$) and the resulting mutant derivative was coexpressed with the GFP-Gpb2 protein to test for protein localization. As noted above, $Gpa2^{G299A}$ recruits GFP-Gpb2 to the plasma membrane (Figure 5). Similarly, $Gpa2^{\Delta\alpha\ (51-57)}$ also brought GFP-Gpb2 to the plasma membrane (Figure 5). Therefore, the sequence spanning amino acids 51–57, which is predicted to be an N-terminal alpha helical region, is not required for Gpa2-Gpb2 binding.

We next addressed whether other sequences in the Gpa2 N-terminal extension are required for Gpb2 interaction. For this purpose, deletions were introduced into the N-terminal region of the $GPA2^{G299A}$ allele to create Δ1–14, Δ1–29, Δ1–44, and Δ1–100 derivatives of $Gpa2^{G299A}$, which were also then fused to the first 10 amino acids from the *S. cerevisiae* Gα subunit Gpa1 that are sufficient for membrane localization (unpublished data; Gillen *et al.*, 1998). Internal deletions were also created (Δ16–84, Δ31–84, Δ46–84, and Δ46–100, Figure 5). This deletion mutant series was coexpressed with GFP-Gpb2 to examine which Gpa2 mutants are capable of recruiting GFP-Gpb2 to the plasma membrane (Figure 5). All deletions generated for this study (except for the Δ46–449 Gpa2 mutant) are predicted to have no significant impact on the secondary structure of Gpa2, based on PHD analysis, and the function and expression of these alleles of $GPA2^{G299A}$ were confirmed by introducing these alleles into wild-type diploid cells and examining pseudohyphal growth (unpublished data). All deletion constructs and representative results are shown in Figure 5.

GFP-Gpb2 did not associate with the plasma membrane when coexpressed with the Δ1–14, Δ1–29, Δ1–44, or Δ1–100 Gpa2 derivatives, indicating that the N-terminus of Gpa2 plays an important role in Gpb2 binding (Figure 5). However, the first 15 or 30 amino acids were not sufficient for Gpb2 binding because neither the Gpa2 Δ16–84 nor the Δ31–84 mutant was able to recruit Gpb2 to the plasma membrane. On the other hand, membrane localization of GFP-Gpb2 was observed when it was coexpressed with the Gpa2 Δ46–84 and Δ46–100 mutants. Taken together, these findings indicate that the first 45 amino acids are necessary for Gpb2 interaction. This N-terminal region alone (1–45 aa) was not sufficient because GFP-Gpb2 was cytoplasmic with the $Gpa2^{\Delta 46-449}$ variant. Structural analyses have revealed that Gβ binding interfaces are present not only in the N-terminus (the αN domain) but also in the central region (β2 to α2 domain) of conventional Gα molecules (Figure 1 and Lambright *et al.*, 1996; Wall *et al.*, 1998). Therefore, by analogy Gpa2 may also require the corresponding internal conserved region in conjunction with the N-terminal 1–45 aa to bind Gpb2, although we cannot exclude a possibility that the $Gpa2^{\Delta 46-449}$ variant failed to recruit Gpb2 to the plasma membrane because of instability. Note that the deletions examined were also introduced into a wild-type Gpa2 construct and tested for GFP-Gpb2 interaction as above, and results were essentially equivalent to the ones with the $Gpa2^{G299A}$ deletion variants with the minor difference that plasma membrane localization of GFP-Gpb2 was weaker when the wild-type Gpa2 deletion variant were coexpressed. This is consistent with the fact that $Gpa2^{G299A}$ binds to Gpb2 more strongly than does wild-type Gpa2 (Figure 4, Harashima and Heitman, 2002, 2004).

We next addressed regions of the Gpa2 molecule involved in association with the Gpr1 receptor. Previously, the Gpr1 C-terminal tail composed of 99 amino acids was isolated in a yeast two-hybrid screen that identified Gpa2 interacting proteins (Xue *et al.*, 1998). Because Gpr1 that is C-terminally

tagged with GFP is nonfunctional (unpublished data), likely because of interference with Gpr1-Gpa2 coupling, we fused GFP to the N-terminus of the 99 amino acid soluble C-terminal tail of Gpr1. The resulting GFP fusion protein (GFP-Gpr1C) was coexpressed with the $Gpa2^{G299A}$ variants to examine roles of the N-terminal extension on interactions with the coupled receptor Gpr1, as above (Figure 5, also see Figure 8).

As shown in Figure 5, any variant of Gpa2 lacking the first 15 amino acids failed to recruit GFP-Gpr1C to the plasma membrane ($Gpa2^{\Delta 1-14}$, $Gpa2^{\Delta 1-29}$, $Gpa2^{\Delta 1-44}$, and $Gpa2^{\Delta 1-100}$), whereas all of the variants containing amino acids 1–15 ($Gpa2^{\Delta 16-84}$, $Gpa2^{\Delta 31-84}$, $Gpa2^{\Delta 46-84}$, and $Gpa2^{\Delta 46-100}$) recruited GFP-Gpr1C, similar to full length $Gpa2^{G299A}$. The only exception was $Gpa2^{\Delta 46-449}$, which failed to recruit the GFP-Gpr1C to the plasma membrane. These observations indicate that the N-terminal region of Gpa2 participates in associating with the receptor C-terminal tail, but that C-terminal regions of Gpa2 likely also participate. Importantly, the C-terminal tail of other Gα subunits is known to be involved in receptor coupling (Slessareva *et al.,* 2003; Herrmann *et al.,* 2004). Consistent with this model, $Gpa2^{\Delta 1-100}$ still interacted with the C-terminal tail of Gpr1 in the yeast two-hybrid assay and Gpa2 function was perturbed by a C-terminal GFP tag (unpublished data). In summary, these data indicate that both the N-terminal and more C-terminal regions of the Gα protein Gpa2 are required for interactions with both Gpb2 and Gpr1.

### *Functional Roles of the Gpa2 N-terminus*

To address roles of the Gpa2 amino terminus, N-terminal deletions were introduced into wild-type Gpa2. The resulting deletion alleles were expressed in diploid or haploid *gpa2* mutant cells to examine whether these mutants complement *gpa2* defects in pseudohyphal growth, invasive growth, and glucose-induced cAMP production (Figure 6). These mutant alleles were also introduced into diploid *gpr1 gpa2* mutant cells to examine whether they require Gpr1 for function or act as dominant alleles that bypass the receptor. Cells expressing $Gpa2^{\Delta 1-100}$ exhibited reduced pseudohyphal and invasive growth and reduced levels of basal and glucose-induced cAMP, indicating that the N-terminal region plays an important functional role or that deletion of the 1–100 amino acids might result in misfolding of Gpa2 (Figures 6). $Gpa2^{\Delta 46-84}$, $Gpa2^{\Delta 46-100}$, and $Gpa2^{\Delta \alpha\ (51-57)}$ all functioned as wild-type Gpa2, likely because Gpb2 and the C-terminal tail of Gpr1 still bind to these deletion proteins (Figure 6 and unpublished data). The Δ1–14, Δ1–29, Δ1–44, Δ16–84, or Δ31–84 *GPA2* mutant genes were largely able to complement *gpa2* mutant phenotypes. One interpretation of these results is that these deletion proteins still functionally interact with Gpr1 and Gpb2 via other Gpa2 domains and are capable of functioning, similar to wild-type Gpa2. Or expression of the deletion Gpa2 proteins from a multicopy plasmid might mask their reduced activity so that expression from a low copy plasmid could elicit altered mutant phenotypes. Alternatively, these results could be due to counterbalancing defects in Gpa2 interaction with Gpr1 and Gpb2 because Gpr1/Gpa2 and Gpb2 control the cAMP signaling pathway positively and negatively, respectively (see *Discussion*).

### *Kelch Gβ Mimic Proteins Gpb1/2 Function on the Plasma Membrane*

Gpb2 is directed to the plasma membrane in a Gpa2 dependent manner, indicating that the kelch Gβ mimic proteins Gpb1/2 may function on the plasma membrane. To examine this hypothesis, the first 10 amino acids of Gpa2 (hereafter, the membrane localization sequence [MLS]) that suffice for membrane localization were fused to the N-terminus of the GFP-Gpb1 or GFP-Gpb2 protein. The resulting fusion proteins were tested for protein localization and complementation of the elevated filamentous phenotype of *gpb1,2* mutant cells (Figure 7). We also tested the effects of fusing a nuclear localization signal (NLS) from the SV40 T antigen to the N-terminus of the GFP-Gpb1 or GFP-Gpb2 protein (Figure 7).

The MLS- and NLS-fused GFP-Gpb1/2 proteins were predominantly localized to the plasma membrane and the nucleus, respectively (Figure 7A). Furthermore, the MLS-GFP-Gpb1/2 fusion proteins complemented the *gpb1,2* double mutant phenotype and restored wild-type pseudohyphal growth (Figure 7B). In contrast, the nuclear localized Gpb1/2 proteins (NLS-GFP-Gpb1/2) were nonfunctional (Figure 7B). These findings provide evidence that Gpb1/2 can function when heterologously targeted to the plasma membrane. These results also indicate that the as yet unidentified second target of Gpb1/2 might be membrane associated.

### *Kelch Gβ Mimic Proteins Gpb1/2 Inhibit Gpr1-Gpa2 Coupling*

Gpa2 interacts with the C-terminal tail of the Gpr1 receptor and recruits the GFP-Gpr1 C-tail fusion protein to the plasma membrane. Here we used this assay to analyze Gpr1-Gpa2 coupling in further detail. GFP-Gpr1C is localized to the plasma membrane when coexpressed with the dominant negative $Gpa2^{G299A}$ allele. Additionally, membrane localization of GFP-Gpr1C was less pronounced when coexpressed with wild-type Gpa2, suggesting that the C-terminal tail of Gpr1 binds more strongly to $Gpa2^{G299A}$ compared to wild-type Gpa2 (Figure 8). On the other hand, interaction of Gpa2 with the C-terminal tail of Gpr1 was reduced even further with the dominant $Gpa2^{Q300L}$ allele (Figure 8). This is consistent with the widely accepted model in which the Gα-GDP complex binds to the cognate GPCR, whereas the Gα-GTP complex dissociates from the GPCR. To confirm the interaction between GFP-Gpr1C and Gpa2, the nonfunctional nuclear localized $Gpa2^{G2A}$-NLS was coexpressed with GFP-Gpr1C. In this case, GFP-Gpr1C was now misdirected to the nucleus (Figure 8).

Because Gpb2 is directed to the plasma membrane in a Gpa2-dependent manner and binds to the N-terminus of Gpa2 where the C-terminal tail of Gpr1 also binds, we hypothesized that Gpb1/2 could negatively regulate Gpa2 function by inhibiting the Gpr1-Gpa2 interaction. To address this hypothesis, the wild-type Gpb1/2 proteins were simultaneously coexpressed with the GFP-Gpr1C and $Gpa2^{G299A}$ proteins. As shown in Figure 8, the membrane localization of GFP-Gpr1 was significantly reduced by coexpression of Gpb1/2, indicating that Gpb1/2 compete with the C-terminal tail of Gpr1 for binding to the N-terminus of Gpa2. Gpb1/2 may thereby control Gpa2 function by impairing receptor coupling. This is in contrast to canonical Gβ subunits, which function to promote interactions of the Gα subunit with the associated GPCR.

## DISCUSSION

### *The Roles of the N-terminal Region of Gpa2*

The $MG^2XXXS^6$ sequence in open reading frames and the glycine residue of the consensus sequence are well defined as a myristoylation consensus sequence and the myristoyl-

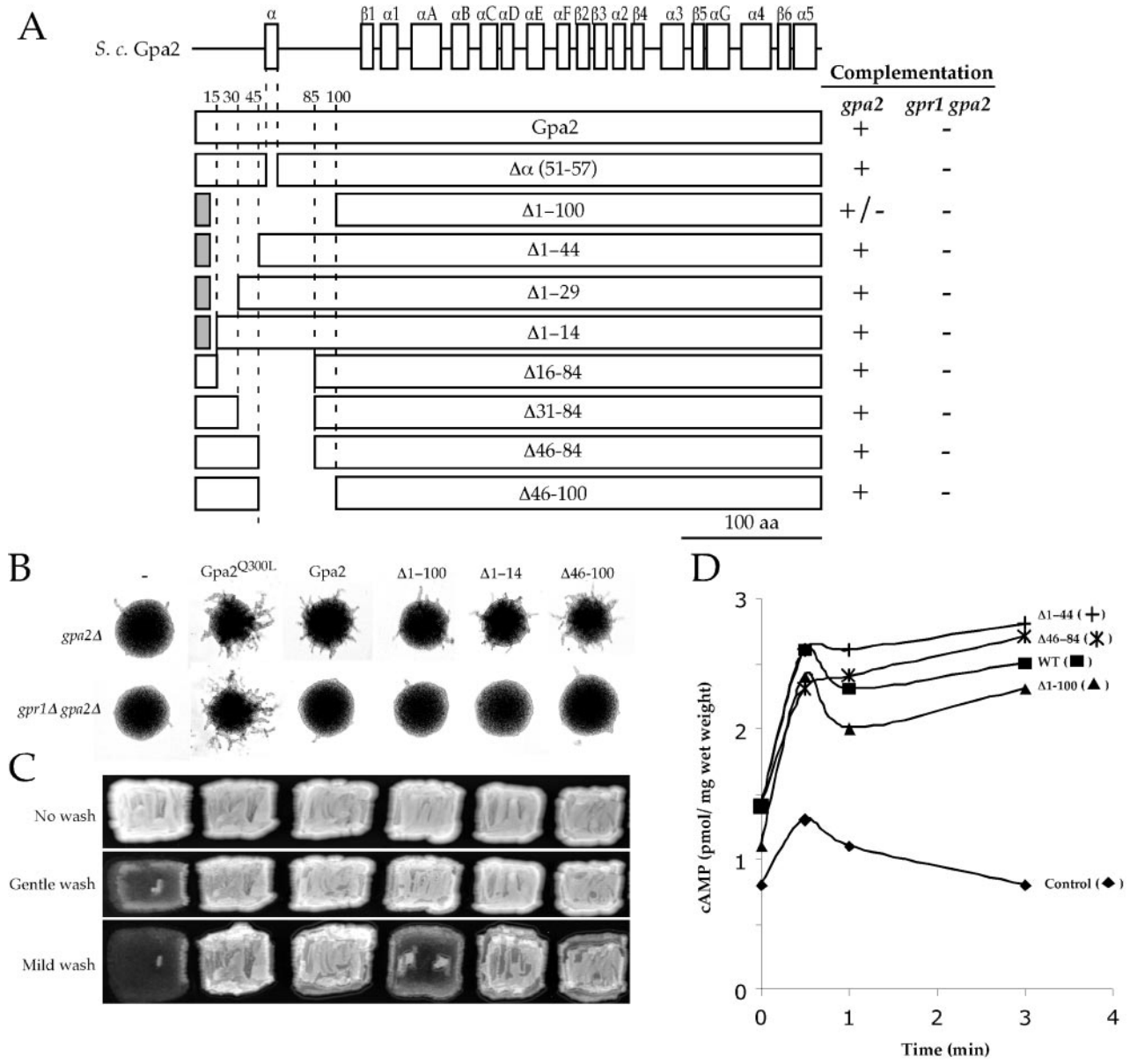


**Figure 6.** Function of the N-terminal deletion Gpa2 proteins in vivo. (A) Schematic of N-terminal deletion Gpa2 variants and complementation results in *gpa2* or *gpr1 gpa2* mutant cells. N-terminal deletions were created in the wild-type *GPA2* gene and introduced into *gpa2* (MLY132$\alpha$ for invasive growth assay and MLY132a/$\alpha$ for pseudohyphal growth assay) or *gpr1 gpa2* (MLY277a/$\alpha$) mutant cells and ability to complement pseudohyphal and invasive growth defects was examined. Representative data are shown in B for pseudohyphal growth and in C for invasive growth. (D) Glucose-induced cAMP production in *gpa2* (MLY132$\alpha$) mutant cells expressing the N-terminal deletion Gpa2 derivatives. The values shown are the mean of two independent experiments, except the control, which is representative of cells carrying the empty vector (pTH19).

ation site. On the other hand, no obvious consensus sequence is established for palmitoylation, yet palmitoylation mostly occurs in a cysteine residue(s) near the N-terminus. The G$\alpha$ subunit Gpa2 contains the $MG^2XXXS^6$ myristoylation consensus sequence and a cysteine at the fourth position of its N-terminus. A cysteine after the N-terminal cysteine appears at the 189th position of the Gpa2 protein. Our biochemical studies revealed that Gpa2 is myristoylated and palmitoylated. Furthermore, the labeling and site-directed mutagenesis studies shown in Figure 2 provide evidence that Gpa2 is myristoylated at $Gly^2$ and, most likely, also palmitoylated at $Cys^4$.

Introduction of site-specific mutations (G2A, C4A, and S6Y) into the *GPA2* and *GPA2-GFP* fusion genes demonstrates that myristoylation and palmitoylation are critical for plasma membrane targeting and function of Gpa2. Although it still remains to be established why myristoylation is essential for G$\alpha$ function, recent studies demonstrate that GPCR-G$\alpha$ fusion proteins, in which G$\alpha$ is localized to the plasma membrane yet no longer lipid modified, are functional in vivo (for review, see Seifert *et al.*, 1999). Furthermore, a nonmyristoylated $G\alpha i2^{Q205L}$ protein is unable to signal and fails to transform rat fibroblasts (Gallego *et al.*, 1992). Consistently, we also found that a nonmyristoylated

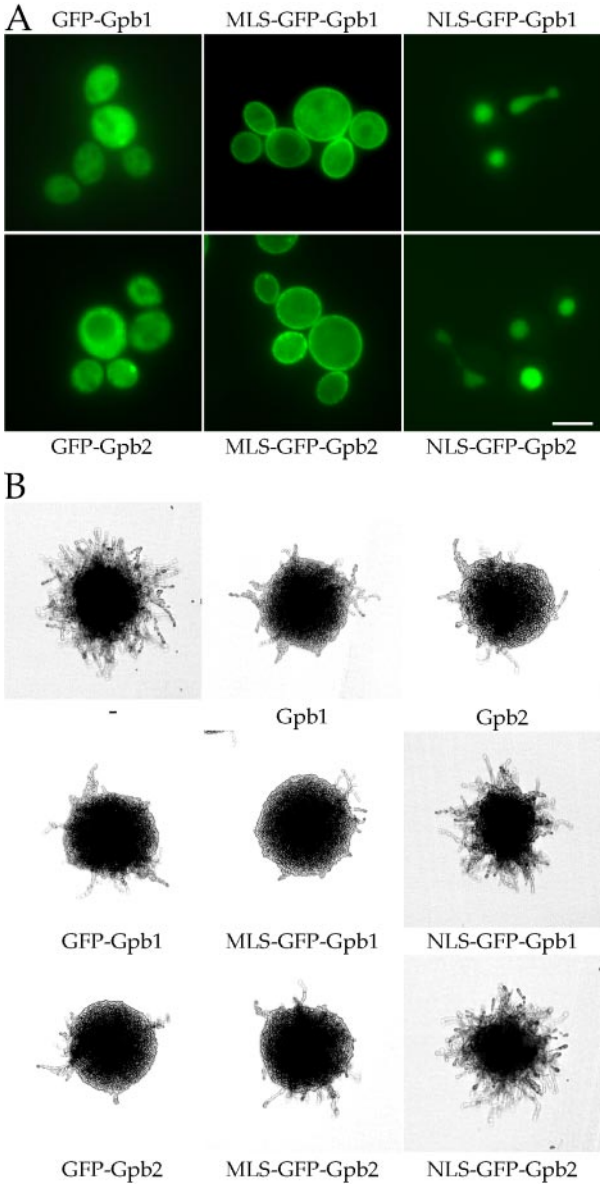


**Figure 7.** Kelch G$\beta$ mimic proteins Gpb1/2 function on the plasma membrane. A membrane localization sequence (MLS) or nuclear localization signal (NLS) was fused to the N-terminus of the functional GFP-Gpb1/2 proteins (pTH106/pTH75) and the resulting fusion proteins (pTH163, pTH164, pTH166, or pTH167) were expressed in diploid *gpb1,2* double mutant cells (THY212a/$\alpha$) to test for protein localization (A) and function (B). The MLS-GFP-Gpb1/2 fusion proteins were recruited to the plasma membrane and were as functional as the wild-type Gpb1/2 proteins, whereas the NLS-GFP-Gpb1/2 fusion proteins were directed to the nucleus and nonfunctional. Cells bearing the empty vector (pTH19) or the *GPB1* (pTH26) or *GPB2* (pTH27) plasmid served as controls. Scale bar, 5 $\mu$m.

dominant Gpa2$^{Q300L}$ mutant (equivalent to G$\alpha$i2 Q205L) is incapable of enhancing filamentous growth in wild-type cells. These findings support a model in which lipid modifications are necessary for plasma membrane targeting that is a prerequisite for G$\alpha$ function. Alternatively, myristoylation may play an important role in G$\alpha$ structure that is required for receptor coupling (Preininger *et al.*, 2003).

In heterotrimeric G proteins, the N-terminus is also involved in interactions with G$\beta\gamma$ dimer, receptors, and effectors. Structural and biochemical studies implicate the N-terminal alpha helix ($\alpha$N domain) in G$\beta\gamma$ dimer and receptor coupling (Lambright *et al.*, 1996; Wall *et al.*, 1998). Gpa2 contains an alpha helix in the extended N-terminus, yet the position of this helix is not conserved (Figure 1). More strikingly, the alpha helix is not involved in coupling to the kelch subunit Gpb2 or to the Gpr1 C-terminal tail. Studies using Gpa2 variants that carry a series of deletions in the Gpa2 N-terminus identified binding domains for the Gpr1 C-terminal tail and Gpb2 that map to amino acids 1–15 and 1–45 and are not predicted to form an alpha helix.

Lipid modifications alone are not sufficient to restore these interactions as the Gpa2 $\Delta$1–14 mutant that is lipid modified on an appended Gpa1$^{1-10}$ peptide did not direct the binding partners to the plasma membrane. Rather, amino acid sequences that lie between residues 1–45 are important for the interactions. Interestingly, the non-alpha helical N-terminus (spanning amino acids 1–6) of G$\alpha$q is known to be involved in receptor selectivity (Kostenis *et al.*, 1997). Therefore, the N-terminus may play a direct role in receptor coupling by providing a binding interface or an indirect role by influencing overall structure. Either possibility is novel and further studies, especially structural studies, should address the role of the N-terminus of Gpa2.

### *The Role of the Gpr1 C-terminal Tail*

Previous studies suggest the presence of preactivation complexes in which an unoccupied, inactive GPCR is coupled to the G$\alpha$ subunit (Samama *et al.*, 1993; Stefan *et al.*, 1998; Dosil *et al.*, 2000). Such preactivation complexes are not necessarily required for formation of the activated ternary complex in which a ligand bound, activated receptor forms a complex with a G protein to stimulate GDP-GTP exchange on G$\alpha$, yet the preactivation complexes are involved in regulation of specificity and intensity of G-protein mediated signaling (Neubig, 1994; Shea and Linderman, 1997). In *S. cerevisiae*, the C-terminal tail of the $\alpha$-factor receptor Ste2 is implicated in the formation of the preactivation complex with its associated G$\alpha$ Gpa1 (Dosil *et al.*, 2000). Although no direct evidence has been reported for a preactivation complex between the Gpr1 receptor and Gpa2, our data support the existence of one. First, the cytoplasmic C-terminal tail of Gpr1 binds to wild-type Gpa2 and a nuclear localized Gpa2$^{G2A}$-NLS. Second, Gpr1 and Gpa2 are still functional in the absence of the G$\beta$ mimic subunits Gpb1/2, suggesting a promiscuous coupling between Gpr1 and Gpa2.

These observations may be relevant to our finding that N-terminal deletion variants of Gpa2 ($\Delta$1–14, $\Delta$1–29, $\Delta$1–44, and $\Delta$1–100) that are unable to bind to the Gpr1 C-terminal tail are still functional and can respond to glucose to stimulate cAMP production. This interpretation may also explain why cells expressing these Gpa2 variants exhibited near wild-type phenotypes. It is conceivable that a reduced affinity of the Gpa2 variants with the Gpr1 receptor could result in a decrease in signaling leading to a low-PKA phenotype. However, these Gpa2 variants also show decreased binding to the kelch subunits Gpb1/2 that negatively control cAMP signaling, affecting Gpb1/2 function to activate the as yet unidentified second target that inhibits cAMP signaling.

### *Kelch Subunits Gpb1/2 Inhibit Gpr1-Gpa2 Coupling*

G-protein activity is controlled at multiple steps including expression, protein localization, GDP-GTP exchange, and GTPase activity. GPCRs activate G proteins by stimulating GDP dissociation from G$\alpha$ and acting as guanine nucleotide exchange factors, thereby leading to G$\alpha$ in the active G$\alpha$-GTP form. On the other hand, the GoLoco family protein

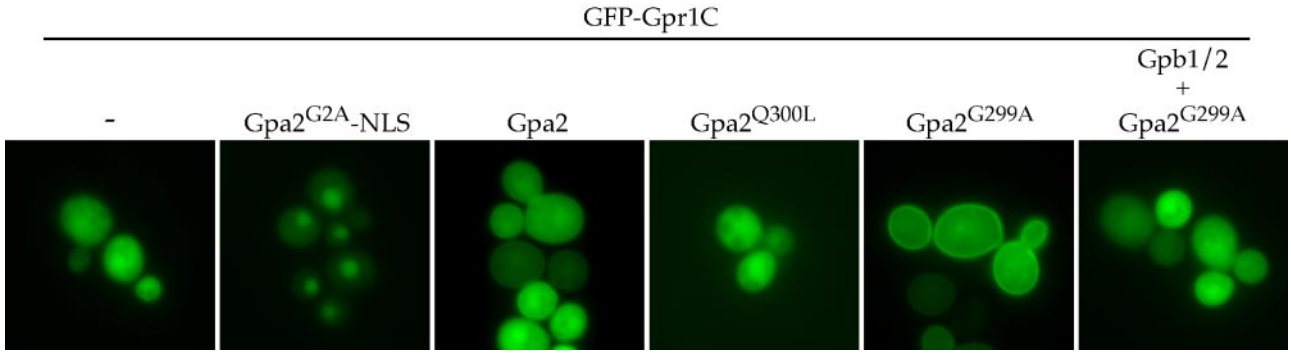


**Figure 8.** Kelch Gβ mimic proteins Gpb1/2 interfere with the interaction between Gpa2 and the C-terminal tail of Gpr1. (A) The GFP-Gpr1C fusion protein (pTH170) was expressed alone or coexpressed with Gpa2 variants, wild-type Gpa2 (pTH47), $Gpa2^{Q300L}$ (pTH48), $Gpa2^{G299A}$ (pTH49), or NLS-$Gpa2^{G2A}$ (pTH149) with or without Gpb1/2 (pTH174/pTH114) in wild-type cells (THY452). Empty vectors (pTH171 and pTH173) were used as controls for the Gpb1/2 plasmids, pTH174 and pTH114. The location of nuclei were confirmed by DAPI staining.

AGS3 functions as a guanine nucleotide dissociation inhibitor (GDI) by inhibiting GDP-GTP exchange (De Vries *et al.*, 2000). Although GoLoco homologues are conserved in multicellular eukaryotes, no such homolog is apparent in the yeast genome.

Our previous studies revealed that the kelch subunits Gpb1 and Gpb2 negatively control Gpa2 and preferentially associate with Gpa2-GDP (Harashima and Heitman, 2002). However, neither loss nor overexpression of Gpb1/2 perturbed Gpa2 membrane localization or expression. In addition, Gpb1/2 did not exhibit GDI activity under standard in vitro conditions (unpublished data). Here we show that Gpb1/2 inhibit Gpa2-Gpr1 coupling. A model governing how the kelch Gpb1/2 subunits control Gpa2 is that Gpb1/2 bind to the Gpa2 N-terminal region spanning amino acids 1–45 and occlude binding of the Gpr1 C-terminal tail to the first fifteen amino acids of Gpa2 (Figure 9).

In canonical heterotrimeric G proteins, Gβγ subunits are required for receptor-Gα coupling. In *S. cerevisiae*, the Gβγ dimer plays an essential role in pheromone receptor-Gα Gpa1 coupling (Blumer and Thorner, 1990). In mammalian systems, a role for the Gβγ subunits in coupling of $\beta_2$-adrenergic receptor-Gαs, $M_2$-muscarinic receptor-Gαo, $A_1$-adenosine and 5-$HT_{1A}$ receptors-Gαi, and $\beta_2$-adrenergic re-

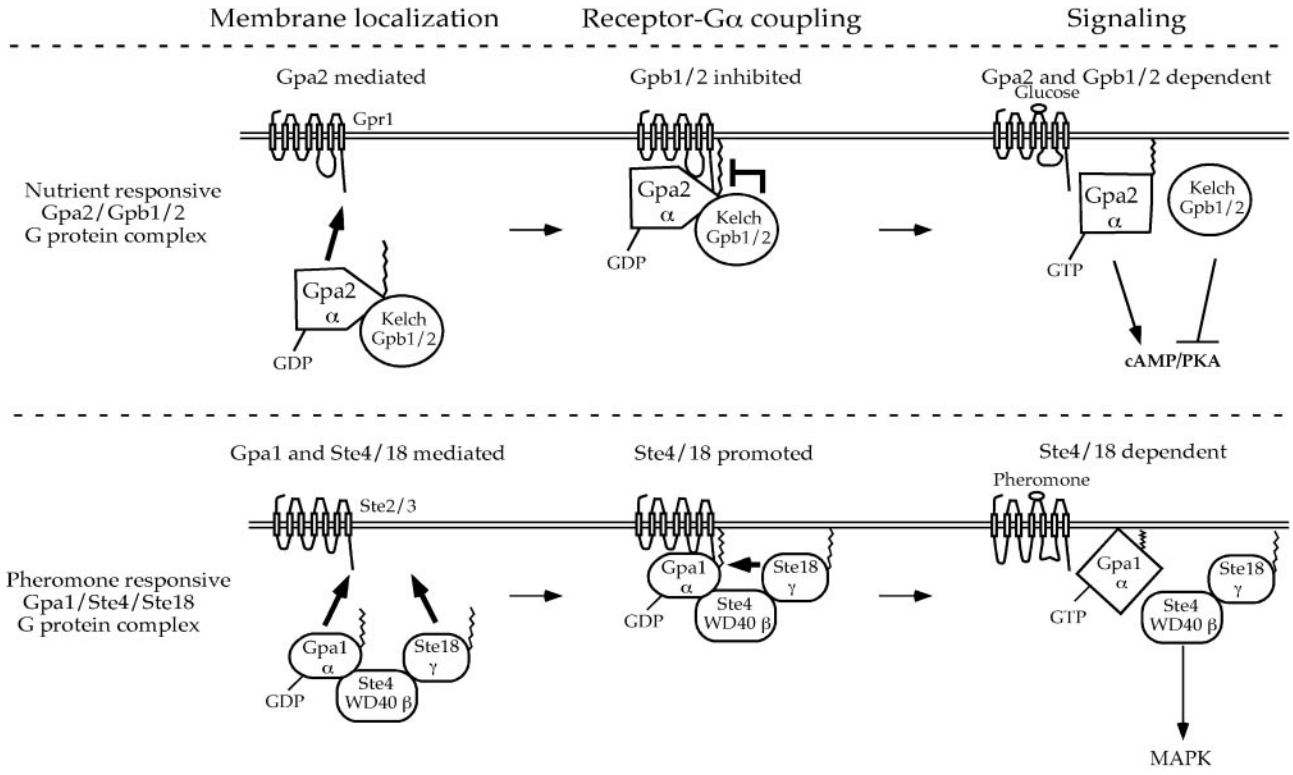


**Figure 9.** Model of canonical heterotrimeric and atypical G protein signaling in budding yeast. The canonical heterotrimeric G protein composed of the Gpa1/Ste4/Ste18 subunits regulates the pheromone responsive MAPK cascade, whereas the atypical heteromeric G protein consisting of the Gpa2/Gpb1/2 subunits controls the nutrient sensing cAMP-PKA signaling pathway. For details, see *Discussion*.

ceptor-Gαi has been established (Richardson and Robishaw, 1999; Hou *et al.*, 2001; Lim *et al.*, 2001; Kühn *et al.*, 2002). This function is opposite to the role of the kelch subunits, yet importantly, yeast and mammalian WD40 repeat Gβγ subunits and the kelch subunits all converge to modulate receptor-Gα coupling. That receptor-Gα coupling is oppositely regulated may depend on how tightly and specifically a given Gα binds to its associated receptor. In yeast, the pheromone receptor Ste2 is functionally coupled to the Gα protein Gpa1 and not to the Gpa2 Gα subunit (Blumer and Thorner, 1990). During diploid filamentation, the glucose receptor Gpr1 is associated with Gpa2 and not with the haploid specific Gα Gpa1. Importantly, the Gpa2 Gα subunit is still partially functional and able to signal in response to the agonist glucose via Gpr1 in the absence of Gpb1/2, suggesting that Gpa2 can functionally couple to its receptor in the absence of Gpb1/2 (Harashima and Heitman, 2002). Therefore, Gpa2 may normally be tightly associated with the Gpr1 receptor, and Gpb1/2 function to compete with this association to reduce signaling in the absence of glucose.

Generally, the intracellular third loop of GPCRs plays a crucial role in interactions with the Gα subunit. Although *S. cerevisiae* Gpa2 has been reported to interact with the intracellular third loop of Gpr1 in the yeast two-hybrid assay (Yun *et al.*, 1997), we were unable to recapitulate this result (unpublished data). This could be attributable to a weak interaction between Gpa2 and the third loop of Gpr1. In contrast, the Gpr1 C-terminal tail avidly binds to Gpa2 in two-hybrid assays (Yun *et al.*, 1997; Xue *et al.*, 1998; Kraakman *et al.*, 1999; Harashima and Heitman, 2002). We also showed that the Gpa2-Gpr1 C-terminal tail interaction can be detected using the GFP tagged C-terminal tail of Gpr1 in vivo (Figures 5 and 8). These data indicate that the Gpr1 C-terminus plays an important role in Gpa2 binding. This atypical feature of the Gpr1 receptor-Gpa2 Gα complex may mirror the unusual aspects by which the kelch subunits Gpb1/2 inhibit the signaling complex.

### *Is Gpa2 an Unusual Gα or an Ancestral Gα Subunit?*

Our studies provide evidence that lipid modifications (myristoylation and palmitoylation) of Gα Gpa2 are necessary and sufficient for Gpa2 plasma membrane targeting but are not required for interaction with the kelch Gβ mimic subunit Gpb2. Instead, Gpa2 directs Gpb2 to the plasma membrane. Mammalian Gα subunits as well as the yeast canonical Gα subunit Gpa1 share similar features. Like Gpa2, lipid modifications but not the Gβγ dimer are required for plasma membrane localization of yeast Gpa1 and mammalian Gα (Song *et al.*, 1996; Gillen *et al.*, 1998; Galbiati *et al.*, 1999). It has also been reported that a nonlipidated Gα still binds to Gβγ subunits in yeast and mammals (Jones *et al.*, 1990; Degtyarev *et al.*, 1994; Song *et al.*, 1996). Studies also provide evidence that Gα, at least in part, directs Gβγ subunits to the plasma membrane in vivo (Song *et al.*, 1996; Takida and Wedegaertner, 2003). Although Gpa2 shares similar features with canonical Gα subunits, a striking contrast is the inability of Gpa2 to form a heterotrimeric G protein. The Gα subunit Gpa1 in the fission yeast *Schizosaccharomyces pombe*, which functions in pheromone-mediated signaling, also fails to form a heterotrimeric G protein with the known Gβγ subunits Git5/11. The kelch protein Ral2 has been proposed as a possible Gpa1-associated subunit based on genetic studies (Fukui *et al.*, 1989; Harashima and Heitman, 2002; Hoffman, 2005).

Another contrast between canonical Gα subunits and Gpa2 is that Gβγ subunits typically promote receptor-Gα coupling, whereas Gpb1/2 inhibit receptor-Gpa2 coupling (Figure 9). The receptor Gpr1 and Gα Gpa2 can still in part function and signal in response to glucose without the Gβ mimic subunits Gpb1/2, indicating a promiscuous and specific coupling between Gpr1 and Gpa2 even in the absence of Gpb1/2 (Harashima and Heitman, 2002). In *S. cerevisiae*, the cAMP-PKA signaling pathway is essential for cell growth and determines cell fates in response to extracellular nutrients (Harashima and Heitman, 2004). Therefore the cAMP-PKA signaling pathway should be strictly controlled, and for this reason, Gpb1/2 may interfere with promiscuous Gpr1-Gpa2 coupling to facilitate responses to extracellular nutrients. On the other hand, in canonical G proteins, the Gβγ dimer may control Gα function by increasing the specificity of receptor coupling (Richardson and Robishaw, 1999; Hou *et al.*, 2001; Lim *et al.*, 2001; Kühn *et al.*, 2002). Importantly, the kelch Gβ mimic subunits Gpb1/2 and canonical Gβγ dimer both regulate receptor-Gα coupling. Thus, the Gpa2/Gpb1/2 protein complex shares features with canonical heterotrimeric G proteins, and we propose Gpa2 is an ancestral subunit rather than an unusual Gα subunit. In this model, eukaryotic cells first acquired a GPCR and associated Gα subunit to sense and signal extracellular cues. Later, seven-bladed β-propeller-type subunits (kelch or WD40 based) were recruited to the GPCR-Gα signaling complex. Finally, farnesylated Gγ subunits were recruited to promote membrane localization. In this model, the atypical features of the nutrient and pheromone GPCR-Gα signaling modules in budding and fission yeasts might mirror features of their ancestral signaling modules from which they derive.

Alternatively, yeasts might uniquely have evolved an "alternative" Gα subunit and established a novel G protein signaling system to sense extracellular stimuli, in which an atypical Gα subunit forms a complex and functions with an unusual binding-partner kelch Gβ mimic protein. Further studies in both unicellular and multicellular organisms would distinguish these possibilities.

## ACKNOWLEDGMENTS

We thank Sayoko Ito-Harashima for providing a yeast strain and Cristl Arndt and Emily Wenink for assistance. We also thank Yong-Sun Bahn, Alex Idnurm, Julian Rutherford, Chaoyang Xue, Andy Alspaugh, Pat Casey, Henrik Dohlman, and Bob Lefkowitz for critical reading. This study was supported by the Department of Defense Neurofibromatosis program (W81xwh-04-01-0208). T.H. was supported by a fellowship from the Children's Tumor Foundation and J.H. is an investigator of the Howard Hughes Medical Institute.

## REFERENCES

Adams, J., Kelso, R., and Cooley, L. (2000). The kelch repeat superfamily of proteins: propellers of cell function. Trends Cell Biol. *10*, 17–24.

Arévalo-Rodríguez, M., and Heitman, J. (2005). Cyclophilin A is localized to the nucleus and controls meiosis in *Saccharomyces cerevisiae*. Eukaryot. Cell *4*, 17–29.

Ashrafi, K., Farazi, T. A., and Gordon, J. I. (1998). A role for *Saccharomyces cerevisiae* fatty acid activation protein 4 in regulating protein N-myristoylation during entry into stationary phase. J. Biol. Chem. *273*, 25864–25874.

Batlle, M., Lu, A. L., Green, D. A., Xue, Y., and Hirsch, J. P. (2003). Krh1p and Krh2p act downstream of the Gpa2p Gα subunit to negatively regulate haploid invasive growth. J. Cell Sci. *116*, 701–710.

Blumer, K. J., and Thorner, J. (1990). β and γ subunits of a yeast guanine nucleotide-binding protein are not essential for membrane association of the α subunit but are required for receptor coupling. Proc. Natl. Acad. Sci. USA *87*, 4363–4367.

Bourne, H. R. (1997). How receptors talk to trimeric G proteins. Curr. Opin. Cell Biol. *9*, 134–142.

Cabrera-Vera, T. M., Vanhauwe, J., Thomas, T. O., Medkova, M., Preininger, A., Mazzoni, M. R., and Hamm, H. E. (2003). Insights into G protein structure, function, and regulation. Endocr. Rev. *24*, 765–781.

Chen, C. A., and Manning, D. R. (2001). Regulation of G proteins by covalent modification. Oncogene *20*, 1643–1652.

Colombo, S. *et al.* (1998). Involvement of distinct G-proteins, Gpa2 and Ras, in glucose- and intracellular acidification-induced cAMP signalling in the yeast *Saccharomyces cerevisiae.* EMBO J. *17*, 3326–3341.

De Vries, L., Fischer, T., Tronchère, H., Brothers, G. M., Strockbine, B., Siderovski, D. P., and Farquhar, M. G. (2000). Activator of G protein signaling 3 is a guanine dissociation inhibitor for $G\alpha_i$ subunits. Proc. Natl. Acad. Sci. USA *97*, 14364–14369.

De Vries, L., and Gist Farquhar, M. (1999). RGS proteins: more than just GAPs for heterotrimeric G proteins. Trends Cell Biol. *9*, 138–144.

Degtyarev, M. Y., Spiegel, A. M., and Jones, T. L. (1994). Palmitoylation of a G protein $\alpha_i$ subunit requires membrane localization not myristoylation. J. Biol. Chem. *269*, 30898–30903.

Dohlman, H. G. (2002). G proteins and pheromone signaling. Annu. Rev. Physiol. *64*, 129–152.

Dohlman, H. G., and Thorner, J. W. (2001). Regulation of G protein-initiated signal transduction in yeast: paradigms and principles. Annu. Rev. Biochem. *70*, 703–754.

Dosil, M., Schandel, K. A., Gupta, E., Jenness, D. D., and Konopka, J. B. (2000). The C terminus of the *Saccharomyces cerevisiae* $\alpha$-factor receptor contributes to the formation of preactivation complexes with its cognate G protein. Mol. Cell. Biol. *20*, 5321–5329.

Evanko, D. S., Thiyagarajan, M. M., and Wedegaertner, P. B. (2000). Interaction with $G\beta\gamma$ is required for membrane targeting and palmitoylation of $G\alpha_s$ and $G\alpha_q$. J. Biol. Chem. *275*, 1327–1336.

Farazi, T. A., Waksman, G., and Gordon, J. I. (2001). The biology and enzymology of protein *N*-myristoylation. J. Biol. Chem. *276*, 39501–39504.

Fishburn, C. S., Pollitt, S. K., and Bourne, H. R. (2000). Localization of a peripheral membrane protein: $G\beta\gamma$ targets $G\alpha_Z$. Proc. Natl. Acad. Sci. USA *97*, 1085–1090.

Fukui, Y., Miyake, S., Satoh, M., and Yamamoto, M. (1989). Characterization of the *Schizosaccharomyces pombe ral2* gene implicated in activation of the *ras1* gene product. Mol. Cell. Biol. *9*, 5617–5622.

Galbiati, F., Volonté, D., Meani, D., Milligan, G., Lublin, D. M., Lisanti, M. P., and Parenti, M. (1999). The dually acylated $NH_2$-terminal domain of $G_{i1\alpha}$ is sufficient to target a green fluorescent protein reporter to caveolin-enriched plasma membrane domains. Palmitoylation of caveolin-1 is required for the recognition of dually acylated G-protein $\alpha$ subunits *in vivo.* J. Biol. Chem. *274*, 5843–5850.

Gallego, C., Gupta, S. K., Winitz, S., Eisfelder, B. J., and Johnson, G. L. (1992). Myristoylation of the $G\alpha_{i2}$ polypeptide, a G protein $\alpha$ subunit, is required for its signaling and transformation functions. Proc. Natl. Acad. Sci. USA *89*, 9695–9699.

Gancedo, J. M. (2001). Control of pseudohyphae formation in *Saccharomyces cerevisiae.* Fems Microbiol. Rev. *25*, 107–123.

Gautam, N., Downes, G. B., Yan, K., and Kisselev, O. (1998). The G-protein $\beta\gamma$ complex. Cell Signal *10*, 447–455.

Gillen, K. M., Pausch, M., and Dohlman, H. G. (1998). N-terminal domain of Gpa1 (G protein $\alpha$ subunit) is sufficient for plasma membrane targeting in yeast *Saccharomyces cerevisiae.* J. Cell Sci. *111*, 3235–3244.

Gilman, A. G. (1987). G-Proteins: transducers of receptor-generated signals. Annu. Rev. Biochem. *56*, 615–649.

Guan, K. L., and Han, M. (1999). A G-protein signaling network mediated by an RGS protein. Genes Dev. *13*, 1763–1767.

Hamm, H. E., Deretic, D., Arendt, A., Hargrave, P. A., Koenig, B., and Hofmann, K. P. (1988). Site of G protein binding to rhodopsin mapped with synthetic peptides from the $\alpha$ subunit. Science *241*, 832–835.

Harashima, T., and Heitman, J. (2002). The G$\alpha$ protein Gpa2 controls yeast differentiation by interacting with kelch repeat proteins that mimic G$\beta$ subunits. Mol. Cell *10*, 163–173.

Harashima, T., and Heitman, J. (2004). Nutrient control of dimorphic growth in *Saccharomyces cerevisiae.* In: Topics in Current Genetics, Vol. 7, ed. J Winderickx and P. M. Taylor, Heidelberg: Springer-Verlag, 131–169.

Herrmann, R., Heck, M., Henklein, P., Henklein, P., Kleuss, C., Hofmann, K. P., and Ernst, O. P. (2004). Sequence of interactions in receptor-G protein coupling. J. Biol. Chem. *279*, 24283–24290.

Hoffman, C. S. (2005). Except in every detail: comparing and contrasting G-protein signaling in *Saccharomyces cerevisiae* and *Schizosaccharomyces pombe.* Eukaryot. Cell *4*, 495–503.

Hou, Y., Chang, V., Capper, A. B., Taussig, R., and Gautam, N. (2001). G Protein $\beta$ subunit types differentially interact with a muscarinic receptor but not adenylyl cyclase type II or phospholipase C-$\beta$2/3. J. Biol. Chem. *276*, 19982–19988.

Ito, N., Phillips, S. E., Stevens, C., Ogel, Z. B., McPherson, M. J., Keen, J. N., Yadav, K. D., and Knowles, P. F. (1991). Novel thioether bond revealed by a 1.7 Å crystal structure of galactose oxidase. Nature *350*, 87–90.

Ito, N., Phillips, S.E.V., Yadav, K.D.S., and Knowles, P. F. (1994). Crystal structure of a free radical enzyme, galactose oxidase. J. Mol. Biol. *238*, 794–814.

Jeansonne, N. E. (1994). Yeast as a model system for mammalian seven-transmembrane segment receptors. Proc. Soc. Exp. Biol. Med. *206*, 35–44.

Johnson, D. R., Bhatnagar, R. S., Knoll, L. J., and Gordon, J. I. (1994). Genetic and biochemical studies of protein N-myristoylation. Annu. Rev. Biochem. *63*, 869–914.

Jones, T. L., Simonds, W. F., Merendino, J. J., Jr., Brann, M. R., and Spiegel, A. M. (1990). Myristoylation of an inhibitory GTP-binding protein $\alpha$ subunit is essential for its membrane attachment. Proc. Natl. Acad. Sci. USA *87*, 568–572.

Journot, L., Pantaloni, C., Bockaert, J., and Audigier, Y. (1991). Deletion within the amino-terminal region of $G_s\alpha$ impairs its ability to interact with $\beta\gamma$ subunits and to activate adenylate cyclase. J. Biol. Chem. *266*, 9009–9015.

Kostenis, E., Degtyarev, M. Y., Conklin, B. R., and Wess, J. (1997). The N-terminal extension of $G\alpha_q$ is critical for constraining the selectivity of receptor coupling. J. Biol. Chem. *272*, 19107–19110.

Kraakman, L., Lemaire, K., Ma, P. S., Teunissen, A.W.R.H., Donaton, M.C.V., Van Dijck, P., Winderickx, J., de Winde, J. H., and Thevelein, J. M. (1999). A *Saccharomyces cerevisiae* G-protein coupled receptor, Gpr1, is specifically required for glucose activation of the cAMP pathway during the transition to growth on glucose. Mol. Microbiol. *32*, 1002–1012.

Kübler, E., Mösch, H. U., Rupp, S., and Lisanti, M. P. (1997). Gpa2p, a G-protein $\alpha$-subunit, regulates growth and pseudohyphal development in *Saccharomyces cerevisiae* via a cAMP-dependent mechanism. J. Biol. Chem. *272*, 20321–20323.

Kühn, B., Christel, C., Wieland, T., Schultz, G., and Gudermann, T. (2002). G-protein $\beta\gamma$-subunits contribute to the coupling specificity of the $\beta_2$-adrenergic receptor to $G_s$. Naunyn Schmiedebergs Arch. Pharmacol. *365*, 231–241.

Lambright, D. G., Sondek, J., Bohm, A., Skiba, N. P., Hamm, H. E., and Sigler, P. B. (1996). The 2.0 Å crystal structure of a heterotrimeric G protein. Nature *379*, 311–319.

Lefkowitz, R. J. (2000). The superfamily of heptahelical receptors. Nat. Cell Biol. *2*, E133–E136.

Lemaire, K., Van de Velde, S., Van Dijck, P., and Thevelein, J. M. (2004). Glucose and sucrose act as agonist and mannose as antagonist ligands of the G protein-coupled receptor Gpr1 in the yeast *Saccharomyces cerevisiae.* Mol. Cell *16*, 293–299.

Lengeler, K. B., Davidson, R. C., D'Souza, C., Harashima, T., Shen, W. C., Wang, P., Pan, X. W., Waugh, M., and Heitman, J. (2000). Signal transduction cascades regulating fungal development and virulence. Microbiol. Mol. Biol. Rev. *64*, 746–785.

Lim, W. K., Myung, C. S., Garrison, J. C., and Neubig, R. R. (2001). Receptor-G protein $\gamma$ specificity: $\gamma$11 shows unique potency for $A_1$ adenosine and 5-$HT_{1A}$ receptors. Biochemistry *40*, 10532–10541.

Linder, M. E., Pang, I. H., Duronio, R. J., Gordon, J. I., Sternweis, P. C., and Gilman, A. G. (1991). Lipid modifications of G protein subunits. Myristoylation of $G_{o\alpha}$ increases its affinity for $\beta\gamma$. J. Biol. Chem. *266*, 4654–4659.

Longtine, M. S., McKenzie III, A., Demarini, D. J., Shah, N. G., Wach, A., Brachat, A., Philippsen, P., and Pringle, J. R. (1998). Additional modules for versatile and economical PCR-based gene deletion and modification in *Saccharomyces cerevisiae.* Yeast *14*, 953–961.

Lorenz, M. C., and Heitman, J. (1997). Yeast pseudohyphal growth is regulated by GPA2, a G protein $\alpha$ homolog. EMBO J. *16*, 7008–7018.

Lorenz, M. C., Pan, X. W., Harashima, T., Cardenas, M. E., Xue, Y., Hirsch, J. P., and Heitman, J. (2000). The G protein-coupled receptor Gpr1 is a nutrient sensor that regulates pseudohyphal differentiation in *Saccharomyces cerevisiae.* Genetics *154*, 609–622.

Mombaerts, P. (2004). Genes and ligands for odorant, vomeronasal and taste receptors. Nat. Rev. Neurosci. *5*, 263–278.

Morales, J., Fishburn, C. S., Wilson, P. T., and Bourne, H. R. (1998). Plasma membrane localization of $G\alpha_z$ requires two signals. Mol. Biol. Cell *9*, 1–14.

Navon, S. E., and Fung, B. K. (1987). Characterization of transducin from bovine retinal rod outer segments. Participation of the amino-terminal region of $T_{\alpha}$ in subunit interaction. J. Biol. Chem. *262*, 15746–15751.

Neubig, R. R. (1994). Membrane organization in G-protein mechanisms. FASEB J. *8*, 939–946.

Pan, X., Harashima, T., and Heitman, J. (2000). Signal transduction cascades regulating pseudohyphal differentiation of *Saccharomyces cerevisiae.* Curr. Opin. Microbiol. *3*, 567–572.

Preininger, A. M., Van Eps, N., Yu, N. J., Medkova, M., Hubbell, W. L., and Hamm, H. E. (2003). The myristoylated amino terminus of $G\alpha_{i1}$ plays a critical role in the structure and function of $G\alpha_{i1}$ subunits in solution. Biochemistry *42*, 7931–7941.

Richardson, M., and Robishaw, J. D. (1999). The $\alpha_{2A}$-adrenergic receptor discriminates between $G_i$ heterotrimers of different $\beta\gamma$ subunit composition in Sf9 insect cell membranes. J. Biol. Chem. *274*, 13525–13533.

Rolland, F., de Winde, J. H., Lemaire, K., Boles, E., Thevelein, J. M., and Winderickx, J. (2000). Glucose-induced cAMP signalling in yeast requires both a G-protein coupled receptor system for extracellular glucose detection and a separable hexose kinase-dependent sensing process. Mol. Microbiol. *38*, 348–358.

Ross, E. M., and Wilkie, T. M. (2000). GTPase-activating proteins for heterotrimeric G proteins: Regulators of G protein signaling (RGS) and RGS-like proteins. Annu. Rev. Biochem. *69*, 795–827.

Rost, B., and Sander, C. (1993). Prediction of protein secondary structure at better than 70% accuracy. J. Mol. Biol. *232*, 584–599.

Samama, P., Cotecchia, S., Costa, T., and Lefkowitz, R. J. (1993). A mutation-induced activated state of the $\beta_2$-adrenergic receptor. Extending the ternary complex model. J. Biol. Chem. *268*, 4625–4636.

Schwartz, M. A., and Madhani, H. D. (2004). Principles of MAP kinase signaling specificity in *Saccharomyces cerevisiae.* Annu. Rev. Genet. *38*, 725–748.

Schwindinger, W. F., and Robishaw, J. D. (2001). Heterotrimeric G-protein $\beta\gamma$-dimers in growth and differentiation. Oncogene *20*, 1653–1660.

Seifert, R., Wenzel-Seifert, K., and Kobilka, B. K. (1999). GPCR-G$\alpha$ fusion proteins: molecular analysis of receptor-G-protein coupling. Trends Pharmacol. Sci. *20*, 383–389.

Shea, L., and Linderman, J. J. (1997). Mechanistic model of G-protein signal transduction. Determinants of efficacy and effect of precoupled receptors. Biochem. Pharmacol. *53*, 519–530.

Sherman, F. (1991). Getting started with yeast. Methods Enzymol. *194*, 3–21.

Slessareva, J. E., Ma, H., Depree, K. M., Flood, L. A., Bae, H., Cabrera-Vera, T. M., Hamm, H. E., and Graber, S. G. (2003). Closely related G-protein-coupled receptors use multiple and distinct domains on G-protein $\alpha$-subunits for selective coupling. J. Biol. Chem. *278*, 50530–50536.

Sondek, J., Bohm, A., Lambright, D. G., Hamm, H. E., and Sigler, P. B. (1996). Crystal structure of a $G_A$ protein $\beta\gamma$ dimer at 2.1 Å resolution. Nature *379*, 369–374.

Song, J., and Dohlman, H. G. (1996). Partial constitutive activation of pheromone responses by a palmitoylation-site mutant of a G protein $\alpha$ subunit in yeast. Biochemistry *35*, 14806–14817.

Song, J., Hirschman, J., Gunn, K., and Dohlman, H. G. (1996). Regulation of membrane and subunit interactions by N-myristoylation of a G protein $\alpha$ subunit in yeast. J. Biol. Chem. *271*, 20273–20283.

Sprang, S. R. (1997). G protein mechanisms: Insights from structural analysis. Annu. Rev. Biochem. *66*, 639–678.

Stefan, C. J., Overton, M. C., and Blumer, K. J. (1998). Mechanisms governing the activation and trafficking of yeast G protein-coupled receptors. Mol. Biol. Cell *9*, 885–899.

Strader, C. D., Fong, T. M., Tota, M. R., Underwood, D., and Dixon, R. A. (1994). Structure and function of G protein-coupled receptors. Annu. Rev. Biochem. *63*, 101–132.

Takida, S., and Wedegaertner, P. B. (2003). Heterotrimer formation, together with isoprenylation, is required for plasma membrane targeting of G$\beta\gamma$. J. Biol. Chem. *278*, 17284–17290.

Tamaki, H., Miwa, T., Shinozaki, M., Saito, M., Yun, C. W., Yamamoto, K., and Kumagai, H. (2000). GPR1 regulates filamentous growth through *FLO11* in yeast *Saccharomyces cerevisiae.* Biochem. Biophys. Res. Commun. *267*, 164–168.

Thiyagarajan, M. M., Bigras, E., Van Tol, H. H., Hébert, T. E., Evanko, D. S., and Wedegaertner, P. B. (2002). Activation-induced subcellular redistribution of $G\alpha_s$ is dependent upon its unique N-terminus. Biochemistry *41*, 9470–9484.

Thompson, J. D., Higgins, D. G., and Gibson, T. J. (1994). CLUSTAL W: improving the sensitivity of progressive multiple sequence alignment through sequence weighting, position-specific gap penalties and weight matrix choice. Nucleic Acids Res. *22*, 4673–4680.

Wall, M. A., Coleman, D. E., Lee, E., Iñiguez-Lluhi, J. A., Posner, B. A., Gilman, A. G., and Sprang, S. R. (1995). The structure of the G protein heterotrimer $G_{i\alpha1\beta1\gamma2}$. Cell *83*, 1047–1058.

Wall, M. A., Posner, B. A., and Sprang, S. R. (1998). Structural basis of activity and subunit recognition in G protein heterotrimers. Structure *6*, 1169–1183.

Wedegaertner, P. B., Bourne, H. R., and von Zastrow, M. (1996). Activation-induced subcellular redistribution of $G_{s\alpha}$. Mol. Biol. Cell *7*, 1225–1233.

Wedegaertner, P. B., Chu, D. H., Wilson, P. T., Levis, M. J., and Bourne, H. R. (1993). Palmitoylation is required for signaling functions and membrane attachment of $G_q\alpha$ and $G_s\alpha$. J. Biol. Chem. *268*, 25001–25008.

Wilson, P. T., and Bourne, H. R. (1995). Fatty acylation of $a_z$. Effects of palmitoylation and myristoylation on $\alpha_z$ signaling. J. Biol. Chem. *270*, 9667–9675.

Wise, A., Grassie, M. A., Parenti, M., Lee, M., Rees, S., and Milligan, G. (1997). A cysteine-3 to serine mutation of the G-protein $G_{i1}\alpha$ abrogates functional activation by the $\alpha_{2A}$-adrenoceptor but not interactions with the $\beta\gamma$ complex. Biochemistry *36*, 10620–10629.

Xue, Y., Batlle, M., and Hirsch, J. P. (1998). GPR1 encodes a putative G protein-coupled receptor that associates with the Gpa2p $G_{\alpha}$ subunit and functions in a Ras-independent pathway. EMBO J. *17*, 1996–2007.

Yamaguchi, Y., Katoh, H., and Negishi, M. (2003). N-terminal short sequences of $\alpha$ subunits of the $G_{12}$ family determine selective coupling to receptors. J. Biol. Chem. *278*, 14936–14939.

Yun, C. W., Tamaki, H., Nakayama, R., Yamamoto, K., and Kumagai, H. (1997). G-protein coupled receptor from yeast *Saccharomyces cerevisiae.* Biochem. Biophys. Res. Commun. *240*, 287–292.

Yun, C. W., Tamaki, H., Nakayama, R., Yamamoto, K., and Kumagai, H. (1998). Gpr1p, a putative G-protein coupled receptor, regulates glucose-dependent cellular cAMP level in yeast *Saccharomyces cerevisiae.* Biochem. Biophys. Res. Commun. *252*, 29–33.

Molecular Cell 22, 819–830, June 23, 2006 ©2006 Elsevier Inc. DOI 10.1016/j.molcel.2006.05.011

# The Kelch Proteins Gpb1 and Gpb2 Inhibit Ras Activity via Association with the Yeast RasGAP Neurofibromin Homologs Ira1 and Ira2

**Toshiaki Harashima,[1,3] Scott Anderson,[2] John R. Yates III,[2] and Joseph Heitman[1,*]**
[1] Department of Molecular Genetics and Microbiology
Duke University Medical Center
Durham, North Carolina 27710
[2] The Scripps Research Institute
La Jolla, California 92037

## Summary

**The G protein-coupled receptor Gpr1 and associated Gα subunit Gpa2 govern dimorphic transitions in response to extracellular nutrients by signaling coordinately with Ras to activate adenylyl cyclase in the yeast *Saccharomyces cerevisiae*. Gpa2 forms a protein complex with the kelch Gβ mimic subunits Gpb1/2, and previous studies demonstrate that Gpb1/2 negatively control cAMP-PKA signaling via Gpa2 and an unknown second target. Here, we define these targets of Gpb1/2 as the yeast neurofibromin homologs Ira1 and Ira2, which function as GTPase activating proteins of Ras. Gpb1/2 bind to a conserved C-terminal domain of Ira1/2, and loss of Gpb1/2 results in a destabilization of Ira1 and Ira2, leading to elevated levels of Ras2-GTP and unbridled cAMP-PKA signaling. Because the Gpb1/2 binding domain on Ira1/2 is conserved in the human neurofibromin protein, an analogous signaling network may contribute to the neoplastic development of neurofibromatosis type 1.**

## Introduction

Molecular switches composed of G protein-coupled receptors (GPCRs) and associated heterotrimeric G proteins transduce extracellular stimuli to intracellular signaling molecules, including the ubiquitous second messenger cAMP. Canonical heterotrimeric G proteins consist of α, β, and γ subunits. Ligand binding induces conformational changes in the receptor, stimulating GDP to GTP exchange on the associated Gα subunits, leading to dissociation of the receptor-Gα subunit complex and release of the Gβγ dimer. Liberated Gα, Gβγ, or both signal via downstream effectors. Signal transduction is attenuated by either intrinsic or RGS-stimulated GTP hydrolysis followed by reassociation of Gα-GDP with the Gβγ dimer (Cabrera-Vera et al., 2003; Dohlman et al., 1991; Ross and Wilkie, 2000).

The budding yeast *Saccharomyces cerevisiae* deploys two distinct GPCR-G protein signaling modules to sense pheromones and nutrients, respectively (Harashima and Heitman, 2004). One is haploid and mating-type specific and involves the pheromone receptors Ste2/3 coupled to the Gα subunit Gpa1 in a canonical heterotrimeric complex with the Gβγ subunits Ste4/18. In response to pheromone, the Ste4/18 dimer dissociates from Gpa1 and activates the pheromone-responsive MAP kinase pathway to enable mating.

The second yeast GPCR signaling cascade involves the GPCR Gpr1, which is expressed in both haploid and diploid cells and activates the associated Gα subunit Gpa2 in response to glucose and structurally related sugars (Lemaire et al., 2004; Lorenz et al., 2000; Xue et al., 1998; Yun et al., 1998). Activated Gpa2 stimulates cAMP production by adenylyl cyclase and engages the PKA signaling pathway (Colombo et al., 1998; Lorenz and Heitman, 1997). In contrast to canonical Gα subunits, Gpa2 is unable to form a heterotrimeric G protein with the known Gβγ subunits Ste4/18. Instead, Gpa2 associates with two kelch proteins, Gpb1 and Gpb2, which are functionally redundant, share ~35% sequence identity, and each contain seven kelch repeat motifs. In a striking example of convergent evolution, both the WD-40 repeat-based Gβ subunits and the kelch repeat enzyme galactose oxidase are known to fold into seven bladed β propeller structures that are essentially superimposable (Harashima and Heitman, 2004).

Mutants lacking the Gpr1 receptor or the coupled Gpa2 subunit are defective in glucose-induced cAMP production and filamentous growth, whereas *gpb1,2* double mutants exhibit increased PKA phenotypes, including enhanced filamentous growth, sensitivity to nitrogen starvation and heat shock, and impaired glycogen accumulation and sporulation (Batlle et al., 2003; Harashima and Heitman, 2002). Introduction of *gpa2* mutations only partially attenuates these *gpb1,2* mutant phenotypes, providing evidence that Gpb1/2 negatively regulate cAMP signaling by inhibiting Gpa2 and an as yet unidentified second target. Mutation of the gene encoding one of the three PKA catalytic subunits, Tpk2, largely suppresses the elevated PKA phenotypes of *gpb1,2* mutants, indicating that this second target may be a component of the cAMP signaling pathway itself (Harashima and Heitman, 2002). Our recent studies provide evidence that Gpb1/2 are recruited to and function at the plasma membrane in a Gpa2-dependent manner, suggesting that the unidentified second target may be membrane-associated (Harashima and Heitman, 2005).

In *S. cerevisiae*, the cAMP-PKA signaling cascade is essential for cell viability. Loss of either adenylyl cyclase (Cyr1) or all three PKA catalytic subunits (Tpk1,2,3) is lethal (Toda et al., 1988; Toda et al., 1987b). On the other hand, elevated PKA activity as a consequence of mutations in the PKA regulatory subunit Bcy1 results in a growth defect (Toda et al., 1987a). Therefore, cAMP signaling must be strictly controlled in response to extracellular cues. Two distinct Gpr1-Gpa2 and Ras-mediated pathways converge on Cyr1. Notably, *ras2* mutants fail to produce cAMP in response to glucose, similar to *gpr1* and *gpa2* mutants, and *gpr1 ras2* and *gpa2 ras2* mutants exhibit a synthetic growth defect, suggesting that Gpr1-Gpa2 and Ras2 play a shared role in glucose-induced cAMP production (Bhattacharya et al., 1995; Kübler et al., 1997; Xue et al., 1998).

*Correspondence: heitm001@duke.edu
[3] Present address: Division of Molecular Cell Biology, National Institute for Basic Biology, Nishigonaka 38, Myodaiji, Okazaki 444-8585, Aichi, Japan.

*S. cerevisiae* expresses two Ras proteins: Ras1 and Ras2 (Powers et al., 1984). Although Ras1 and Ras2 are functionally redundant for cell growth, Ras2 plays the predominant role in cAMP signaling in response to glucose. Ras activity is controlled positively by the guanine nucleotide exchange factors Cdc25 and Sdc25 (GEFs) and negatively by the GTPase activating proteins Ira1 and Ira2 (GAPs) (Crechet et al., 1990; Munder and Furst, 1992; Tanaka et al., 1990a, 1991). Ras2 is known to bind to and activate Cyr1, yet how Ras2 regulates Cyr1 in response to glucose is not understood at a molecular level (Field et al., 1988; Mintzer and Field, 1994). Previous studies have implicated Cdc25 in responses to glucose (Gross et al., 1999; Munder and Kuntzel, 1989; Portillo and Mazon, 1986). On the other hand, Ira1 has been shown to interact with Cyr1 and may promote its membrane localization (Mitts et al., 1991). *ira1,2* double mutant cells exhibit constitutively elevated Ras2-GTP levels and are unable to further mount a Ras2-GTP increase in response to glucose (Colombo et al., 2004). Therefore, both Cdc25 and Ira1/2 may coordinately activate Ras2 and adenylyl cyclase in response to glucose.

The RasGAP Ira1/2 proteins are large (~350 kDa) proteins that are conserved from yeast to humans (Tanaka et al., 1989, 1990b). In humans, the RasGAP activity of the Ira1/2 homolog neurofibromin is implicated in one of the most common genetic diseases, neurofibromatosis type I (NF1) (Ballester et al., 1990; Cawthon et al., 1990; Viskochil et al., 1990; Wallace et al., 1990; Xu et al., 1990a). Although the *IRA1*, *IRA2*, and *NF1* genes were cloned more than a decade ago, how the RasGAP activity of these proteins is controlled is largely unknown. Here, we identified the yeast neurofibromin homologs Ira1/2 as targets of the kelch Gβ mimic subunits Gpb1/2. Gpb1/2 bind to a conserved C-terminal domain, stabilize Ira1/2, and thereby serve to govern cAMP-PKA signaling by constraining Ras2-GTP excursions. These findings have profound potential implications for our understanding of NF1 functions in normal cell growth control and its dysregulation in individuals with NF1.

## Results

### Kelch Gβ Mimic Proteins Act Upstream of the PKA Pathway

We hypothesized that the second target of the kelch Gβ mimic Gpb1/2 proteins might be either an early or a later component of the PKA pathway. Here, epistasis analysis was used to pinpoint the site of Gpb1/2 action. In models in which Gpb1/2 function downstream of Cyr1, *gpb1,2* mutations would be predicted to rescue the growth defect of *ras2 gpa2* double mutant cells. To test this hypothesis, two diploid mutants (*gpa2/gpa2 ras2/RAS2* and *gpb1,2/gpb1,2 gpa2/GPA2 ras2/ras2*) were constructed, sporulated, and dissected. As shown in Figure 1A, *gpb1,2 ras2 gpa2* cells were as growth impaired as *ras2 gpa2* cells, providing evidence that Gpb1/2 instead act early in the pathway via Cyr1 or one of its regulatory elements such as Ras1/2, Cdc25, or Ira1/2.

To examine genetic interactions between *gpb1,2* and *ras2* mutations, the *RAS2* gene was deleted in *gpb1,2* cells and the resulting *gpb1,2 ras2* cells were tested for filamentous growth, *FLO11* expression, sensitivity to nitrogen starvation, and glycogen accumulation (Figures 1B–1F). Consistent with our previous findings, *gpb1,2* cells exhibited elevated pseudohyphal and invasive growth, increased *FLO11* expression, sensitivity to nitrogen starvation, and reduced glycogen accumulation. Introduction of a *gpa2* mutation partially suppressed these *gpb1,2* mutant phenotypes (Figure 1 and Harashima and Heitman [2002]). On the other hand, introduction of a *ras2* mutation more completely suppressed these *gpb1,2* mutant phenotypes. Steady-state and glucose-induced cAMP levels were also determined. As shown previously (Harashima and Heitman, 2002), an increased basal level of cAMP was observed in *gpb1,2* cells, and this elevated cAMP level was restored to the wild-type level by a *ras2* mutation (Figure 1G). Introduction of a *ras1* mutation was unable to suppress any of the *gpb1,2* mutant phenotypes (data not shown). Taken together, these genetic studies support the hypothesis that Gpb1/2 act directly on Ras2 or one of its regulators such as the RasGEF Cdc25 or the RasGAP Ira1/2 proteins.

### RasGAP Proteins Ira1/2 Interact with the Kelch Gβ Mimic Subunits Gpb1/2

Possible targets of Gpb1/2 were identified by mass spectrometry analysis of the Gpb1/2 native protein complex. For this purpose, the FLAG epitope tag was fused to the carboxy terminus of Gpb1 and to the amino terminus of Gpb2. These FLAG-Gpb1/2 proteins were expressed from an attenuated *ADH1* promoter on a 2 μm plasmid. Expression of the FLAG-tagged proteins restored wild-type filamentous growth of the *gpb1,2* double mutant strain, indicating that both fusion proteins are functional (data not shown). Because endogenous Gpa2 and Gpb1/2 may compete for Gpb1/2 with other targets, the FLAG-Gpb1/2 proteins were expressed in *gpa2 gpb1,2* triple mutant cells. Crude cellular extracts were prepared, and Gpb1/2 and interacting proteins were coimmunoprecipitated by using an anti-FLAG affinity matrix. The native protein complexes were eluted with FLAG peptide, and the eluted proteins were analyzed by mass spectrometry (see Experimental Procedures).

This analysis revealed a number of candidate Gpb1/2-interacting proteins. Importantly, the list of Gpb2-interacting proteins included Ira1 and Ira2, and no other components of the cAMP-PKA signaling cascade (including Cdc25, Ras1/2, Cyr1, Pde1/2, Bcy1, Tpk1/2/3, Flo8, or Sfl1) were identified (data not shown). Because Gpb1 and Gpb2, and also Ira1 and Ira2, represent partially redundant protein pairs, we hypothesized that Gpb1 and Gpb2 might bind to both Ira1 and Ira2. To address this possibility, Gpb1 was N-terminally tagged and expressed, and Gpb1/2-Ira1/2 interactions were examined in cells that also expressed a functional version of the Ira1 or Ira2 protein fused with three copies of the hemagglutinin epitope tag (3HA) (Figure 2). Importantly, this coimmunoprecipitation analysis revealed that Gpb1 and Gpb2 both interact with both Ira1 and Ira2 (Figures 2A and 2B).

Gpb1/2 contain a unique N-terminal domain and a C-terminal domain containing seven kelch repeats. Our previous studies revealed that the kelch domains of Gpb2 bind to Gpa2 but the unique N-terminal domain does not (Harashima and Heitman, 2002). To examine which domain(s) is required for the Gpb1/2-Ira1/2

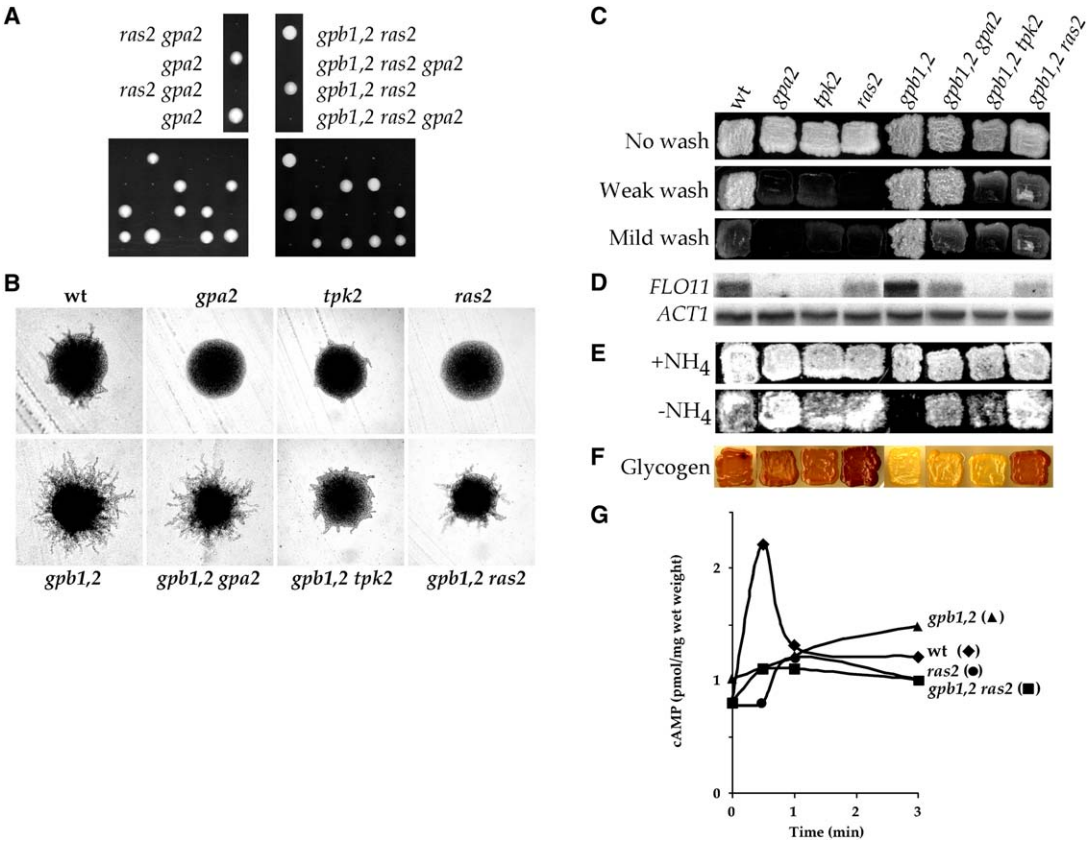


Figure 1. Genetic Interactions between *gpb1,2* and *ras2* Mutations

(A) *gpb1,2* mutations are unable to suppress the synthetic growth defect of *gpa2 ras2* mutant cells. Diploid *gpa2::G418/gpa2::hph ras2::nat/RAS2* (left) and *gpb1,2::loxP/gpb1,2::loxP gpa2::loxP-G418/GPA2 ras2::nat/ras2::nat* (right) cells were sporulated and dissected.

(B–F) *ras2* mutations alleviate increased PKA phenotypes associated with *gpb1,2* mutations, including enhanced pseudohyphal growth (B), hyperinvasive growth (C), increased *FLO11* expression (D), sensitivity to nitrogen starvation (E), and reduced glycogen accumulation (F).

(G) Glucose-induced cAMP production was examined. Glucose was added to glucose-starved cells, and at the indicated time points, cells were collected and cAMP levels were determined.

interaction, the FLAG tag was fused to either the N terminus of the N-terminal unique domain (FLAG-Gpb2N) or to the C-terminal kelch domain (FLAG-Gpb2C), and the resulting fusion proteins and FLAG-Gpb2 were coexpressed with the Ira1-3HA protein in vivo (Figure 2C). In contrast to the Gpa2-Gpb1/2 interaction, neither the Gpb2 N-terminal nor the C-terminal domain alone was sufficient to bind to Ira1. Therefore, both Gpb2 domains are required for interaction with Ira1. We note that the unique N-terminal and the C-terminal kelch domains are both essential for Gpb1/2 function in vivo (Harashima and Heitman, 2002).

Because the *gpb1,2* mutant phenotypes were suppressed by *ras2* mutations and Gpb1/2 bind to the RasGAP proteins Ira1/2, Gpb1/2 could associate with Ira1/2 and function via Ras2. However, Gpb1/2 interacted with Ira1/2 in the absence of Ras2 as strongly as in the presence of Ras2 (Figure 2D). Therefore, Ras2 is dispensable for the Gpb1/2-Ira1/2 interactions, and Gpb1/2 may control Ras activity through direct interaction with Ira1/2.

### Gpb1/2 Are Genetically Implicated in Both Gpa2- and Ras-Mediated Signaling

*ras2* mutants are defective in filamentous growth, whereas wild-type cells expressing a dominant active *RAS2*$^{G19V}$ allele that lacks intrinsic GTPase activity exhibit elevated filamentous growth. Consistent with these findings, cells lacking Ira1, Ira2, or both Ira1 and Ira2 were also hyperfilamentous (Figure 3A). Importantly, *ira1,2* cells expressing Gpb1/2 and *ira1,2 gpb1,2* quadruple mutant cells lacking Gpb1/2 were morphologically indistinguishable from each other. These findings support models in which the hyperfilamentous phenotype conferred by the *gpb1,2* mutations may be exerted via Ira1/2.

Expression of the dominant active *GPA2*$^{Q300L}$ and *RAS2*$^{G19V}$ alleles dramatically enhances filamentous growth of wild-type cells (Figure 3B). In contrast, little if any further effect was observed when these dominant active mutant alleles were expressed in the hyperfilamentous *gpb1,2* double mutant, supporting models in which Gpa2 and Ras2 are activated by the *gpb1,2* mutations and Gpb1/2 function to negatively control the activity of both (Figure 3B).

If Gpb1/2 regulate Ira1/2, and the hyperfilamentous phenotype of the *gpb1,2* mutant is due to reduced Ira1/2 RasGAP activity, increased expression of the *IRA2* gene should suppress the *gpb1,2* mutant phenotype. In fact, overexpression of the *IRA2* gene attenuated pseudohyphal differentiation of the *gpb1,2* mutant (Figure 3C).

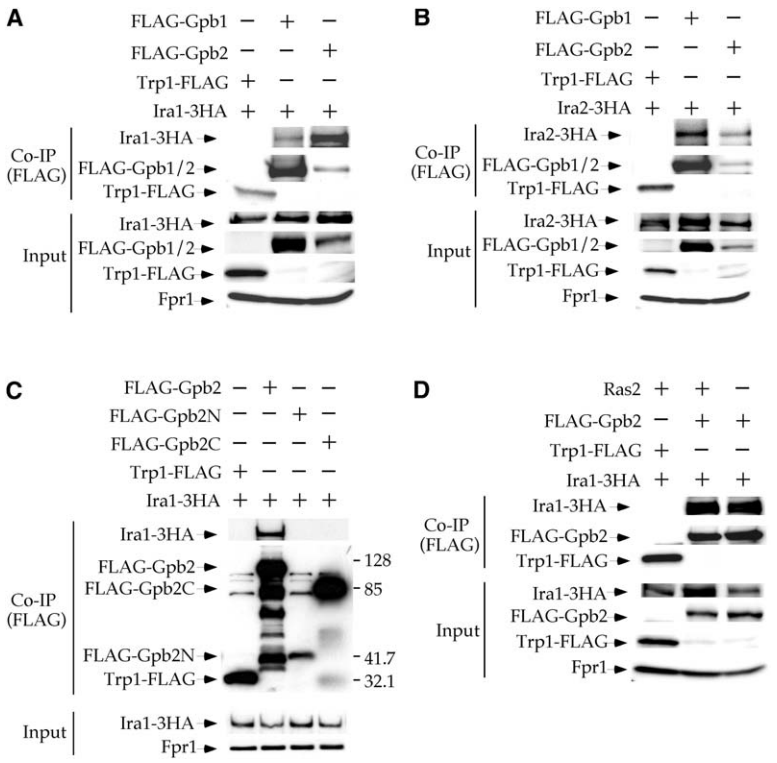


Figure 2. Kelch Gβ Mimic Subunits Interact with RasGAP Ira1/2

(A and B) Ira1 (A) and Ira2 (B) physically bind to Gpb1/2 in vivo. The N-terminally FLAG-tagged Gpb1 (pTH111) and Gpb2 (pTH88) proteins were expressed in yeast cells that also express C-terminally 3HA-tagged Ira1 or Ira2 and immunoprecipitated.

(C) Gpb2 requires both the unique N-terminal and the C-terminal kelch domains to interact with Ira1. The N-terminally FLAG-tagged Gpb2 N-terminal region (FLAG-Gpb2N), C-terminal kelch domains (FLAG-Gpb2C), or full-length Gpb2 (FLAG-Gpb2) was coexpressed with the Ira1-3HA protein in vivo. Positions of molecular marker (128, 85, 41.7, and 32.1 k) are indicated to the right of the panel.

(D) Ras2 is dispensable for the Gpb2-Ira1 interaction. Gpb2-Ira1 interactions were examined in the presence and absence of Ras2 by using cells that express FLAG-Gpb2.

Note that the first lane in the Co-IP panels of (A) and (B) was spliced to eliminate a space and that the data in each panel are directly comparable.

In (A)–(D), protein complexes were captured on anti-FLAG affinity gel and detected with anti-FLAG or anti-HA. Input levels of Ira1/2 were captured on anti-HA agurose beads, eluted, and analyzed by Western blot using anti-HA antibody (see the Experimental Procedures for details).

Consistently, neither loss of the *IRA1/2* genes nor introduction of the *RAS2*$^{G19V}$ gene exaggerated mutant phenotypes (including hyperinvasion, nitrogen starvation sensitivity, and decreased glycogen) associated with an elevated PKA activity in *gpb1,2* cells (Figures 3D–3F). On the other hand, overproduction of Ira2 was able to alleviate these *gpb1,2* mutant phenotypes (Figures 3D–3F). In addition, the increased basal and glucose-induced cAMP levels in *gpb1,2* cells were significantly attenuated by Ira2 overproduction (Figure 3G).

In summary, these genetic data provide evidence that Gpb1/2 negatively control cAMP signaling via Ira1/2.

## Gpb1/2 Control Ira1/2 RasGAP Activity

Biochemical and genetic data indicate that Ira1/2 represent secondary targets of Gpb1/2 and that Gpb1/2 function to enhance Ira1/2 activity. To investigate this at a mechanistic level, we quantified Ras2-GTP levels by measuring Ras2 protein binding to the Raf1 kinase that specifically interacts with Ras-GTP (Colombo et al., 2004). A low copy number plasmid carrying the wild-type *RAS2* or dominant active *RAS2*$^{G19V}$ gene was introduced into wild-type, *gpb1,2*, *ira1*, *ira2*, and *ira1,2* cells. Transformants were grown in synthetic medium to mid-logarithmic growth phase, and crude cell extracts were prepared to assess the steady state levels of Ras2-GTP.

As shown previously, the Ras-GTP level was increased ~5-fold in *ira1* and *ira2* cells, (Figure 4A and Tanaka et al. [1990a]). Similarly, *gpb1,2* cells also exhibited an ~5 fold increase in Ras2-GTP levels, indicative of reduced RasGAP activity (Figure 4A). The Ras-GTP level in *ira1,2* cells was further increased and comparable to that in wild-type and *gpb1,2* cells expressing the *RAS2*$^{G19V}$ gene, in which an ~25-fold increase in Ras-GTP was observed (Figure 4A). These observations are in accord with the previous finding documenting that Ras2-GTP levels were indistinguishable between wild-type and *ira1,2* cells when the *RAS2*$^{G19V}$ gene was expressed (Tanaka et al., 1990a). In summary, loss of Gpb1/2 results in an elevation of Ras2-GTP, possibly by reducing, but not eliminating, the RasGAP activity of Ira1/2.

## Gpb1/2 Control Protein Levels of Ira1/2

To elucidate how Gpb1/2 control Ira1/2 RasGAP activity, we investigated the levels of the Ira1/2 proteins as well as Ira1/2-Ras2 interactions in the presence and absence of Gpb1/2. To examine protein levels, the functional Ira1/2-3HA proteins were expressed. Neither Ira1 nor Ira2 was detectable by Western blot analysis using crude cell extracts because of low expression levels (data not shown). The Ira1/2-3HA proteins were therefore enriched by immunoprecipitation using anti-HA-conjugated agarose beads, which also enabled an examination of the levels of the Ras2 protein bound to the Ira1/2-3HA affinity captured proteins (Figure 4B).

As shown in Figure 4B, loss of Gpb1/2 resulted in a marked decrease in the levels of both Ira1 and Ira2 and a concomitant loss of Ras2 as an Ira1/2-interacting protein. Reintroduction of the *GPB1* and *GPB2* genes complemented this defect and restored the levels of Ira1/2 to the wild-type levels, indicating that Gpb1/2 govern the stability of Ira1/2.

To confirm this model, protein stability of Ira1/2 was examined in the presence and absence of Gpb1/2 by a pulse-chase analysis (Figures 4C and 4D). In wild-type cells, the Ira1/2 and Fpr1 proteins were stable over time, and the half life ($t_{1/2}$) of these proteins was more

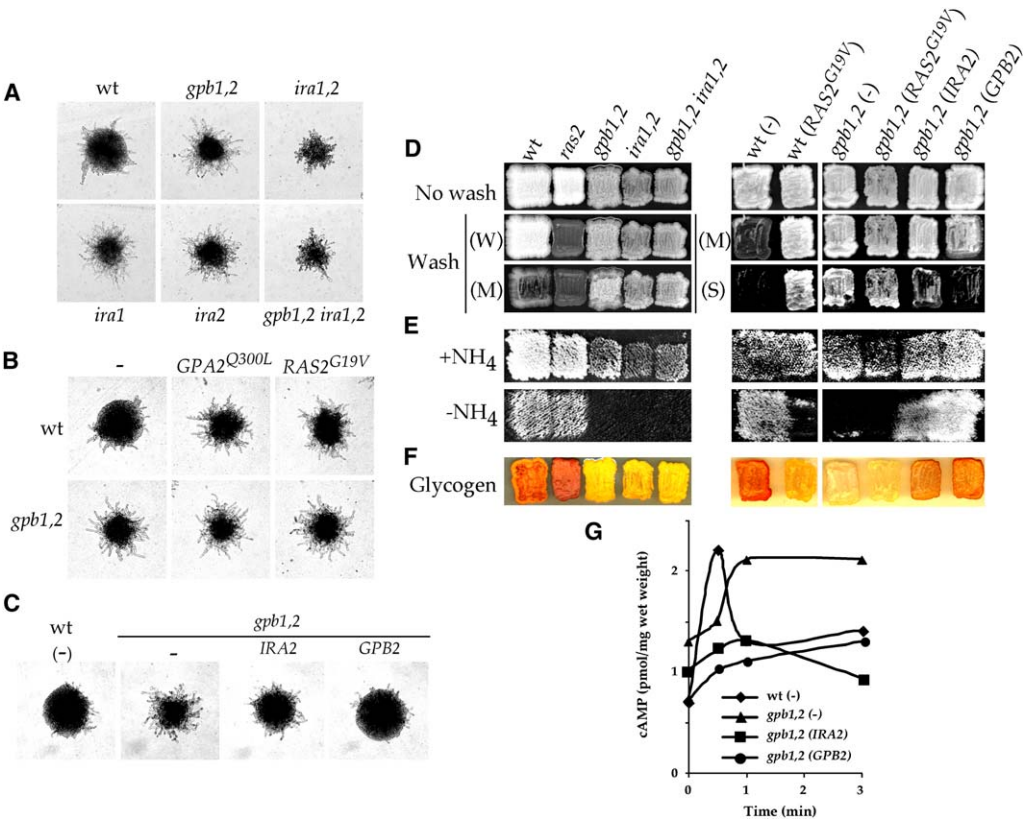


Figure 3. Genetic Interactions between *gpb1,2* and *ira1,2* Mutations

(A) Isogenic diploid strains indicated were assayed for pseudohyphal growth.

(B) The dominant active $GPA2^{Q300L}$ and $RAS2^{G19V}$ alleles were introduced into diploid wild-type and *gpb1,2* cells and tested for filamentous growth.

(C) Ira2 overproduction suppressed the increased filamentous phenotype of *gpb1,2* cells.

(D) Haploid cells indicated were tested for invasive growth. Cells were grown on YPD at 30ºC for 5 days and photographed after weak (W), mild (M), or strong (S) washing.

(E) Cells were grown on YPD at 30ºC for 2 days and replica plated onto nitrogen-replete ($+NH_4$) and no nitrogen ($-NH_4$) media to test for nitrogen starvation sensitivity. After 6 (left) or 10 (right) days at 30ºC, cells were replica plated onto YPD again and incubated under the same conditions.

(F) Glycogen levels of cells grown on YPD at 30ºC for 2 days were determined by using iodine vapor.

(G) cAMP levels were determined in response to glucose readdition as described in the legend of Figure 1.

than 4 hr ($t_{1/2} > 4$ hr, Figures 4C and 4D and data not shown). Similarly, the Fpr1 protein in *gpb1,2* cells was as stable as in wild-type cells (Figures 4C and 4D and data not shown). However, levels of the Ira1/2 proteins decreased rapidly, and the half-life of Ira1 and Ira2 was reduced to ~30 and 25 min, respectively (Figures 4C and 4D). Therefore, we conclude that Gpb1/2 bind to and stabilize Ira1/2 and that loss of Gpb1/2 leads to reduced Ira1/2 protein levels.

### Gpb1/2 Stabilize Ira1/2 by Binding to a C-Terminal Domain

To establish how Gpb1/2 control stability of the Ira1/2 proteins, the Gpb1/2 binding domain on Ira1/2 was identified. For this purpose, deletions were created in the endogenous Ira1 C terminus by inserting the 3HA epitope and expressing these deletion derivatives in an otherwise wild-type background (Figure 5). Plasmids expressing the FLAG-Gpb1/2 proteins were then introduced into the resulting Ira1 deletion mutant cells, and Gpb1/2-Ira1 interactions were examined by FLAG-mediated coimmunoprecipitation (Figures 5A and 5B).

By Western blot analysis, the level of the C-terminally truncated 1–2925 aa Ira1 protein was significantly reduced and the shorter 1–2714 aa and 1–2432 aa Ira1 proteins were undetectable in this assay (Figure 5A and "Input" panel in Figure 5B). Because Gpb1/2 control the stability of the Ira1/2 proteins, deletion of a Gpb1/2 binding site should result in a decrease in Ira1/2 protein levels. Thus, we hypothesized that the Gpb1/2 binding site might be present in the C-terminal region of Ira1 necessary for Ira1 stability. In fact, Gpb1/2 bound to the Ira1 deletion protein retaining 1–2925 aa, but not to the derivative containing only 1–1257 aa (Figure 5A and "Co-IP" panel in Figure 5B). Furthermore, two N-terminal deletion derivatives that retain amino acid residues 2433–3092 and 2715–3092 were stably expressed and both associated with Gpb1/2 (Figure 5C). A C-terminal region spanning 2715–2925 aa of Ira1 also bound to Gpb1/2 (Figure 5D), and loss of this region resulted in instability of this Ira1 deletion derivative in accord with the role of Gpb1/2 in Ira1 protein stability (Figure 5A and data not shown). Taken together, these results reveal that the Gpb1/2 binding domain (GBD) maps between

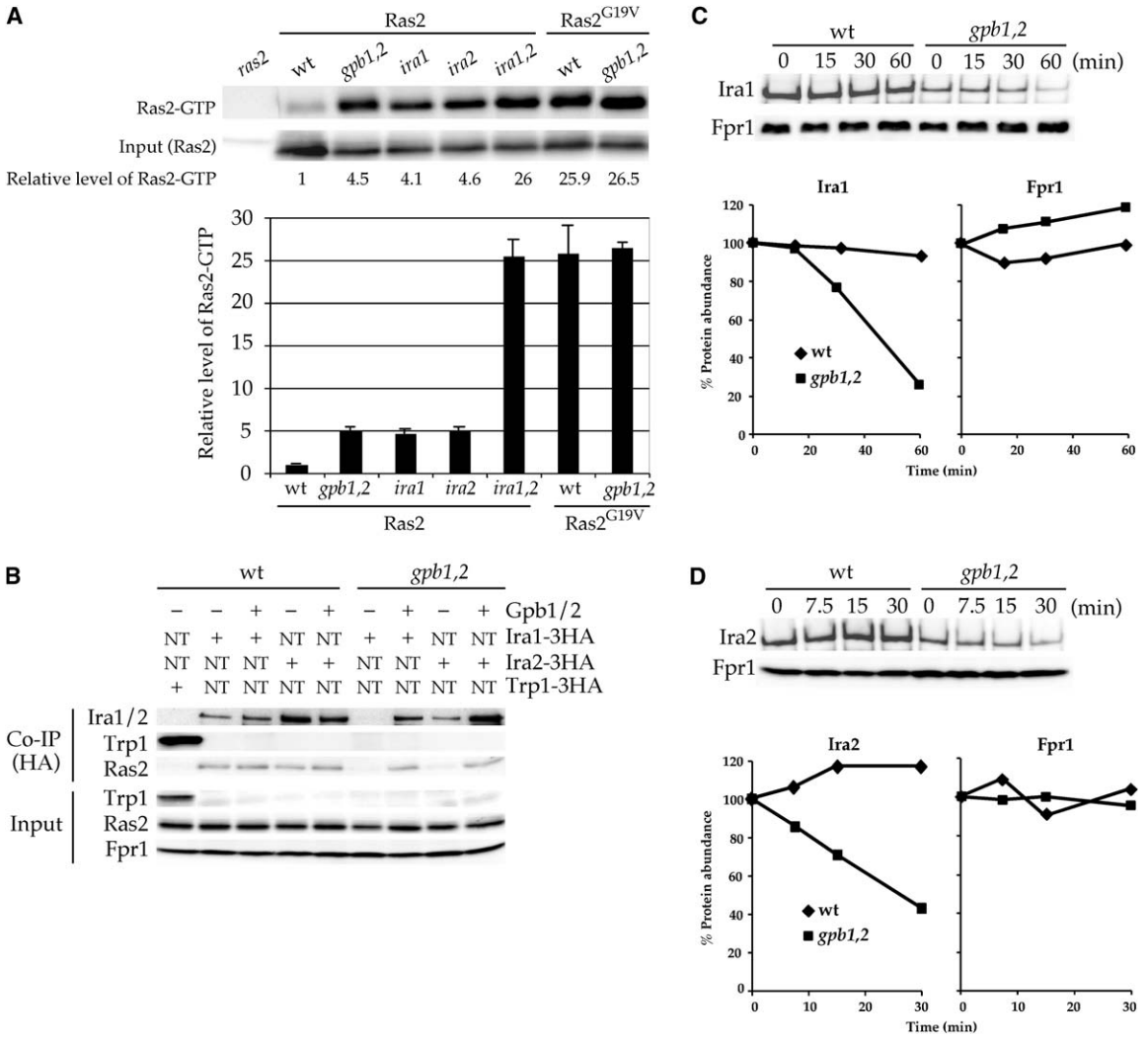


Figure 4. Gpb1/2 Stabilize Ira1/2

(A) The relative increase in Ras2-GTP was examined in haploid cells that express the wild-type or dominant active (G19V) *RAS2* gene. Representative data are shown in the top panel. Purified Ras2-GTP from *ira1,2* double mutant cells expressing the wild-type Ras2 protein and wild-type and *gpb1,2* mutant cells that express the dominant active $Ras2^{G19V}$ protein was 5-fold diluted prior to Western analysis, as the levels of Ras2-GTP in these cells were higher than those in the other cells. Levels of Ras-GTP and total cellular Ras protein ("Input") were densitometrically quantified. Ras2-GTP levels were then normalized to "Input" Ras2 levels and shown as a relative level to Ras2-GTP in wild-type cells in the bottom panel. The values shown in the bottom panel are the means of two or three independent experiments with the standard error of the mean.
(B) The *GPB1/2* genes were introduced into wild-type and *gpb1,2* cells expressing either *IRA1-3HA* or *IRA2-3HA* to examine protein stability of Ira1/2 and the Ras2-Ira1/2 interactions. "NT" indicates the nontagged, wild-type Ira1, Ira2, or Trp1 protein. Based on densitometric analysis, the steady-state protein levels of Ira1/2 were reduced in *gpb1,2* cells by at least 2- to 10-fold compared to wild-type cells.
(C and D) Protein stability of Ira1/2 was investigated by cycloheximide-chase assay in the presence and absence of Gpb1/2. Levels of Ira1/2-3HA and Fpr1 were densitometorically quantified, and the percentage of protein abundance of Ira1/2 and Fpr1 at "Time 0" is shown in the bottom panel. Note that the first and the last lanes in the "Ras2-GTP" and "Input" panels in (A) were spliced to eliminate a space or a lane and that the data in each panel are directly comparable.

amino acids 2715 and 2925 of Ira1. Significantly, this region is conserved in homologs of Ira1, including the human neurofibromin protein (see Discussion).

Equivalent deletions were also introduced into Ira2 (Figure S1 available in the Supplemental Data with this article online). The level of the Ira2 C-terminal deletion protein retaining 1–2922 aa was reduced, and this Ira2 deletion derivative was still able to interact with Gpb1/2 (Figures S1A and S1B). An Ira2 variant that preserves 1–2702 aa, but not the GBD, was now undetectable (Figure S1B). These findings are similar to the equivalent Ira1 deletion proteins (1–2925 aa and 1–2714 aa) (Figure 5). Both Gpb1 and Gpb2 bind to Ira2 deletion derivatives retaining amino acids 2703–3079 and 2703–2922 that are homologous to the regions spanning the corresponding amino acids 2715–3092 and 2715–2925 of Ira1 (Figures S1C and S1D). These results provide evidence that the GBD maps to the corresponding regions of both Ira1 and Ira2.

### The C Terminus of Ira1/2 Is Required for Function

Biochemical studies reveal that deletion of the C-terminal 167 amino acids, and deletion of the C-terminal 378 amino acids or the GBD in the Ira1 protein reduce and

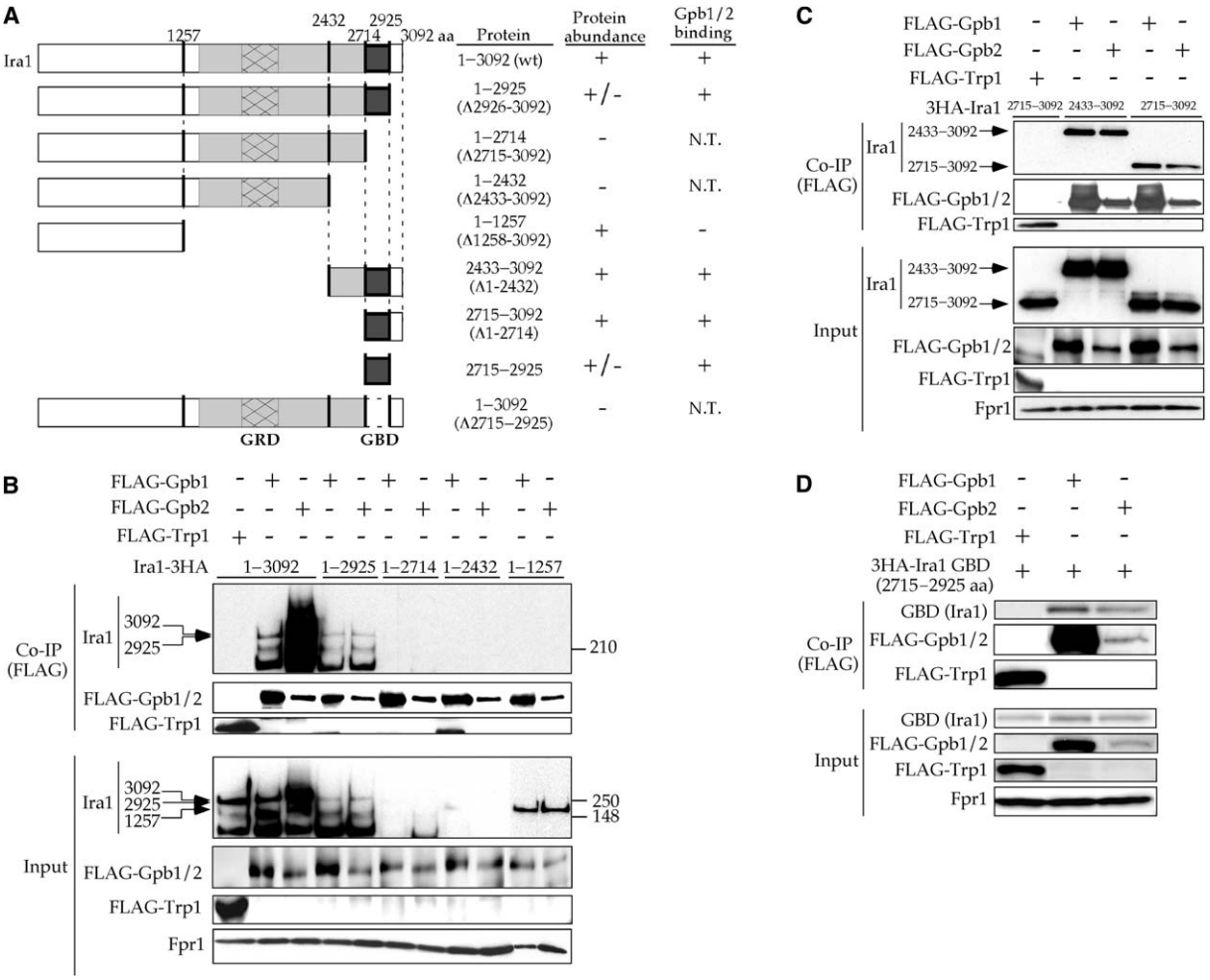


Figure 5. Gpb1/2 Bind to the C Terminus of Ira1

(A) Schematic of Ira1 deletion proteins created and summary of results obtained from assays of protein abundance (Input) and Gpb1/2 binding (Co-IP) as below. Positions of deletions created in Ira1 are shown and numbered. A conserved region between Ira1/2 and human neurofibromin is shaded in gray. The GAP-related domain (GRD) and the Gpb1/2 binding domain (GBD) are shown as hatched and dark gray rectangles, respectively.

(B) Protein interactions were investigated by using crude cell extracts from cells expressing the 3HA-tagged full-length Ira1 (1–3092 aa) or Ira1 C-terminal deletion variants. Positions of full-length wild-type Ira1 and deletion variants (1–2925 and 1 ~ 1257 aa) are indicated to the left of the panel. Positions at which molecular weight markers (250, 210, and 148 k) migrated are indicated to the right of the panels. The deletion of 167 amino acids leads to reduced protein levels of Ira1 from 3- to 7-fold in comparison of the full-length Ira1 protein level, and the further deletion (378 aa) results in undetectable levels ("Input"). Note that some smaller Ira1-3HA species were also detected via the C-terminal HA tag, indicating that these are proteolysis products lacking N-terminal regions. This further supports the assignment of the GBD to the C-terminal region of Ira1.

(C) N-terminal deletion Ira1 variants were tested for interaction with Gpb1/2. Positions of the Ira1 deletion variants (2433–3092 and 2715–3092 aa) are indicated to the left of the panel.

(D) A putative GBD of Ira1 spanning 2715–2925 aa was examined for Gpb1/2 interactions. Note that the last two lanes in (B) and the first lane in (D) were spliced to remove a space and that the Western data in each panel are directly comparable.

abolish protein stability, respectively. To test for a physiological relevance of these results, homozygous diploid cells that express these Ira1 C-terminal deletions (Δ2926–3092, Δ2715–3092, and ΔGBD) were constructed and assessed for pseudohyphal differentiation (Figure 6A). Haploid cells that carry these Ira1 C-terminal deletions were also tested for invasive growth, nitrogen starvation sensitivity, and glycogen accumulation (Figures 6B–6D). Cells expressing the truncated Ira1 derivative that contains 1–2925 aa and also includes the GBD exhibited significantly increased filamentous growth and sensitivity to nitrogen starvation and decreased glycogen (Figure 6). Cells expressing the shorter Ira1 derivatives that lack the GBD (1–2714 aa or ΔGBD) were markedly hyperfilamentous and phenotypically indistinguishable from *gpb1,2* or *ira1* null mutant cells, suggesting that these two Ira1 deletion derivatives are nonfunctional (Figure 6). This is consistent with instability of these deletion proteins (Figure 5). Therefore, the GBD and the extreme C-terminal region are both involved in protein stability and physiological functions of the Ira1 protein.

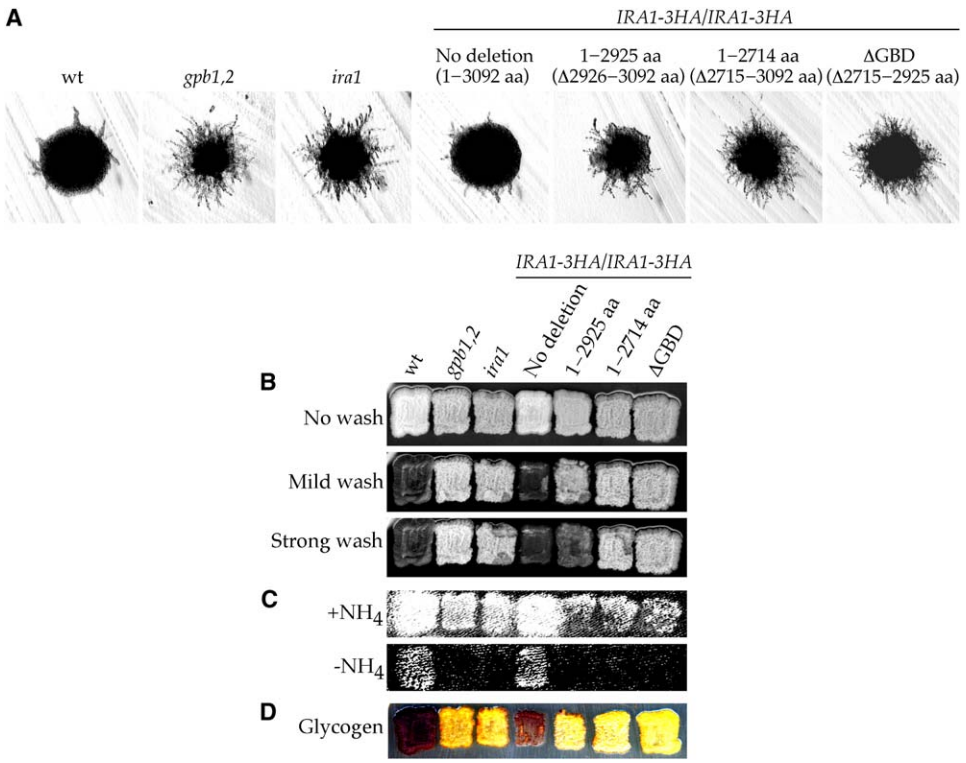


Figure 6. The C Terminus of Ira1/2 Is Necessary for Function

Homozygous diploid cells were tested for filamentous growth (A). Invasive growth (B), nitrogen starvation sensitivity (C), and glycogen accumulation (D) were examined by using isogenic haploid cells. To assay for nitrogen starvation sensitivity, cells were replica plated onto YPD after 7 days on nitrogen replete or depleted medium.

## Discussion

### Kelch Gpb1/2 Proteins Stabilize the RasGAP Proteins Ira1/2

The central finding of our study is the discovery that the activity of the yeast RasGAP neurofibromin homologs Ira1/2 is controlled by two components of the GPCR-Gα signaling module: Gpb1 and Gpb2. Our studies provide evidence that Gpb1/2 bind to and control the stability of Ira1/2 and thereby affect intracellular Ras-GTP levels. In conjunction with their role in binding the Gpa2-GDP complex and inhibiting receptor-Gα coupling, Gpb1/2 serve as potent molecular brakes to constrain signaling via the PKA signaling pathway during both vegetative growth and dimorphic transitions (Figure 7).

Deletion analysis enabled the definition of two C-terminal domains involved in the protein stability of Ira1/2. Namely, the Gpb1/2 binding domain (GBD) spanning 2715–2925 aa in Ira1 and the corresponding region in Ira2 (2703–2922 aa) and the more extreme C-terminal region of Ira1/2 that is unique to the yeast proteins (Figure 5 and Figure S1). The two domains have an additive effect, because the Ira1/2 C-terminally truncated proteins lacking the yeast-specific domain were still detectable, yet deletions eliminating both domains or the GBD alone resulted in undetectable levels of the Ira1/2 C-terminal deletion variants (1–2714 aa Ira1, Ira1ΔGBD, and 1–2702 aa Ira2). Consistent with this, Ira1/2 protein levels were significantly reduced in *gpb1,2* cells compared with those in wild-type cells (Figures 4B and 5 and Figure S1). Therefore, two distinct mechanisms appear to govern the stability of Ira1/2. Importantly, Ira1 was found to be ubiquitinated in a proteomic analysis of membrane-associated proteins (Hitchcock et al., 2003). This finding indicates that Ira1/2 protein stability might be controlled by a ubiquitin/proteasome-dependent mechanism as is neurofibromin (see below), and Gbp1/2 could inhibit Ira1/2 ubiquitination or interactions with the proteasome and thereby stabilize Ira1/2. Further studies will be required to elucidate in further detail the molecular mechanisms by which the yeast neurofibromin homologs Ira1/2 are stabilized. These would also shed light on how RasGAP activity of neurofibromin is controlled in response to extracellular stimuli.

Interestingly, in previous studies, a transversion mutation resulting in a premature nonsense codon at the 2700th amino acid was identified in Ira2, truncating the penultimate 222 amino acids, including the Gpb1/2 binding domain, and resulting in a loss of Ira2 function (Halme et al., 2004). These studies provide complementary support for our finding that the C-terminal domain of Ira1/2 is critical for biological function. Importantly, the role of the GBD is also likely to be conserved in human neurofibromin because the GBD is conserved among the yeast and mammalian neurofibromin homologs. Therefore, our findings should shed light on how the GAP activity of the neurofibromin homologs is controlled and its dysregulation in the ontogeny of NF1.

Ira1 and Ira2 share ~45% sequence similarity and are functionary redundant, yet each may also play specific

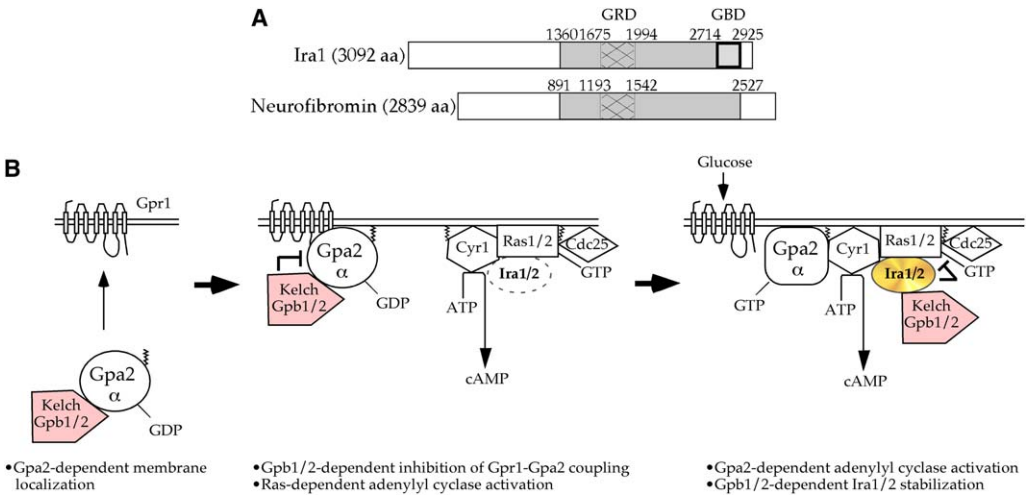


Figure 7. A Dual Role of the Kelch Proteins Gpb1/2 as Molecular Brakes on cAMP Signaling

(A) A schematic of the yeast neurofibromin homolog Ira1 and human neurofibromin proteins. A conserved region including the GRD and the GBD is shown in gray. GRD, hatched rectangle; GBD, bold rectangle.

(B) A model for how the kelch Gβ mimic proteins Gpb1/2 control cAMP signaling. See details in the text.

roles in Ras regulation. First, *ira1,2* double mutants exhibit more severe phenotypes compared to each single mutant. For instance, *ira1,2* double mutants exhibit an increased sensitivity to heat shock, enhanced filamentous growth, and increased Ras-GTP levels compared to *ira1* or *ira2* single mutants (Figure 3; [Tanaka et al., 1990a, 1990b]). Second, overproduction of the *IRA2* gene is able to suppress the heat shock sensitivity of *ira1,2* cells, but overexpression of the *IRA1* gene does not (Tanaka et al., 1990b). Similarly, we note that overexpression of *IRA2* suppresses the *gpb1,2* double mutant phenotype, whereas overexpression of *IRA1* does not (data not shown, Figure 3). Third, *ira1* mutations suppress the lethality of *cdc25* mutations more efficiently than *ira2* mutations (Tanaka et al., 1990b). Therefore, Ira1/2 may be controlled by both common and specific regulators. Indeed, Tfs1, which is a member of the phosphatidylethanolamine binding protein family and known as a cytoplasmic inhibitor CPY, specifically binds to and inhibits Ira2, although the mechanisms by which Tfs1 controls RasGAP activity of Ira2 remain unclear (Chautard et al., 2004).

### Gpb1/2 Link Signaling from the Gα Subunit Gpa2 to Ras

Our studies demonstrate that a central molecular link between the GPCR Gpr1-Gα Gpa2 signaling module and Ras is exerted via the RasGAP Ira1/2. Our recent studies also demonstrate that Gpb1/2 preferentially bind to the GDP bound form of Gpa2 and Gpb1/2 are recruited to the plasma membrane in a Gpa2-dependent manner and function to inhibit coupling between the Gpr1 receptor and Gpa2 (Harashima and Heitman, 2002, 2005). We hypothesize that the following molecular events transpire when the ligand glucose binds to the Gpr1 receptor (Figure 7). First, GDP-GTP exchange occurs on Gpa2 and Gpb1/2 dissociate from Gpa2-GTP. Second, Gpa2-GTP stimulates cAMP production via adenylyl cyclase and the liberated Gpb1/2 subunits then interact with and stabilize the Ira1/2 proteins. On the other hand, Ras is also activated in response to glucose by a Cdc25-mediated GDP-GTP exchange reaction. The Gpb1/2 bound and stabilized Ira1/2 proteins now bind to Ras-GTP and stimulate GTP hydrolysis, attenuating Ras-mediated activation of Cyr1. These mechanisms provide the cell with an elaborate and balanced regulatory network that constrains cAMP signaling within a tightly controlled physiological range. In this model, Gpb1/2 play a dual inhibitory role to inhibit receptor-Gα coupling and to extinguish signaling by Ras-GTP via their action to stabilize and thereby promote the RasGAP activity of Ira1/2.

A recent report has suggested that Gpb1/2 might act late in the PKA pathway to regulate signaling, possibly via direct actions on the PKA catalytic or regulatory subunit or on a protein phosphatase that impinges on PKA (Lu and Hirsch, 2005). Although such a model is conceivable, no direct evidence linking Gpb1 or Gpb2 to either PKA subunits or candidate regulators was presented. Instead, our genetic and physical evidence presented here support a model in which Gpb1/2 directly impinge upon Ira1/2 in the PKA signaling pathway. In addition, simultaneous loss of Gpb1/2 was unable to suppress the growth defect of *gpa2 ras2* cells (Figure 1A). However, given the complex nature of the PKA signaling cascade, one idea in which these two apparently conflicting models might be reconciled would be to consider that the signaling cascade might exist as a supramolecular complex, in which it might be difficult to assign a strictly linear signaling pathway. Given the size of the Ira1/2 proteins, it would not be surprising if these were to act as scaffolds for PKA signaling via interactions with Ras, Gpb1/2, and other signaling components. In such a model, Gpb1/2 might exert regulatory roles at multiple steps in the cascade. Further studies will be required to elucidate the potent inhibitory action of Gpb1/2 on the PKA signaling pathway.

### A Yeast Model for NF1

NF1 is an autosomal-dominant disorder that occurs in approximately one in every 3500 newborn infants.

Mutations in the *NF1* gene result in pleiotropic manifestations that include learning disabilities, small stature, bony abnormalities, and benign neurofibromas involving peripheral nerves. In some cases, NF1 patients present with malignant tumors involving peripheral nerve sheath tumors, optic gliomas, or the hematopoietic system (Zhu and Parada, 2002).

The human Ira1/2 homolog neurofibromin is a large protein (~300 kDa) that shares sequence identity with members of the RasGAP family, including p120GAP, and *Drosophila* NF1 (Buchberg et al., 1990; Cawthon et al., 1990; Marchuk et al., 1991; Wallace et al., 1990; Xu et al., 1990b). The RasGAP activity of neurofibromin has a pivotal role in Ras-dependent NF1 development because expression of the GAP-related domain (GRD) of neurofibromin can alleviate these $NF1^{-/-}$-deficient phenotypes (DeClue et al., 1992; Hiatt et al., 2001). In addition to regulating Ras activity, neurofibromin also governs G protein-mediated adenylyl cyclase activity in the fruit fly *Drosophila melanogaster* to control learning and memory, neuropeptide responses, and regulation of body size (Guo et al., 1997, 2000; Hannan et al., 2006; The et al., 1997; Tong et al., 2002). Expression of a human *NF1* gene complements the phenotypes in $NF1^{-/-}$ flies associated with an adenylyl cyclase defect (Tong et al., 2002). Similarly, neurofibromin controls adenylyl cyclase activity in response to the neuropeptide PACAP in mammals (Dasgupta et al., 2003; Tong et al., 2002). Therefore, neurofibromin governs adenylyl cyclase activity not only in yeast but also in flies and in mammals. Importantly, Ira1 binds to Cyr1, and this interaction plays a crucial role in Cyr1 activation (Mitts et al., 1991). Because heterologous expression of the GRD from mammalian neurofibromin rescues yeast *ira1* and *ira2* mutant phenotypes (Ballester et al., 1989; Ballester et al., 1990; Martin et al., 1990; Tanaka et al., 1990a; Xu et al., 1990a), Ira1/2 are structural and functional counterparts of mammalian neurofibromin and play key conserved roles in regulating both Ras and adenylyl cyclase.

Our studies identified the GBD in the C-terminal region of the yeast Ira1/2 proteins; importantly, this region is conserved in the fly and mammalian homologs (2247–2417 aa in human NF1, Figure 7). Analysis of the mutational spectra in the *NF1* gene from NF1 patients reveals that many mutations lie downstream of the GRD and many missense, frameshift, nonsense, and splice site mutations map near or even within the GBD homologous region (Ars et al., 2003; Fahsold et al., 2000; Origone et al., 2002). These downstream mutations presumably leave the GRD functional but may affect protein stability of neurofibromin and lead to the development of NF1. Importantly, neurofibromin stability is controlled via proteolysis by a ubiquitin/proteasome system (Cichowski et al., 2003). Mammalian cells express a myriad of kelch repeat proteins, and most of these remain to be characterized at a functional level. In many previous examples, signaling precedents established first in yeast were later found to also operate in multicellular eukaryotes. Our studies suggest that kelch repeat proteins related to Gpb1/2 may play an analogous role in controlling neurofibromin stability and signaling in flies and humans and might therefore provide clues to understand how NF1 develops and stimulate the development of therapeutic interventions.

## Experimental Procedures

### Strains, Media, and Plasmids

Media and standard yeast experimental procedures were as described (Sherman, 1991). A heterozygous diploid *gpb1,2::loxP/gpb1,2::loxP gpa2::loxP-G418/GPA2 ras2::nat/ras2::nat* strain was isolated after a cross between stains THY387a and THY389α. Yeast strains and plasmids used in this study are summarized in Tables S1 and S2.

### Phenotypic Analysis

Pseudohyphal and invasive growth assays, sensitivity to nitrogen starvation, glycogen accumulation, Northern analysis, and cAMP assay were conducted as described previously (Harashima and Heitman, 2002). In cAMP assay data shown in Figures 1G and 3G, the values shown are the mean of two independent experiments.

### Preparation of Crude Cell Extracts

Total cell extracts from yeast cells that were grown to midlog phase ($OD_{600} \cong 0.8$) in YPD or synthetic drop-out media were prepared in lysis buffer (50 mM HEPES [pH 7.6], 120 mM NaCl, 0.3% CHAPS, 1 mM EDTA, 20 mM NaF, 20 mM β-glycerophosphate, 0.1 mM Na-orthovanadate, 0.5 mM DTT, protease inhibitors [Calbiochem, cocktail IV], and 0.5 mM PMSF) by using a bead beater. Because the levels of the full-length Ira1/2 and Ira1/2 N- and C-terminal deletion variant proteins in crude extracts were too low to detect by Western blot, the full-length and deletion Ira1/2 proteins were immunoprecipitated by using anti-HA agarose beads, eluted, subjected to Western analysis, and examined for protein stability and indicated as "Input" in Figures 2, 4, and 5 and Figure S1.

### Immunoprecipitation and Western Blot Analysis

HA-tagged Ira1/2 proteins were captured by using anti-HA agarose beads (F-7, Santa Cruz Biotechnology). The beads were then washed three times with lysis buffer, once with PBS, and once with elution buffer (50 mM HEPES [pH 7.6], 100 mM KCl, 1 mM EDTA, 20 mM β-glycerophosphate, 0.5 mM DTT, protease inhibitors [Calbiochem, cocktail IV], and 0.5 mM PMSF) for 5 min each. After washing, the immunoprecipitated proteins were eluted by the addition of HA peptide (Roche) at a final concentration of ~800 μg/ml in elution buffer with incubation for 30 min at 30ºC. FLAG-tagged proteins were immunoprecipitated with anti-FLAG M2 affinity gel (SIGMA), the beads were washed, and protein complexes were then eluted by incubating for 30 min at room temperature with FLAG peptide (SIGMA) at a final concentration of ~500 μg/ml in elution buffer. The eluted proteins were subjected to Western analysis with anti-HA (F-7 or Y-11, Santa Cruz Biotechnology) and anti-FLAG M2 antibodies (SIGMA). Endogenous Ras2 protein levels were analyzed with an anti-Ras2 antibody (yC-19, Santa Cruz Biotechnology). The Fpr1 protein served as a loading control and was examined with a polyclonal anti-Fpr1 antibody (Harashima and Heitman, 2002).

### Mass Spectrometry

The eluted protein samples were TCA precipitated, washed with acetone, resuspended in Tris buffer, 8 M urea, pH 8.6, reduced with 100 mM TCEP, and alkylated with 55 mM iodoacetamide. Trypsin digestion was performed in the presence of 1 mM $CaCl^2$ to enhance specificity. Peptide mixtures were analyzed as described by Washburn et al. (2001). A FLAG-tagged GFP protein (pTH100) served as a mock control.

### Ras-GTP Detection

Total cellular extracts were prepared as above and employed for coimmunoprecipitation by using a GST-fused Ras binding domain (RBD) from the Raf1 kinase that preferentially binds to Ras-GTP (EZ-DETECT Ras activation kit, PIERCE Biotechnology). Experimental procedures were followed per the manufacturer's instructions.

### Cycloheximide-Chase Assay

Cycloheximide (CHX) was added to exponentially growing cells at a final concentration of 50 μg/ml to inhibit de novo protein synthesis. At the time points indicated, cells were collected and washed. Total cell extracts were prepared and subjected to immunoprecipitation for Ira1/2 or SDS-PAGE for Fpr1 as above.

## Supplemental Data

Supplemental Data include Supplemental Experimental Procedures, Supplemental References, one figure, and two tables and can be found with this article online at http://www.molecule.org/cgi/content/full/22/6/819/DC1/ or will be provided upon request from the authors.

## Acknowledgments

We thank Akio Toh-e for providing a plasmid and Cristl Arndt and Emily Wenink for assistance. We also thank Julian Rutherford, Chaoyang Xue, and Yong-Sun Bahn for critical reading and Andy Alspaugh, Henrik Dohlman, Bob Lefkowitz, and Pat Casey for encouragement. We are indebted to Yoshinori Ohsumi for his tremendous support during the revision of this manuscript. This study was supported by the Neurofibromatosis program of the Department of Defense (W81xwh-04-01-0208). T.H. was supported by a fellowship from the Children's Tumor Foundation. J.H. was an investigator of the Howard Hughes Medical Institute. Funding from the National Institute of Health (P41 RR11823-10) to J.R.Y. is gratefully acknowledged.

Received: August 6, 2005
Revised: March 14, 2006
Accepted: May 8, 2006
Published: June 22, 2006

## References

Ars, E., Kruyer, H., Morell, M., Pros, E., Serra, E., Ravella, A., Estivill, X., and Lázaro, C. (2003). Recurrent mutations in the *NF1* gene are common among neurofibromatosis type 1 patients. J. Med. Genet. *40*, e82.

Ballester, R., Michaeli, T., Ferguson, K., Xu, H.P., McCormick, F., and Wigler, M. (1989). Genetic analysis of mammalian GAP expressed in yeast. Cell *59*, 681–686.

Ballester, R., Marchuk, D., Boguski, M., Saulino, A., Letcher, R., Wigler, M., and Collins, F. (1990). The *NF1* locus encodes a protein functionally related to mammalian GAP and yeast *IRA* proteins. Cell *63*, 851–859.

Batlle, M., Lu, A.L., Green, D.A., Xue, Y., and Hirsch, J.P. (2003). Krh1p and Krh2p act downstream of the Gpa2p Gα subunit to negatively regulate haploid invasive growth. J. Cell Sci. *116*, 701–710.

Bhattacharya, S., Chen, L., Broach, J.R., and Powers, S. (1995). Ras membrane targeting is essential for glucose signaling but not for viability in yeast. Proc. Natl. Acad. Sci. USA *92*, 2984–2988.

Buchberg, A.M., Cleveland, L.S., Jenkins, N.A., and Copeland, N.G. (1990). Sequence homology shared by neurofibromatosis type-1 gene and *IRA-1* and *IRA-2* negative regulators of the *RAS* cyclic AMP pathway. Nature *347*, 291–294.

Cabrera-Vera, T.M., Vanhauwe, J., Thomas, T.O., Medkova, M., Preininger, A., Mazzoni, M.R., and Hamm, H.E. (2003). Insights into G protein structure, function, and regulation. Endocr. Rev. *24*, 765–781.

Cawthon, R.M., Weiss, R., Xu, G.F., Viskochil, D., Culver, M., Stevens, J., Robertson, M., Dunn, D., Gesteland, R., O'Connell, P., et al. (1990). A major segment of the neurofibromatosis type 1 gene: cDNA sequence, genomic structure, and point mutations. Cell *62*, 193–201.

Chautard, H., Jacquet, M., Schoentgen, F., Bureaud, N., and Bénédetti, H. (2004). Tfs1p, a member of the PEBP family, inhibits the Ira2p but not the Ira1p Ras GTPase-activating protein in *Saccharomyces cerevisiae*. Eukaryot. Cell *3*, 459–470.

Cichowski, K., Santiago, S., Jardim, M., Johnson, B.W., and Jacks, T. (2003). Dynamic regulation of the Ras pathway via proteolysis of the NF1 tumor suppressor. Genes Dev. *17*, 449–454.

Colombo, S., Ma, P.S., Cauwenberg, L., Winderickx, J., Crauwels, M., Teunissen, A., Nauwelaers, D., de Winde, J.H., Gorwa, M.F., Colavizza, D., and Thevelein, J.M. (1998). Involvement of distinct G-proteins, Gpa2 and Ras, in glucose- and intracellular acidification-induced cAMP signalling in the yeast *Saccharomyces cerevisiae*. EMBO J. *17*, 3326–3341.

Colombo, S., Ronchetti, D., Thevelein, J.M., Winderickx, J., and Martegani, E. (2004). Activation state of the Ras2 protein and glucose-induced signaling in *Saccharomyces cerevisiae*. J. Biol. Chem. *279*, 46715–46722.

Crechet, J.B., Poullet, P., Mistou, M.Y., Parmeggiani, A., Camonis, J., Boy-Marcotte, E., Damak, F., and Jacquet, M. (1990). Enhancement of the GDP-GTP exchange of Ras proteins by the carboxyl-terminal domain of Scd25. Science *248*, 866–868.

Dasgupta, B., Dugan, L.L., and Gutmann, D.H. (2003). The neurofibromatosis 1 gene product neurofibromin regulates pituitary adenylate cyclase-activating polypeptide-mediated signaling in astrocytes. J. Neurosci. *23*, 8949–8954.

DeClue, J.E., Papageorge, A.G., Fletcher, J.A., Diehl, S.R., Ratner, N., Vass, W.C., and Lowy, D.R. (1992). Abnormal regulation of mammalian $p21^{ras}$ contributes to malignant tumor growth in von Recklinghausen (type 1) neurofibromatosis. Cell *69*, 265–273.

Dohlman, H.G., Thorner, J., Caron, M.G., and Lefkowitz, R.J. (1991). Model systems for the study of seven-transmembrane-segment receptors. Annu. Rev. Biochem. *60*, 653–688.

Fahsold, R., Hoffmeyer, S., Mischung, C., Gille, C., Ehlers, C., Kücükceylan, N., Abdel-Nour, M., Gewies, A., Peters, H., Kaufmann, D., et al. (2000). Minor lesion mutational spectrum of the entire *NF1* gene does not explain its high mutability but points to a functional domain upstream of the GAP-related domain. Am. J. Hum. Genet. *66*, 790–818.

Field, J., Nikawa, J., Broek, D., MacDonald, B., Rodgers, L., Wilson, I.A., Lerner, R.A., and Wigler, M. (1988). Purification of a *RAS*-responsive adenylyl cyclase complex from *Saccharomyces cerevisiae* by use of an epitope addition method. Mol. Cell. Biol. *8*, 2159–2165.

Gross, A., Winograd, S., Marbach, I., and Levitzki, A. (1999). The N-terminal half of Cdc25 is essential for processing glucose signaling in *Saccharomyces cerevisiae*. Biochemistry *38*, 13252–13262.

Guo, H.F., The, I., Hannan, F., Bernards, A., and Zhong, Y. (1997). Requirement of *Drosophila* NF1 for activation of adenylyl cyclase by PACAP38-like neuropeptides. Science *276*, 795–798.

Guo, H.F., Tong, J., Hannan, F., Luo, L., and Zhong, Y. (2000). A neurofibromatosis-1-regulated pathway is required for learning in *Drosophila*. Nature *403*, 895–898.

Halme, A., Bumgarner, S., Styles, C., and Fink, G.R. (2004). Genetic and epigenetic regulation of the *FLO* gene family generates cell-surface variation in yeast. Cell *116*, 405–415.

Hannan, F., Ho, I., Tong, J., Zhu, Y., Nurnberg, P., and Zhong, Y. (2006). Effect of neurofibromatosis type I mutations on a novel pathway for adenylyl cyclase activation requiring neurofibromin and Ras. Hum. Mol. Genet. *15*, 1087–1098, Published online March 2, 2006.

Harashima, T., and Heitman, J. (2002). The Gα protein Gpa2 controls yeast differentiation by interacting with kelch repeat proteins that mimic Gβ subunits. Mol. Cell *10*, 163–173.

Harashima, T., and Heitman, J. (2004). Nutrient control of dimorphic growth in *Saccharomyces cerevisiae*. In Topics in Current Genetics, *Vol. 7*, J.G. Winderickx and P.M. Taylor, eds. (Heidelberg, Germany: Springer-Verlag), pp. 131–169.

Harashima, T., and Heitman, J. (2005). Gα subunit Gpa2 recruits kelch repeat subunits that inhibit receptor-G protein coupling during cAMP-induced dimorphic transitions in *Saccharomyces cerevisiae*. Mol. Biol. Cell *16*, 4557–4571.

Hiatt, K.K., Ingram, D.A., Zhang, Y., Bollag, G., and Clapp, D.W. (2001). Neurofibromin GTPase-activating protein-related domains restore normal growth in *Nf1−/−* cells. J. Biol. Chem. *276*, 7240–7245.

Hitchcock, A.L., Auld, K., Gygi, S.P., and Silver, P.A. (2003). A subset of membrane-associated proteins is ubiquitinated in response to mutations in the endoplasmic reticulum degradation machinery. Proc. Natl. Acad. Sci. USA *100*, 12735–12740.

Kübler, E., Mösch, H.U., Rupp, S., and Lisanti, M.P. (1997). Gpa2p, a G-protein α-subunit, regulates growth and pseudohyphal development in *Saccharomyces cerevisiae* via a cAMP-dependent mechanism. J. Biol. Chem. *272*, 20321–20323.

Lemaire, K., Van de Velde, S., Van Dijck, P., and Thevelein, J.M. (2004). Glucose and sucrose act as agonist and mannose as

antagonist ligands of the G protein-coupled receptor Gpr1 in the yeast *Saccharomyces cerevisiae*. Mol. Cell *16*, 293–299.

Lorenz, M.C., and Heitman, J. (1997). Yeast pseudohyphal growth is regulated by GPA2, a G protein α homolog. EMBO J. *16*, 7008–7018.

Lorenz, M.C., Pan, X.W., Harashima, T., Cardenas, M.E., Xue, Y., Hirsch, J.P., and Heitman, J. (2000). The G protein-coupled receptor Gpr1 is a nutrient sensor that regulates pseudohyphal differentiation in *Saccharomyces cerevisiae*. Genetics *154*, 609–622.

Lu, A., and Hirsch, J.P. (2005). Cyclic AMP-independent regulation of protein kinase A substrate phosphorylation by Kelch repeat proteins. Eukaryot. Cell *4*, 1794–1800.

Marchuk, D.A., Saulino, A.M., Tavakkol, R., Swaroop, M., Wallace, M.R., Andersen, L.B., Mitchell, A.L., Gutmann, D.H., Boguski, M., and Collins, F.S. (1991). cDNA cloning of the type 1 neurofibromatosis gene: complete sequence of the *NF1* gene product. Genomics *11*, 931–940.

Martin, G.A., Viskochil, D., Bollag, G., McCabe, P.C., Crosier, W.J., Haubruck, H., Conroy, L., Clark, R., O'Connell, P., Cawthon, R.M., et al. (1990). The GAP-related domain of the neurofibromatosis type 1 gene product interacts with *ras* p21. Cell *63*, 843–849.

Mintzer, K.A., and Field, J. (1994). Interactions between adenylyl cyclase, CAP and RAS from *Saccharomyces cerevisiae*. Cell. Signal. *6*, 681–694.

Mitts, M.R., Bradshaw-Rouse, J., and Heideman, W. (1991). Interactions between adenylate cyclase and the yeast GTPase-activating protein Ira1. Mol. Cell. Biol. *11*, 4591–4598.

Munder, T., and Kuntzel, H. (1989). Glucose-induced cAMP signaling in *Saccharomyces cerevisiae* is mediated by the Cdc25 protein. FEBS Lett. *242*, 341–345.

Munder, T., and Furst, P. (1992). The *Saccharomyces cerevisiae CDC25* gene product binds specifically to catalytically inactive ras proteins in vivo. Mol. Cell. Biol. *12*, 2091–2099.

Origone, P., De Luca, A., Bellini, C., Buccino, A., Mingarelli, R., Costabel, S., La Rosa, C., Garrè, C., Coviello, D.A., Ajmar, F., et al. (2002). Ten novel mutations in the human neurofibromatosis type 1 (NF1) gene in Italian patients. Hum. Mutat. *20*, 74–75.

Portillo, F., and Mazon, M.J. (1986). The *Saccharomyces cerevisiae* start mutant carrying the *cdc25* mutation is defective in activation of plasma membrane ATPase by glucose. J. Bacteriol. *168*, 1254–1257.

Powers, S., Kataoka, T., Fasano, O., Goldfarb, M., Strathern, J., Broach, J., and Wigler, M. (1984). Genes in *S. cerevisiae* encoding proteins with domains homologous to the mammalian ras proteins. Cell *36*, 607–612.

Ross, E.M., and Wilkie, T.M. (2000). GTPase-activating proteins for heterotrimeric G proteins: regulators of G protein signaling (RGS) and RGS-like proteins. Annu. Rev. Biochem. *69*, 795–827.

Sherman, F. (1991). Getting started with yeast. Methods Enzymol. *194*, 3–21.

Tanaka, K., Matsumoto, K., and Toh-e, A. (1989). *IRA1*, an inhibitory regulator of the *RAS*-cyclic AMP pathway in *Saccharomyces cerevisiae*. Mol. Cell. Biol. *9*, 757–768.

Tanaka, K., Nakafuku, M., Satoh, T., Marshall, M.S., Gibbs, J.B., Matsumoto, K., Kaziro, Y., and Toh-e, A. (1990a). *S. cerevisiae* genes *IRA1* and *IRA2* encode proteins that may be functionally equivalent to mammalian *ras* GTPase activating protein. Cell *60*, 803–807.

Tanaka, K., Nakafuku, M., Tamanoi, F., Kaziro, Y., Matsumoto, K., and Toh-e, A. (1990b). *IRA2*, a second gene of *Saccharomyces cerevisiae* that encodes a protein with a domain homologous to mammalian *ras* GTPase-activating protein. Mol. Cell. Biol. *10*, 4303–4313.

Tanaka, K., Lin, B.K., Wood, D.R., and Tamanoi, F. (1991). *IRA2*, an upstream negative regulator of RAS in yeast, is a RAS GTPase-activating protein. Proc. Natl. Acad. Sci. USA *88*, 468–472.

The, I., Hannigan, G.E., Cowley, G.S., Reginald, S., Zhong, Y., Gusella, J.F., Hariharan, I.K., and Bernards, A. (1997). Rescue of a *Drosophila NF1* mutant phenotype by protein kinase A. Science *276*, 791–794.

Toda, T., Cameron, S., Sass, P., Zoller, M., Scott, J.D., Mcmullen, B., Hurwitz, M., Krebs, E.G., and Wigler, M. (1987a). Cloning and characterization of *BCY1*, a locus encoding a regulatory subunit of the cyclic AMP-dependent protein kinase in *Saccharomyces cerevisiae*. Mol. Cell. Biol. *7*, 1371–1377.

Toda, T., Cameron, S., Sass, P., Zoller, M., and Wigler, M. (1987b). Three different genes in *S. cerevisiae* encode the catalytic subunits of the cAMP-dependent protein kinase. Cell *50*, 277–287.

Toda, T., Cameron, S., Sass, P., and Wigler, M. (1988). *SCH9*, a gene of *Saccharomyces cerevisiae* that encodes a protein distinct from, but functionally and structurally related to, cAMP-dependent protein kinase catalytic subunits. Genes Dev. *2*, 517–527.

Tong, J., Hannan, F., Zhu, Y., Bernards, A., and Zhong, Y. (2002). Neurofibromin regulates G protein-stimulated adenylyl cyclase activity. Nat. Neurosci. *5*, 95–96.

Viskochil, D., Buchberg, A.M., Xu, G., Cawthon, R.M., Stevens, J., Wolff, R.K., Culver, M., Carey, J.C., Copeland, N.G., Jenkins, N.A., et al. (1990). Deletions and a translocation interrupt a cloned gene at the neurofibromatosis type 1 locus. Cell *62*, 187–192.

Wallace, M.R., Marchuk, D.A., Andersen, L.B., Letcher, R., Odeh, H.M., Saulino, A.M., Fountain, J.W., Brereton, A., Nicholson, J., Mitchell, A.L., et al. (1990). Type 1 neurofibromatosis gene: identification of a large transcript disrupted in three NF1 patients. Science *249*, 181–186.

Washburn, M.P., Wolters, D., and Yates, J.R., 3rd. (2001). Large-scale analysis of the yeast proteome by multidimensional protein identification technology. Nat. Biotechnol. *19*, 242–247.

Xu, G.F., Lin, B., Tanaka, K., Dunn, D., Wood, D., Gesteland, R., White, R., Weiss, R., and Tamanoi, F. (1990a). The catalytic domain of the neurofibromatosis type 1 gene product stimulates *ras* GTPase and complements *ira* mutants of *S. cerevisiae*. Cell *63*, 835–841.

Xu, G.F., O'Connell, P., Viskochil, D., Cawthon, R., Robertson, M., Culver, M., Dunn, D., Stevens, J., Gesteland, R., White, R., et al. (1990b). The neurofibromatosis type 1 gene encodes a protein related to GAP. Cell *62*, 599–608.

Xue, Y., Batlle, M., and Hirsch, J.P. (1998). *GPR1* encodes a putative G protein-coupled receptor that associates with the Gpa2p $G_{\alpha}$ subunit and functions in a Ras-independent pathway. EMBO J. *17*, 1996–2007.

Yun, C.W., Tamaki, H., Nakayama, R., Yamamoto, K., and Kumagai, H. (1998). Gpr1p, a putative G-protein coupled receptor, regulates glucose-dependent cellular cAMP level in yeast *Saccharomyces cerevisiae*. Biochem. Biophys. Res. Commun. *252*, 29–33.

Zhu, Y., and Parada, L.F. (2002). The molecular and genetic basis of neurological tumours. Nat. Rev. Cancer *2*, 616–626.

Dear Joe,

On behalf of the Children's Tumor Foundation and scientists working in the neurofibromatosis field, we would like to invite you to speak as a special guest at the International NF Conference. The 2007 meeting will be held at Canyons Resort near Park City, Utah from June 10-12. This yearly conference is the premier meeting for the NF1 and NF2 fields, however each year a handful of guest speakers are invited. Therefore we would be honored to have you speak about your work relating to IRA-interacting proteins. If you would like to share any work relating to NF1 specifically you are welcome to do so, however it is up to your discretion.

The Canyons Resort is only 35 minutes away from Salt Late City International Airport, and therefore is fairly easy to get to. We will begin to plan our schedule once we have heard back form our invited guest speakers and are willing to accommodate any restrictions or preferences relating to dates that you can speak. Notably, the Canyons Grand Summit Hotel is a AAA Four-Diamond resort, rising from the heart of the resort village at The Canyons. The hotel is located at the base of the Flight of the Canyons high-speed gondola. Park City's Historic Main Street (and superb restaurants) are located 4 miles away and the Resort is surrounded with mountains and hiking trails are easily accessible within 2 minutes of walking distance. Utah is beautiful in June, therefore this will be a superb setting for this meeting.

We would appreciate it if you could let us know about your availability at your earliest convenience. Once you have responded we will put you in touch with organizers at the Children's Tumor Foundation. We are looking forward to hearing from you and hope that you will be able to join us.

Best Regards,

Karen Cichowski and Eric Legius
NF Conference Co-Chairs, 2007

Title: The kelch proteins Gpb1 and Gpb2 inhibit Ras activity via association with the yeast RasGAP neurofibromin homologs Ira1 and Ira2

Author & Affiliation:
Toshiaki Harashima, Ph.D.
National Institute for Basic Biology, Okazaki, Japan; Email: t0084h@nibb.ac.jp

Full Author List:
Joseph Heitman, MD, Ph.D.
Duke University Medical Center, Durham, NC, USA

Title:

The G protein coupled receptor Gpr1 and associated Gα subunit Gpa2 govern dimorphic transitions in response to extracellular nutrients by signaling coordinately with Ras to activate adenylyl cyclase in the yeast *Saccharomyces cerevisiae*[1]. Although Gpa2 positively controls the cAMP signaling pathway, it does not form a conventional heterotrimeric G protein. Instead, Gpa2 forms a protein complex with kelch proteins Gpb1 and Gpb2 that contain seven kelch repeats to fold into seven bladed β propeller structure strikingly similar to a fold by seven WD-40 repeats in Gβ subunits. Our studies demonstrate that Gpb1/2 negatively control cAMP-PKA signaling and function as novel Gα Gpa2 protein partners, signaling effectors, and Gβ structural mimics, based on genetic and biochemical evidence[2, 3]. In addition, Gpb1/2 target the yeast RasGAP neurofibromin homologs Ira1 and Ira2 to down-regulate Ras activity[4]. Gpb1/2 bind to a conserved C-terminal domain of Ira1/2, and loss of Gpb1/2 or loss of the Gpb1/2 binding domain (GBD) in Ira1/2 results in a destabilization of Ira1 and Ira2, leading to elevated levels of Ras2-GTP and unbridled cAMP-PKA signaling. Therefore, Gpb1/2 inhibit Ras activity by stabilizing the RasGAP Ira1/2 proteins via their association with the GBD. Because the GBD on Ira1/2 is conserved in the human neurofibromin protein, an analogous

signaling network may contribute to the neoplastic development of neurofibromatosis type 1. Importantly, neurofibromin stability is controlled via proteolysis by a ubiquitin/proteasome system and mutations in the corresponding region of the GBD on neurofibromin have been identified in NF1 patients[5, 6, 7, 8].


Ref. 1. Lorenz, M. C., Pan, X. W., Harashima, T., Cardenas, M. E., Xue, Y., Hirsch, J. P., and Heitman, J. (2000). The G protein-coupled receptor Gpr1 is a nutrient sensor that regulates pseudohyphal differentiation in *Saccharomyces cerevisiae*. Genetics *154*, 609-622.

Ref.2. Harashima, T., and Heitman, J. (2002). The Gα protein Gpa2 controls yeast differentiation by interacting with kelch repeat proteins that mimic Gβ subunits. Mol Cell *10*, 163-173.

Ref. 3. Harashima, T., and Heitman, J. (2005). Gα subunit Gpa2 recruits kelch repeat subunits that inhibit receptor-G protein coupling during cAMP-induced dimorphic transitions in *Saccharomyces cerevisiae*. Mol Biol Cell *16*, 4557-4571.

Ref. 4. Harashima, T., Anderson, S., Yates JR 3rd, and Heitman, J. (2006) The kelch proteins Gpb1 and Gpb2, inhibit Ras activity by association with the yeast RasGAP neurofibromin homologs Ira1 and Ira2. Mol Cell 22: 819-830

Ref. 5. Cichowski, K., Santiago, S., Jardim, M., Johnson, B. W., and Jacks, T. (2003). Dynamic regulation of the Ras pathway via proteolysis of the NF1 tumor suppressor. Genes Dev *17*, 449-454.

Ref. 6. Ars, E., Kruyer, H., Morell, M., Pros, E., Serra, E., Ravella, A., Estivill, X., and Lázaro, C. (2003). Recurrent mutations in the *NF1* gene are common among neurofibromatosis type 1 patients. J Med Genet *40*, e82.

Ref. 7. Fahsold, R., Hoffmeyer, S., Mischung, C., Gille, C., Ehlers, C., Kücükceylan, N., Abdel-Nour, M., Gewies, A., Peters, H., Kaufmann, D*., et al.* (2000). Minor lesion mutational spectrum of the entire *NF1* gene does not explain

its high mutability but points to a functional domain upstream of the GAP-related domain. Am J Hum Genet *66*, 790-818.

Ref. 8. Origone, P., De Luca, A., Bellini, C., Buccino, A., Mingarelli, R., Costabel, S., La Rosa, C., Garrè, C., Coviello, D. A., Ajmar, F.*, et al.* (2002). Ten novel mutations in the human neurofibromatosis type 1 (NF1) gene in Italian patients. Hum Mutat *20*, 74-75.

This study is supported by DOD Idea Award, Children's Tumor Foundation Young Investigator Award, and Howard Hughes Medical Institute.

Molecular Biology of the Cell
Vol. 19, 000–000, July 2008

# An Mep2-dependent Transcriptional Profile Links Permease Function to Gene Expression during Pseudohyphal Growth in *Saccharomyces cerevisiae*

**Julian C. Rutherford,*† Gordon Chua,‡§ Timothy Hughes,‡ Maria E. Cardenas,* and Joseph Heitman*‖**

Departments of *Molecular Genetics and Microbiology and ‖Medicine, Duke University Medical Center, Durham, NC, 27710; and ‡Banting and Best Department of Medical Research, University of Toronto, Toronto, Ontario, Canada M5G 1L6

Submitted January 16, 2008; Revised April 3, 2008; Accepted April 14, 2008
Monitoring Editor: Carole Parent

**The ammonium permease Mep2 is required for the induction of pseudohyphal growth, a process in *Saccharomyces cerevisiae* that occurs in response to nutrient limitation. Mep2 has both a transport and a regulatory function, supporting models in which Mep2 acts as a sensor of ammonium availability. Potentially similar ammonium permease-dependent regulatory cascades operate in other fungi, and they may also function in animals via the homologous Rh proteins; however, little is known about the molecular mechanisms that mediate ammonium sensing. We show that Mep2 is localized to the cell surface during pseudohyphal growth, and it is required for both filamentous and invasive growth. Analysis of site-directed Mep2 mutants in residues lining the ammonia-conducting channel reveal separation of function alleles (transport and signaling defective; transport-proficient/signaling defective), indicating transport is necessary but not sufficient to sense ammonia. Furthermore, Mep2 overexpression enhances differentiation under normally repressive conditions and induces a transcriptional profile that is consistent with activation of the mitogen-activated protein (MAP) kinase pathway. This finding is supported by epistasis analysis establishing that the known role of the MAP kinase pathway in pseudohyphal growth is linked to Mep2 function. Together, these data strengthen the model that Mep2-like proteins are nutrient sensing transceptors that govern cellular differentiation.**

## INTRODUCTION

Ammonia is an important nutrient for many microorganisms and plants, and in animals the catabolism of amino acids produces ammonia as a by-product that must be excreted from the body to prevent its toxic accumulation. The Amt/Mep/Rh proteins form an evolutionary conserved family of permeases that mediate ammonium transport across cell membranes (reviewed in Andrade and Einsle, 2007). Structural and biochemical studies of bacterial members of this transporter family reveal that the Amt/Mep/Rh proteins form a trimeric complex that facilitates passive diffusion of ammonia gas (Khademi *et al.*, 2004; Zheng *et al.*, 2004; Andrade and Einsle, 2007; Ishikita and Knapp, 2007). AQ:1 Conserved key residues required for ammonium translocation have been identified by site-directed mutagenesis and provide evidence that the mechanism of ammonium transport is evolutionarily conserved (Javelle, *et al.*, 2006; Marini *et al.*, 2006).

Previous studies support the model that certain members of the Amt/Mep/Rh family play a direct role in fungal development as ammonium receptors. The high-affinity ammonium permeases of *Saccharomyces cerevisiae*, *Candida albicans*, and *Ustilago maydis* are required for filamentous growth in response to low ammonium conditions (Lorenz and Heitman, 1998a; Smith *et al.*, 2003; Biswas and Morschhäuser, 2005). The fission yeast *Schizosaccharomyces pombe* undergoes haploid invasive growth during ammonium limitation, and this is dependent on the ammonium permease Amt1, and, to a lesser extent, its paralogue, Amt2 (Mitsuzawa, 2006). Haploid invasive growth and mating by the basidiomycetous fungus *Cryptococcus neoformans* is induced by ammonium limitation and requires the high-affinity ammonium permease, Amt2 (Rutherford *et al.*, 2008). However, the mechanisms that link ammonium transport to development are not understood. One hypothesis is that these permeases act as ammonium sensors, or transceptors, that regulate downstream effector molecules (Lorenz and Heitman, 1998a). This mechanism couples the physical process of nutrient transport to nutrient sensing and is distinct from a regulatory mechanism that responds to the changing metabolized levels of a transported nutrient (Holsbeeks *et al.*, 2004).

Current evidence supports the hypothesis that fungal high-affinity permeases function as ammonium sensors. *S. cerevisiae* cells lacking the high-affinity permease Mep2 do not undergo pseudohyphal growth or exhibit any change in the activity of nitrogen metabolic enzymes (Lorenz and Heitman, 1998a). The C-terminal cytoplasmic domain of the *C. albicans* Mep2 protein is essential for the induction of filamentous growth but dispensable for transport activity

This article was published online ahead of print in *MBC in Press* (http://www.molbiolcell.org/cgi/doi/10.1091/mbc.E08-01-0033) on April 23, 2008.

Present addresses: † Institute for Cell and Molecular Biosciences, Medical School, Newcastle University, United Kingdom; § Department of Biological Sciences, University of Calgary, Canada.

Address correspondence to: Joseph Heitman (heitm001@duke.edu).

(Biswas and Morschhäuser, 2005). Therefore, the roles of Mep2 in ammonium transport and induction of filamentous growth are separable. Independently of its role in pseudohyphal growth, Mep2 acts as a transceptor in the cAMP-independent activation of the protein kinase A (PKA) pathway after ammonium addition to starved cells (Van Nuland *et al.*, 2006). This rapid response is not dependent on ammonium metabolism and can be induced by the transport of the nonmetabolizable ammonium analogue methylamine, which establishes the paradigm of Mep2 as a transceptor. It is not clear whether Mep2 has an equivalent transceptor function during pseudohyphal growth or whether it interacts with any of the established signal transduction pathways that are essential for this process. Epistasis analysis is consistent with the RAS-cAMP being a possible downstream target of Mep2 (Lorenz and Heitman, 1998a); however, a direct interaction between Mep2 and any signaling pathway has not been demonstrated in relation to pseudohyphal growth.

In this report, we present evidence that Mep2 forms a multimeric complex localized to the cell membrane during pseudohyphal growth. Similar to *S. pombe* and *C. neoformans*, haploid *S. cerevisiae* cells undergo invasive growth in response to ammonium limitation and exhibit morphological changes analogous to those observed in pseudohyphal cells. We find that invasive growth requires Mep2, the Npr1 kinase, and elements of the PKA and mitogen-activated protein (MAP) kinase pathways. Furthermore, Mep2-dependent pseudohyphal and invasive growth requires two conserved histidine residues within the hydrophobic channel of Mep2 that have been predicted to be essential for ammonium translocation through the permease. Remarkably, constitutive Mep2 expression induces pseudohyphal growth on nitrogen-replete medium. Under these conditions, Mep2 induces a haploid- and diploid-specific transcriptional profile that includes genes known or predicted to be differentially regulated during pseudohyphal growth. Included within this group of genes are those controlled by the MAP kinase-regulated transcription factor Ste12. Consistent with a functional link between Mep2 and Ste12, constitutive *MEP2* overexpression restores pseudohyphal growth in cells lacking PKA pathway elements but not in cells lacking Ste12. In accord with this finding, overexpression of Ste12, or of the MADS box transcription factor Mcm1, restores pseudohyphal growth in cells lacking Mep2 under ammonium limiting conditions. Therefore, the established role of the MAP kinase pathway in pseudohyphal growth may, in part, be due to its role as a downstream effector of the ammonium receptor function of Mep2. Collectively, these data further support a role for the Mep2 family of permeases as sensors of ammonium availability.

## EXPERIMENTAL PROCEDURES

### *Strains and Growth Media*

T1,AQ:2 The *S. cerevisiae* strains used in this study are listed in Table 1. *S. cerevisiae* cells were grown in synthetic minimal medium with either 2% glucose, raffinose, or galactose as the carbon source. To induce pseudohyphal growth, cells were grown with 50 μM ammonium sulfate as the nitrogen source. Otherwise, cells were grown with the standard concentration of ammonium sulfate in yeast nitrogen base (5 g/l). Yeast cells were transformed as described previously (Schiestl and Gietz, 1989).

### *Plasmids*

T2 The plasmids used in this study are listed in Table 2. All manipulations of DNA fragments and plasmids were carried out using standard procedures and the *Escherichia coli* strain DH5α (Sambrook *et al.*, 1989). All DNA sequences encoding Mep2, epitope-tagged Mep2, and mutant derivatives of these were generated and inserted into the vector pRS316 (*URA3*) by homologous recombination (Ma *et al.*, 1987). In each case, the *MEP2* gene included its own promoter (1 kb), and, except in the Mep2-green fluorescent protein (GFP) fusion encoding plasmid and its mutant derivatives, the *MEP2* terminator. The Mep2-GFP encoding sequences were amplified from the relevant strain of the yeast GFP clone collection to include the *ADH1*-terminating sequences (Huh *et al.*, 2003). All Mep2-FLAG fusions contain the N4Q mutation to prevent glycosylation of Mep2 (Marini and André, 2000). *MCM1*, including its own promoter and terminator, was inserted into the vector pRS426 (*URA3*) by homologous recombination. All newly generated plasmid inserts were verified by DNA sequencing. The plasmid pYes2.1-Mep2, a kind

**Table 1.** Yeast strains used in this study

| Strain | Reference |
|---|---|
| Congenic with σ1278b | |
| HLY352 *MAT***a**/α *ste12::LEU2/ste12::LEU2* | Liu *et al.* (1993) |
| MLY41 *MAT***a** *ura3-52* | Lorenz and Heitman (1997) |
| MLY54a *MAT***a** *ura3-52 npr1::LEU2 leu2::hisG* | Lorenz and Heitman (1998a) |
| MLY54a/α *MAT***a**/α *ura3-52/ura3-52 npr1::LEU2/npr1::LEU2 leu2::hisG/leu2::hisG* | Lorenz and Heitman (1998a) |
| MLY61a/α *MAT***a**/α *ura3-52/ura3-52* | Lorenz and Heitman (1997) |
| MLY104a *MAT***a** *ura3-52 mep1::LEU2 leu2::hisG* | Lorenz and Heitman (1998a) |
| MLY108a *MAT***a** *ura3-52 mep2::G418* | Lorenz and Heitman (1998a) |
| MLY128a *MAT***a** *ura3-52 mep3::G418* | Lorenz and Heitman (1998a) |
| MLY132a *MAT***a** *ura3-52 gpa2::G418* | Lorenz and Heitman (1997) |
| MLY132a/α *MAT***a**/α *ura3-52/ura3-52 gpa2::G418/gpa2::G418* | Lorenz and Heitman (1997) |
| MLY140a/α *MAT***a**/α *ura3-52/ura3-52 ure2::G418/ure2::G418* | Lorenz and Heitman (1998a) |
| MLY183a *MAT***a** *ura3-52 tec1::G418* | Lorenz and Heitman (1998b) |
| MLY186a *MAT***a** *ura3-52 ras1::G418* | Lorenz unpublished |
| MLY187a *MAT***a** *ura3-52 ras2::G418* | Lorenz *et al.* (2000b) |
| MLY187a/α *MAT***a**/α *ura3-52/ura3-52 ras2::G418/ras2::G418* | Lorenz *et al.* (2000b) |
| MLY216a *MAT***a** *ura3-52 ste12::G418* | Lorenz unpublished |
| MLY232a *MAT***a** *ura3-52 gpr1::G418* | Lorenz *et al.* (2000b) |
| MLY232a/α *MAT***a**/α *ura3-52/ura3-52 gpr1::G418/gpr1::G418* | Lorenz *et al.* (2000b) |
| XPY5-1a *MAT***a** *ura3-52 tpk2::G418* | Pan and Heitman (1999) |
| XP5a/α *MAT***a**/α *ura3-52/ura3-52 tpk2::G418/tpk2::G418* | Pan and Heitman (1999) |
| XPY14-1a *MAT***a** *ura3-52 tpk1::G418 tpk3::G418* | Pan and Heitman, (1999) |
| XPY207a *MAT***a** *ura3-52 she2::G418* | Pan and Heitman (1999) |
| Other strains | |
| SY1 *MAT***a** *ura3-52 leu2-3 his4-619 GAL sec6-4* | Novick *et al.* (1980) |
| Mep2-GFP *MATα his3Δ1 leu2Δ0 lys2Δ0 ura3Δ0 MEP2::GFP-HIS3* | Huh *et al.* (2003) |

balt2/zmk-mbc/zmk-mbc/zmk00708/zmk8596-08z | xppws | S=1 | 5/19/08 | 13:20 | 4/Color Figure(s): F1–5,7 | Art: 3353680 | Input-jt



**Table 2.** Plasmids used in this study

| Plasmid | Function | Reference |
|---|---|---|
| pJRH1 | Mep2-GFP *CEN* | This study |
| pJRH2 | Mep2-D186A-GFP *CEN* | This study |
| pJRH3 | Mep2-H194A-GFP *CEN* | This study |
| pJRH4 | Mep2-H348A-GFP *CEN* | This study |
| pJRH7 | Mep2-N4Q-FLAG *CEN* | This study |
| pJRH8 | Mep2-N4Q-H194A-FLAG *CEN* | This study |
| pJRH9 | Mep2-N4Q-H348A-FLAG *CEN* | This study |
| pJRH10 | Mep2-N4Q-D186A-FLAG *CEN* | This study |
| pJRH11 | Mep2-N4Q-T288A-FLAG *CEN* | This study |
| pJRH17 | *MCM1* 2$\mu$ | This study |
| pML151 | *MEP2* 2$\mu$ | Lorenz and Heitman (1998a) |
| pYES2.1-*MEP2* | *GAL-MEP2* 2$\mu$ | Smith *et al.* (2003) |
| pNC252 | *GAL-STE12 CEN* | Liu *et al.* (1993) |
| pSC4 | *STE12 CEN* | Fields and Herskowitz (1987) |
| pSL1509 | *STE11-4 CEN* | Stevenson *et al.* (1992) |
| pMW2 | *RAS2$^{Val19}$ CEN* | Ward *et al.* (1995) |

All novel plasmids were generated using pRS316 (*URA3*) except pJRH17 (pRS426-*URA3*).

AQ:3 gift from Mike Perlin, was used to express *MEP2* to high levels from the galactose-inducible promoter (Smith *et al.*, 2003).

### *Membrane Preparation, Immunoprecipitation, and Western Immunoblotting*

The preparation of cell membranes was carried out as described previously (Galan *et al.*, 1996). Briefly, yeast cells in the exponential growth phase were harvested by centrifugation, washed in distilled water, and suspended in lysis buffer (0.1 M Tris-HCl, pH 7.5, 0.15 M NaCl, 5 mM EDTA) and a mixture of proteinase inhibitors (cocktail IV; Calbiochem, San Diego, CA) and 0.5 mM phenylmethylsulfonyl fluoride. Glass beads (0.45 $\mu$m in diameter) were added, and the cells were lysed by vigorous vortex mixing for 3 min. The resulting homogenate was diluted threefold with lysis buffer and centrifuged at 3000 rpm for 3 min at 4°C. The plasma membrane-enriched fraction was collected by centrifugation for 45 min at 12,000 rpm at 4°C and then suspended in lysis buffer and trichloroacetic acid (10%). For Western analysis, the precipitates were neutralized and dissolved in 20 $\mu$l of 1 M Tris base plus 80 $\mu$l of sample buffer (100 mM Tris-HCl, pH 6.8, 4 mM EDTA, 4% SDS, 20% glycerol, and 0.02% bromphenol blue) containing 2% 2-mercaptoethanol and heated at 37°C for 15 min. For immunoprecipitation, 2-mercaptoethanol was omitted from the samples, which were diluted with 0.6 ml of TNET buffer (50 mM Tris-HCl, pH 7.4, 150 mM NaCl, 5 mM EDTA, and 1% Triton X-100) plus the proteinase inhibitors described. Western analysis was carried out using antibodies, either monoclonal ANTI-FLAG M2 (Sigma-Aldrich, St. Louis, MO), monoclonal anti-GFP (Roche Diagnostics, Indianapolis, IN), or anti-Pma1 (Cardenas *et al.*, 1990), and the relevant horseradish peroxidase-conjugated anti-IgG second antibody, followed by ECL chemiluminescence (GE AQ:4 Healthcare, Chalfont St. Giles, United Kingdom). In the experiments using the *npr1*$\Delta$ strain, relative abundance of Mep2-FLAG was quantified using Quantity One version 4.6.2. (Bio-Rad, Hemel Hempstead, United Kingdom). Immunoprecipitation was carried out as described previously (Harashima and Heitman, 2002) by using EZview Red ANTI-FLAG M2 affinity gel (Sigma-Aldrich). Native Mep2 was resolved by suspending membrane samples in 1× Tris-glycine native sample buffer and separating on 6% NOVEX Tris-glycine gels with Tris-glycine native running buffer (Invitrogen).

### *Protein Localization*

Cells containing plasmid expressed Mep2-GFP were grown in synthetic minimal media and examined for protein localization under a fluorescent microscope (Axioskop2 Plus; Carl Zeiss, Thornwood, NY).

### *Pseudohyphal and Invasive Growth*

Cells undergoing pseudohyphal and invasive growth assays were grown for 6 d on low-ammonium SLAD medium (50 $\mu$M ammonium sulfate) and investigated as described previously (Harashima *et al.*, 2006).

### *Microarray Analysis*

S288C haploid and $\sum$1278b diploid wild-type strains containing a 2$\mu$ plasmid consisting of a *GAL1/10*-driven *MEP2* gene were grown concurrently with isogenic strains containing an empty vector to mid-log phase in selective liquid medium plus 2% raffinose. *MEP2* gene expression was induced for 3 h in 2% galactose. Comparison of the S288C and $\sum$1278b diploid wild-type strains was carried out in synthetic complete medium with 2% glucose. RNA preparation, hybridization, image acquisition, and data processing for microarrays were performed as described previously (Grigull *et al.*, 2004). Each microarray experiment was replicated in dye reverse.

## RESULTS

### *Mep2 Forms a Multimeric Complex In Vivo*

To facilitate studies of the role of Mep2 in the initiation of pseudohyphal growth, a plasmid was generated expressing Mep2 fused to a C-terminal FLAG epitope (Mep2-N4Q-FLAG) from the *MEP2* endogenous promoter. In this allele, the fourth asparagine residue of Mep2 was substituted with glutamine, which prevents glycosylation but does not significantly influence the ability of Mep2 to transport ammonium or induce pseudohyphal growth (Marini and André, 2000). The Mep2-N4Q-FLAG protein is functional; transformation of cells lacking endogenous Mep2 with the Mep2-N4Q-FLAG plasmid restored pseudohyphal growth and growth under ammonium limiting conditions (Figure 5).

The bacterial Amt ammonium permeases form trimeric membrane protein complexes (Conroy *et al.*, 2004; Zheng *et al.*, 2004). Potential multimeric forms of *S. cerevisiae* Mep2 have also been detected following SDS electrophoresis (Marini and André, 2000). We observed that Mep2-N4Q-FLAG migrated at a size consistent with that of a trimeric complex under native electrophoresis conditions (Figure 1A). To confirm that Mep2 monomers interact in vivo, Fl, AQ:24 Mep2-N4Q-FLAG was coexpressed with Mep2 fused to

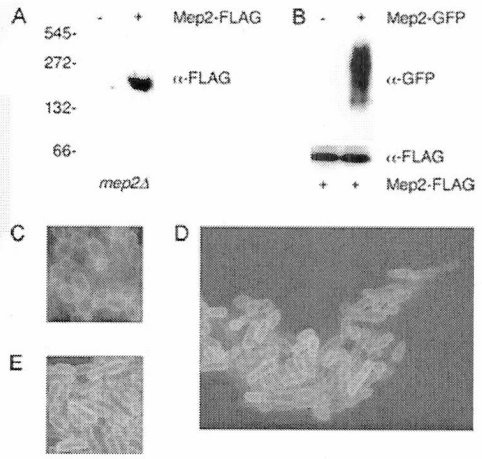


**Figure 1.** Mep2 forms a multimeric complex and is membrane localized in cells undergoing pseudohyphal growth. (A) Membrane fractions from haploid *mep2*$\Delta$ cells containing a plasmid expressing Mep-N4Q-FLAG or a control vector that had been grown in low-ammonium medium (SLAD) were resolved under native conditions, and the FLAG epitope was detected by Western analysis. (B) Mep2-FLAG was immunoprecipitated from control cells and cells expressing an Mep2-GFP fusion protein that had been grown in SLAD medium. Diploid MLY108a/$\alpha$ cells (*mep2*$\Delta$/*mep2*$\Delta$) expressing Mep2-GFP were grown on low-ammonium medium (SLAD) plates for 6 d. The Mep2 fusion protein was localized by direct epifluorescence microscopy in cells at the center of the colony (C), within cells that had formed pseudohyphae (C), and at the edge of the colony (E).

green fluorescent protein. Immunoprecipitation of Mep2-N4Q-FLAG resulted in coimmunoprecipitation of Mep2-GFP, confirming the two epitope-tagged Mep2 derivatives interact (Figure 1B).

### *Mep2 Localization on the Cell Membrane Requires the Exocyst Complex*

Diploid *S. cerevisiae* cells undergo polarized growth during pseudohyphal growth that is, in some respects, similar to polarized growth of haploid cells during mating. In response to mating pheromone, cells develop a mating projection, or shmoo, that grows toward the mating partner to enable cell–cell contact (Jackson and Hartwell, 1990). Proteins important for polarized growth during mating are localized to the shmoo (Bagnat and Simons, 2002). Because pseudohyphal growth involves polarized growth, the extent to which Mep2 is localized to the growing tip of a filament during pseudohyphal growth was examined.

Cells expressing the Mep2-GFP fusion protein were grown on solid agar under pseudohyphal conditions. Within the center of the colony, cells were oval in shape (Figure 1C), whereas cells at the colony edge exhibited the elongated morphology characteristic of pseudohyphal growth (Figure 1E). In both cases, Mep2-GFP was expressed and localized throughout the cell membrane. In addition, Mep2-GFP was localized throughout the cell membrane of cells that had grown away from the center of the colony (Figure 1D). Unlike the signaling components important for mating, Mep2-GFP does not exhibit any preferential localization to any discrete area in the cell membrane or at the growing tip of the cell during pseudohyphal growth.

We next examined whether Mep2 might be transiently localized during its initial expression after the transition from high- to low-ammonium media (Marini *et al.*, 1997) (Figure 2A). Under these conditions, Mep2-GFP localizes to the entire cell membrane within 2 h (Figure 2A). In budding cells, however, Mep2-GFP is initially (within 30 min) localized to small daughter cells, and in larger daughter cells, to the bud neck (Figure 2B). Longer incubation periods resulted in Mep2-GFP becoming gradually localized throughout more of the cell membrane, until Mep2-GFP covered the entire cell membrane by 2 h. The polarized transport of vesicles to the mother-bud neck or the bud tip is dependent on the actin cytoskeleton and the Myo2 myosin motor protein (Pruyne *et al.*, 1998; Karpova *et al.*, 2000). An alternative mechanism to ensure daughter-cell–specific protein expression is myosin-dependent mRNA transport from mother to daughter cell (Takizawa *et al.*, 1997). To distinguish between these two mechanisms, the localization of Mep2-GFP was analyzed in cells lacking the She2 protein and cells that contain the temperature-sensitive *sec6-4* allele. She2 is an RNA binding protein essential for daughter-cell–specific mRNA transport (Long *et al.*, 2000), whereas Sec6 is an integral component of the exocyst complex that mediates polarized targeting of secretory vesicles to sites of active exocytosis (TerBush *et al.*, 1996; TerBush and Novick, 1995). Mep2-GFP exhibited a wild-type pattern of localization in a *she2*Δ mutant strain; however, this pattern of localization was absent in *sec6-4* cells grown at the restrictive temperature (Figure 2C). Thus, Mep2 distribution on the cell membrane involves the exocyst complex.

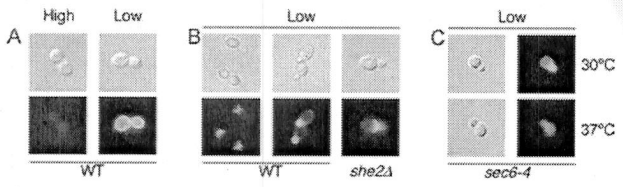


**Figure 2.** Mep2 is localized to the cell membrane via the exocyst complex. Direct epifluorescence microscopy of cells expressing Mep2-GFP was performed with wild-type cells that were grown in high-ammonium medium, pelleted, washed and then grown in high- or low (50 μM)-ammonium sulfate medium for 2 h (A), wild-type and *she2*Δ cells that were transferred from growth in high-ammonium to low-ammonium medium and grown for 20 min (B), and *sec6-4* cells that were grown at the permissive and nonpermissive temperature in low-ammonium medium (C).

### *Mep2 Is Correctly Localized in Mutants Lacking Npr1 and Ure2 and Is Required for Pseudohyphal Growth on Nitrogen Sources Other Than Ammonium*

To further analyze the link between Mep2 localization and pseudohyphal signaling, the localization of Mep2 was analyzed in mutants lacking Ure2 and Npr1 that do not form pseudohyphae (Lorenz and Heitman, 1998a). Ure2 is a regulatory protein that binds to the Gln3 transcription factor and thereby represses transcription of nitrogen catabolite-regulated genes (Blinder *et al.*, 1996). The Npr1 kinase regulates sorting and localization of the general amino acid permease Gap1 (De Craene *et al.*, 2001). We observed that Mep2-GFP is normally localized to the plasma membrane in both *ure2* and *npr1* mutant strains when grown under high and low levels of ammonium (Figure 3A). Therefore, the loss of either Ure2 or Npr1 results in the derepression of *MEP2* gene expression, and the lack of pseudohyphal growth of these mutants cannot be attributed to the lack of Mep2 localization to the cell membrane. In addition, the GFP fluorescence observed in *npr1*Δ cells expressing Mep2-GFP was greater than in wild-type cells, and Mep2-N4Q-FLAG ex-

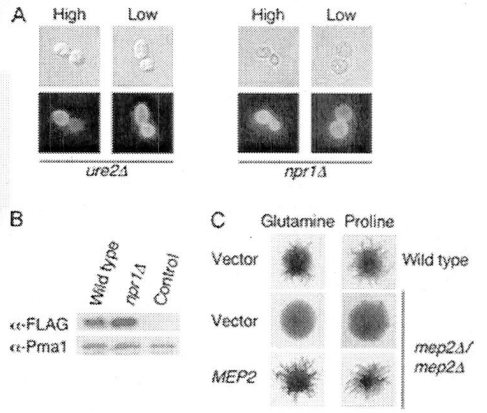


**Figure 3.** Mep2 is correctly localized in mutants lacking Npr1 and Ure2, and it is required for pseudohyphal growth on nitrogen sources other than ammonium. (A) Epifluorescence microscopy of *ure2*Δ and *npr1*Δ cells containing Mep2-GFP that had been grown in high-ammonium medium, pelleted, washed, and then grown in high- or low-ammonium sulfate medium for 2 h. (B) The levels of Mep2-N4Q-FLAG within the membrane fraction of wild-type and *npr1*Δ cells grown in low (50 μM) ammonium sulfate medium were quantified by Western analysis. Levels of the plasma membrane $H^+$-ATPase Pma1 served as a loading control. Cells not expressing Mep2-N4Q-FLAG served as a negative control. (C) Diploid wild-type and *mep2*Δ cells containing either a control plasmid or low copy plasmid expressing *MEP2* from its own promoter were grown with either glutamine (100 μM) or proline (100 μM) as the sole nitrogen source for 6 d.

pression was also ~30% higher in these cells as detected by Western blotting (Figure 3B).

Our previous studies reported that Mep2 induced pseudohyphal growth in response to growth on ammonium alone and not when cells were grown on alternative sources of nitrogen (Lorenz and Heitman, 1998a). This suggested that ammonium transport through Mep2 is required for the initiation of pseudohyphal growth. Conversely, studies in *C. albicans* have found that Mep2 is required for the induction of filamentous growth in response to nitrogen sources other than ammonium (Biswas and Morschhäuser, 2005). We re-analyzed the growth of diploid *mep2*Δ mutants on agar media containing either glutamine or proline as a nitrogen source. Under these conditions, wild-type cells produced pseudohyphae, whereas the diploid *mep2*Δ mutant strain did not (see *Discussion*). Expression of the *MEP2* gene in the diploid *mep2*Δ strain from a centromeric plasmid restored the ability of the mutant strain to undergo pseudohyphal growth (Figure 3C). Therefore, consistent with what has been described in *C. albicans*, Mep2 is required for the initiation of pseudohyphal growth on nitrogen sources other than ammonium.

### *Mep2 Induces Haploid Invasive Growth in Response to Ammonium Limiting Conditions*

Dimorphic growth by *S. cerevisiae* in response to ammonium limitation has traditionally been investigated using diploid cells. Haploid *S. cerevisiae* cells undergo invasive growth when grown in rich medium or in response to fusel alcohols (Roberts and Fink, 1994; Lorenz *et al.*, 2000a), but their response to ammonium levels has not been extensively studied. The finding that the basidiomycetous fungus *C. neoformans* and the fission yeast *S. pombe* undergo haploid invasive growth in response to ammonium limitation suggests that this pattern of growth may be conserved within fungi (Mitsuzawa, 2006; Rutherford et al., 2008). Growth of wild-type cells on low-ammonium media resulted in invasive growth and was dependent on the presence of Mep2 but not on the presence of the Mep1 or Mep3 ammonium permeases (Figure 4A). Complementation of the *mep2*Δ mutation with *MEP2* regulated by its native promoter from a low copy number centromeric plasmid restored invasive growth (Figure 5D). Microscopic examination of the areas of invasive growth revealed formation of chains of elongated cells (Figure 4B). Consistent with the morphology of cells undergoing pseudohyphal growth, some haploid cells exhibited an elongated cell shape when grown under ammonium Limiting conditions (Figure 4C).

The extent of invasive growth under low ammonium conditions was then analyzed in mutant strains lacking genes involved in diploid pseudohyphal growth. Tpk1, Tpk2, and Tpk3 are the PKA catalytic subunits, and Ste12 and Tec1 are transcription factors regulated by the MAP kinase pathway. Mutants lacking Npr1, Tpk2, Ste12, or Tec1 exhibited reduced invasive growth under ammonium limiting conditions. Interestingly, a *tpk1 tpk3* double mutant exhibited increased invasive growth under the same conditions. The link between ammonium-responsive invasive growth is consistent with the finding that cAMP can restore invasive growth in a *S. pombe* mutant that lacks *amt1*Δ (Mitsuzawa, 2006). The Gpr1 G protein-coupled receptor and the Gα subunit Gpa2 activate the cAMP–PKA pathway and are required for pseudohyphal growth. Ras2 is a guanosine triphosphate-binding protein that activates both the cAMP–PKA and the MAP kinase pathways (reviewed in Pan *et al.*, 2000). Mutants lacking Gpr1, Gpa2, Ras1, or Ras2 exhibited

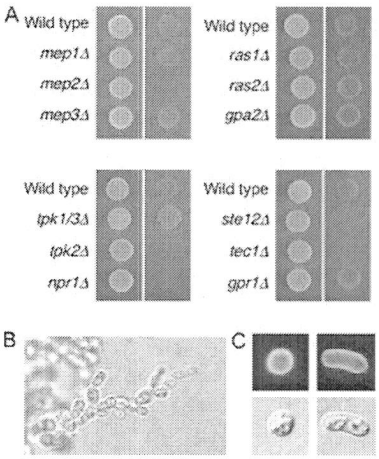


**Figure 4.** Mep2 is required for haploid invasive growth under nitrogen limiting conditions. (A) Haploid wild-type and mutant cells containing a control plasmid were spotted onto low ammonium sulfate (50 μM) solid medium lacking uracil and grown for 6 d. Panels show cells before (left) and after (right) cells have been washed off the surface of the plate to reveal the extent of invasive growth. (B) The morphology of invading cells was visualized with a Zeiss Axiophot 2 Plus fluorescence microscope revealing, in some areas, filaments of pseudohyphal-like chains of cells. (C) Wild-type cells expressing Mep2-GFP that had undergone haploid invasive growth exhibit either morphology consistent with cell cycle arrest or pseudohyphal-like elongation.

invasive growth equivalent to wild-type haploid cells under ammonium limiting conditions (Figure 4A).

### *Ammonium Transport Is Linked to Pseudohyphal and Invasive Growth*

Transceptors bind and/or transport nutrients as part of their sensing mechanism. If Mep2 functions as a transceptor, then mutations that affect transport would be predicted to play a role in pseudohyphal differentiation. In contrast, if Mep2 signals in the absence of its ligand, then mutations that prevent Mep2 from binding or transporting ammonia/ammonium might mimic the ligand free receptor state and activate pseudohyphal growth. These opposing models were tested by identifying and mutating residues involved in Mep2 transport function. An aspartate residue in AmtB that is conserved throughout the Mep/Amt/Rh family is required for ammonium transport (Javelle *et al.*, 2004). In addition, two conserved histidine residues that line the hydrophobic channel of the ammonium permease family are essential for ammonium transport by AmtB (Javelle *et al.*, 2006). These residues are equivalent to D186, H194, and H348 in Mep2 of *S. cerevisiae*.

Individual alanine substitutions of residues D186, H194, and H348 were generated in the Mep2-N4Q-FLAG and Mep2-GFP fusion proteins. The H194A and H348A Mep2 proteins were stably expressed based on Western blot analysis, and they were also localized to the surface of the plasma membrane in the context of a GFP fusion protein (Figure 5, A and B, and Table 3). In contrast, the $Mep2^{D186A}$ mutant protein was unstable, and instead of plasma membrane localization, it seemed to be localized to endogenous membranes, consistent with a recent report (Marini *et al.*, 2006). Cells expressing the $Mep2^{H194A}$ and $Mep2^{H348A}$ proteins did not undergo pseudohyphal growth in response to low ammonium, even though both proteins were stably expressed and correctly localized (Figure 5C) (Table 3). Un-

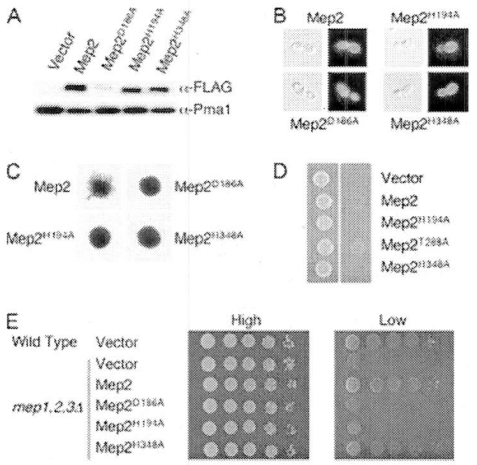


**Figure 5.** Mep2 transport function is linked to pseudohyphal differentiation. (A) The levels of Mep2-N4Q-FLAG and derived mutants within the membrane fraction of cells grown in low- (50 μM) ammonium sulfate medium were quantified by Western analysis. Levels of the plasma membrane $H^+$-ATPase Pma1 served as a loading control. (B) Localization of Mep2 was visualized using diploid *mep2*Δ/*mep2*Δ cells that contained plasmids expressing wild-type and mutant GFP-tagged Mep2 that had been grown in low-ammonium sulfate (50 μM) medium for 2 h. (C) Pseudohyphal growth was assayed using diploid *mep2*Δ/*mep2*Δ cells that contained plasmids expressing wild-type and mutant Mep2 that were grown on low ammonium sulfate (50 μM) medium for 6 d. (D) Haploid *mep2*Δ mutant cells containing relevant plasmids were spotted onto low-ammonium sulfate (50 μM) medium lacking uracil and grown for 6 d. Panels show cells before (left) and after (right) cells have been washed off the surface of the medium to reveal the extent of invasive growth. (E) Wild-type and mutant cells containing the relevant plasmids were grown overnight in complete medium (CMD-ura), washed, and serially diluted onto medium containing high or low (50 μM) levels of ammonium sulfate.

der ammonium limiting conditions, the $Mep2^{H194A}$ protein did not support growth of a strain lacking the three Mep permeases of *S. cerevisiae*, whereas cells expressing $Mep2^{H348A}$ grew to the same extent as wild-type cells. Thus, neither the transport-defective H194A mutant nor the transport-proficient H348A mutant support pseudohyphal differentiation, indicating that transport is not sufficient for signaling, and that signaling requires functions in addition to transport (Figure 5E and Table 3).

In addition, the ability of these Mep2 mutants to support haploid invasive growth under ammonium limiting conditions was assessed. Consistent with the analysis of diploid pseudohyphal growth, haploid cells expressing the $Mep2^{H194A}$ and $Mep2^{H348A}$ proteins failed to undergo invasive growth in response to low ammonium. Conversely, expression of a $Mep2^{T288A}$ mutant protein that exhibits defects in pseudohyphal growth supported haploid invasive growth under the same conditions (Figure 5D). The T288 residue of Mep2 is a potential PKA phosphorylation site that may link the PKA signaling cascade to Mep2 signaling activities under certain conditions (Smith *et al.*, 2003).

**Table 3.** Summary of phenotypes of diploid (pseudohyphal growth, growth on low ammonium) and haploid (invasive growth) mep1,2,3Δ cells expressing wild-type or mutant Mep2 permeases (see Fig. 5)

| | Mep2 localized to membrane | Pseudohyphal growth | Growth on low ammonium | Invasive growth |
|---|---|---|---|---|
| Mep2 | + | + | + | + |
| $Mep2^{D186A}$ | − | − | − | NT |
| $Mep2^{H194A}$ | + | − | − | − |
| $Mep2^{H348A}$ | + | − | + | − |

### *Mep2 Levels Correlate with Extent of Pseudohyphal Growth*

Analysis in *C. albicans* has established that the ability of Mep2 to induce pseudohyphal growth is dependent on its expression levels (Biswas and Morschhäuser, 2005). In accord with these studies, we have found that in *S. cerevisiae*, Mep2 expression levels are important for its regulatory function. *MEP2* expression from a high copy plasmid resulted in more robust pseudohyphal growth compared with expression from a low copy number centromeric plasmid (Figure 6A). Similarly, growth of cells on galactose as opposed to glucose resulted in a significant reduction in the level of pseudohyphal growth, and this was correlated with reduced Mep2-N4Q-FLAG expression (Figure 6, B and C). F6

These findings, together with studies on *C. albicans* Mep2, suggested that uncoupling *MEP2* expression from nitrogen catabolite repression might induce pseudohyphal growth under noninducing conditions. To test this hypothesis, a diploid wild-type strain was transformed with a plasmid expressing *MEP2* from a galactose-inducible promoter. Limited, but distinct, pseudohyphae were observed in cells grown in galactose nitrogen-replete conditions, whereas no pseudohyphae were observed in control cells (Figure 6D). This establishes that ammonium limitation per se is not required for the induction of the ammonium-responsive dimorphic switch in *S. cerevisiae*.

The influence of Mep2 expression levels suggested an explanation for an intriguing observation with the $Mep2^{T288A}$ mutant protein. $Mep2^{T288A}$ lacks a putative PKA phosphorylation site and does not induce pseudohyphal growth in *mep2* mutant cells (Smith *et al.*, 2003) (Figure 6E). However, when the $Mep2^{T288A}$ protein is expressed in cells lacking all three

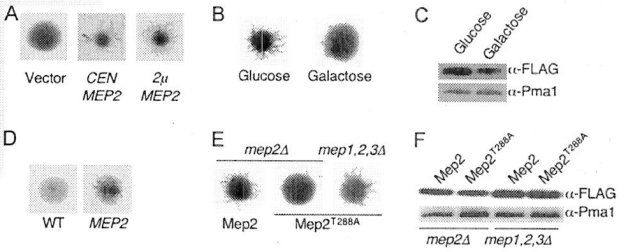


**Figure 6.** Mep2 function correlates with its expression levels. Pseudohyphal growth was assayed after growth for 6 d by using diploid *mep2*Δ/*mep2*Δ cells that contained either low or high copy plasmids expressing *MEP2* (A); wild-type cells grown with either glucose or galactose as the carbon source (B), wild-type cells grown with or without galactose-regulated *MEP2* were grown on synthetic medium with galactose as the carbon source and high levels of ammonium (D); and diploid *mep2*Δ/*mep2*Δ cells or diploid *mep1,2,3*Δ/*mep1,2,3*Δ cells expressing the $Mep2^{T288A}$ variant (E). The levels of Mep2-FLAG within wild-type cells grown on different carbon sources and low (50 μM)-ammonium sulfate (C) or $Mep2^{T288A}$-FLAG within diploid *mep2*Δ/*mep2*Δ cells and diploid *mep1,2,3*Δ/*mep1,2,3*Δ cells grown in low (50 μM)-ammonium sulfate medium (F) were quantified by Western analysis. Levels of the plasma membrane $H^+$-ATPase Pma1 served as a loading control.

ammonium permeases (*mep1*, -2, and -3), pseudohyphal growth is induced at the wild-type level (Figure 6E). One potential explanation for this phenotype is that cells lacking all three ammonium permeases are more starved for nitrogen and therefore induce the expression of Mep2-T288A to a higher level. This increased expression could compensate for the reduced activity of the $Mep2^{T288A}$ protein. When levels of Mep2-FLAG and $Mep2^{T288A}$-FLAG were analyzed in *mep2* versus *mep1*, -2, and -3 mutant cells, both Mep2 proteins were more highly expressed in the *mep1,2,3*Δ strain (Figure 6F), supporting the interpretation that increased levels of the signaling compromised T288A mutant enable signaling function.

### *MEP2 Overexpression Induces Transcription of Genes Implicated in Filamentous Growth and Known Targets of Ste12*

One hypothesis that is consistent with the role of Mep2 as a sensor of ammonium availability is that it interacts with a signal transduction pathway that activates downstream effectors that control gene expression. To test this hypothesis, the transcriptional profile of S288C haploid cells expressing the galactose-inducible *MEP2* allele was assessed during growth in ammonium-rich medium. Initially we determined whether the polymorphisms in the ∑1278b genome would affect hybridizations on our yeast open reading frame (ORF) microarrays by comparing global gene expression between S288C and ∑1278b diploid wild-type strains. Only 24 and 43 genes exhibited a greater than twofold increase and decrease in expression, respectively, between the two genetic backgrounds. Among the differentially regulated genes, the only functional enrichment observed was for glycolysis genes (*CDC19*, *TDH1–3*) that were down-regulated greater than twofold in ∑1278b (GO: 0006096; p = 2.71E-6). These results indicate that the polymorphisms in the ∑1278b strains have minimal effects on hybridization of our yeast ORF microarrays.

AQ: 6

The high expression of *MEP2* under ammonium-rich conditions compared with cells with normal endogenous *MEP2* expression levels resulted in induction of 219 genes that exhibited a twofold or greater increase in expression or more (Supplemental Table 1). These include genes involved in the cell cycle (e.g., *CLB1*, *STB1*, *FAR3*, *SIC1*, and *WHI5*), cell wall maintenance (e.g., *MOB2*, *SKG1*, and *EXG1*) and signal transduction (e.g., *CDC25*, *SDC25*, *STE12*, *RGA1*, and *RTS1*). The most striking feature of the *MEP2*-induced profile in haploid cells was the induction of 35 transposable element genes, consisting mainly of members of the Ty1 family of retrotransposons (Supplemental Table 1). These mobile genetic elements replicate through an RNA intermediate and consist of two direct long terminal repeats that flank the TYA and TYB open reading frames. The promoter of Ty1 elements contains binding sites for multiple transcription factors. Important for this study, the Ty1 promoter contains a filamentation response element within its promoter that responds to nitrogen limitation via the combinatorial activity of Ste12 and Tec1 (Conte *et al.*, 1998; Morillon *et al.*, 2002). Interestingly, in addition to the Ty1 genes, other genes where Ste12 is known to bind to their promoters were also induced in response to constitutive *MEP2* expression. These genes include *AGA1*, *SCW11*, *HXK1*, *GAP1*, *PRY3*, and *PRM6* (Zeitlinger *et al.*, 2003; Borneman *et al.*, 2006, 2007). This profile, when considered in conjunction with those data that support a signaling role for Mep2, suggests that the Ste12 transcription factor is a downstream effector of Mep2 function.

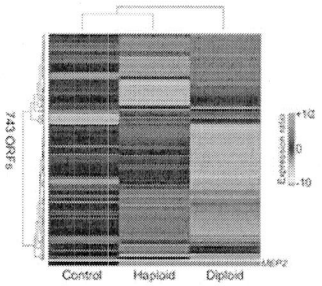


**Figure 7.** Transcriptional profiles of *MEP2* overexpression in a S288C haploid (middle) and ∑1278b diploid (right) wild-type strain. Genes that are differentially regulated greater than twofold in at least one of the microarray experiments are shown in the clustergram. The control experiment (left) compares S288C and ∑1278b diploid wild-type strains to determine whether hybridizations differ between the two genetic backgrounds on the yeast ORF microarrays. Only 77 genes were differentially regulated greater than twofold between the two genetic backgrounds. The bottom bar indicates *MEP2* expression in each microarray experiment.

The identification of a Mep2-dependent transcriptional profile in haploid cells that included genes involved in pseudohyphal growth prompted similar experiments in pseudohyphal-competent Σ1278b diploid yeast cells. The transcriptional profile of wild-type diploid cells was compared with diploid cells expressing *MEP2*. Remarkably, the profile of genes exhibiting twofold or greater differential expression was the reciprocal of that identified in the haploid experiment. Therefore, in most cases, genes that were induced by the constitutive expression of *MEP2* in haploid cells were repressed in diploid cells. Conversely, genes induced in diploid cells containing the *GAL-MEP2* plasmid were repressed in haploid cells (Figure 7).

F7

The genes induced in diploid cells by *MEP2* expression are involved in similar cellular processes as those identified in haploid cells, although the same individual genes are rarely induced in both experiments. Therefore, genes involved in cell wall maintenance, the cell cycle, and mitochondrial function were induced in response to *MEP2* overexpression in diploid cells (Supplemental Table 2). In contrast to the haploid profile, however, the transposable element genes were not collectively induced. This observation may be due in part to lower transcription rates of Ty1 elements reported in diploid cells compared with haploid cells (Morillon *et al.*, 2002). In addition, a large number of genes involved in glucose, methionine, and sulfur metabolism were uniquely induced in diploid cells. Several genes linked to dimorphic growth were induced, including *BEM4* (bud emergence), *CBK1* (protein kinase), and with just under a twofold induction, *GIC2* (bud emergence), *FLO11* (cell surface glycoprotein), and *DIA1* (invasive growth). Interestingly, *FLO11* (*MUC1*), which is essential for pseudohyphal growth, is induced to a higher level in diploid cells (1.8-fold increase) than in haploid cells (1.3-fold increase) in response to Mep2 overexpression. Similar to the Mep2 induced profile in haploid cells, many genes that are targets of Ste12 were induced in diploid cells. These genes include *GIC2*, *CDC19*, *SCH9*, *FLO11*, *CWP2*, and *AGA1* (Zeitlinger *et al.*, 2003; Borneman *et al.*, 2006, 2007).

The Mep2 transcriptional profile also included genes that have a role in cell signaling in addition to the MAPK–Ste12 pathway. *TSC11* encodes a member of the TORC2 complex. Consistent with the involvement of Tor signaling, the gene encoding the Tsc11 subunit of the TORC2, which is proposed to regulate actin cytoskeleton polarization and cell

integrity, is induced by Mep2 expression in diploid cells (Barbet *et al.*, 1996; Schmidt *et al.*, 1996; Schmidt *et al.*, 1997; Cutler *et al.*, 2001; Wedaman *et al.*, 2003). *SCH9* encodes a protein kinase recently shown to be a major target of TORC1 for regulating ribosome biogenesis, translation initiation, and entry into G0 phase, was similarly induced (Urban *et al.*, 2007). The product of *RTS3* is predicted to form part of the protein phosphatase type 2A complex (PP2A) and physically interacts with catalytic and regulatory subunits of protein phosphatase 2A and the PP2A-related phosphatase Sit4–Sap185 complex (Ho *et al.*, 2002; Samanta and Liang, 2003; Gavin *et al.*, 2006). Interestingly, *RTS3* is one of the few genes to be induced in both haploid and diploid cells overexpressing Mep2. In addition, the functional homologue of *RTS3*, *RTS1*, and the regulator of PP2A activity, *RRD2*, were induced by Mep2 expression in haploid and diploid cells, respectively. Rrd2 interacts with the Tap42-PP2Ac complex that is required for a Tor-dependent filamentous signaling pathway (Cutler *et al.*, 2001; Zheng and Jiang, 2005). This suggests that Mep2 expression under nitrogen-sufficient conditions results in the differential regulation of PP2A activity, which might explain the number of identified genes that are involved in both the cell cycle and cell wall integrity and cAMP pathways (Cutler *et al.*, 2001).

### *Constitutive Mep2 Expression Restores Pseudohyphal Growth in Mutants Lacking cAMP–PKA Signaling but Not the MAP Kinase-regulated Transcription Factor Ste12*

The established role of the MAP kinase pathway in pseudohyphal growth suggested that Mep2-dependent induction of Ty1 elements resulted from activity of the Ste12/Tec1 transcription factors. The absence of induction of the equivalent elements in diploid cells could be the result of loss of Ste12/Tec1 activity in diploid cells or to a cell-type–specific regulatory mechanism. The pleiotropic transcriptional regulator Mcm1 is a MADS box protein involved in cell cycle progression, arginine metabolism, cell wall maintenance, cell type determination, pheromone response, and mating (Sengupta and Cochran, 1990; Lydall *et al.*, 1991; Messenguy and Dubois, 1993). The transcriptional activation of a-specific genes results from dimerization of Ste12 and Mcm1 at target promoters (Sengupta and Cochran, 1990; Mueller and Nordheim, 1991). Conversely, Mat$\alpha$2–Mcm1 complexes repress the expression of a-specific genes in diploid cells (Keleher *et al.*, 1989). In addition, Mcm1 regulates Ty1 expression and binds to regulatory sequences independent of Ste12, unlike the pheromone-induced genes that are regulated by a Mcm1–Ste12 heterodimer (Errede, 1993). The cell-type–specific response to Mep2 expression observed in the microarray studies and the identification of genes regulated by Ste12 and the cell cycle suggested that Ste12 and/or Mcm1 could be downstream effectors of Mep2.

To examine this hypothesis, the ability of the *GAL-MEP2* allele to induce pseudohyphal growth in mutants lacking components of the PKA pathway or Ste12 was analyzed. *MEP2* overexpression restored pseudohyphal growth in mutants lacking Tpk2, Gpa2, Gpr1, or Ras2 (Figure 8A). However, *MEP2* overexpression did not restore pseudohyphal growth in a strain lacking Ste12 (Figure 8A). As a control, complementation of the *ste12*$\Delta$ mutant with a plasmid expressing *STE12* or a hyperactive *RAS2* allele restored wild-type pseudohyphal growth in the *ste12*$\Delta$ strain (Figure 8B). Analogous experiments were conducted to determine whether activation of either the PKA or the MAP kinase pathway restores pseudohyphal growth in a *mep2*$\Delta$ mutant. Expression of alleles that constitutively activate the PKA pathway, the MAP kinase pathway, as well as overexpression

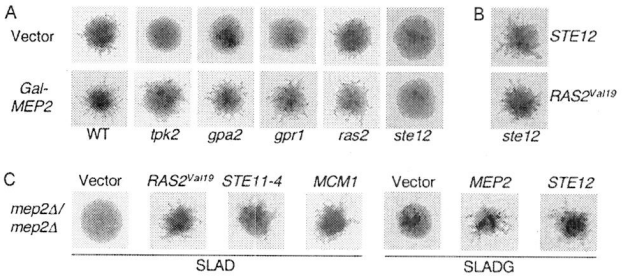


**Figure 8.** Epistasis analysis provides evidence that Mep2 and Ste12 are functionally related. After growth on galactose low-ammonium sulfate (50 $\mu$M) plates for 6 d at 30°C, pseudohyphal growth was assayed in diploid mutants lacking Tpk2, Gpa2, Gpr1, Ras2 and Ste12 that expressed *MEP2* from a galactose-inducible promoter (A) and diploid *ste12*$\Delta$/*ste12*$\Delta$ cells that contained either a galactose-inducible *STE12* gene or the $RAS2^{Val19}$ allele (B). (C) Cells lacking Mep2 and containing plasmids expressing *MCM1*, the $RAS2^{Val19}$ allele, the *STE11-4* allele, *GAL-MEP2*, or *GAL-STE12*.

of Ste12, all restored pseudohyphal growth of the *mep2*$\Delta$ mutant (Figure 8C). Together, these experiments are consistent with Mep2 and Ste12 acting in either the same pathway during pseudohyphal growth or in parallel interdependent pathways. Overexpression of the Ste12 interacting transcription factor Mcm1 also restored pseudohyphal growth in the *mep2*$\Delta$ strain, providing further functional evidence linking Mep2 and the MAP kinase pathway (Figure 8C).

## DISCUSSION

Nitrogen availability regulates the initiation of diploid filamentous growth, haploid invasive growth, and mating in different model fungi. These developmental processes occur when ammonium is limiting, and they are dependent on members of the AmtB/Mep/Rh family of ammonium permeases. Here, we present evidence that supports the hypothesis that Mep2 functions as an ammonium sensor; importantly, we document that the transport activity of Mep2 is linked to both differentiation and the control of gene expression.

The localization and oligomerization state of Mep2 are consistent with other members of the AmtB/Mep2/Rh family of transporters. We have demonstrated that Mep2 monomers interact to form a trimeric complex. Our data doe not exclude the possibility that Mep2 could form heterotrimeric complexes with the nonpseudohyphal-inducing Mep1 and Mep3 ammonium permeases. When initially expressed, Mep2 is localized to the growing bud or the bud neck, a process that is dependent on the exocyst complex. Thereafter, Mep2 is localized throughout the plasma membrane.

A central question relating to Mep2 function is the extent to which ammonium binding, transport, or both are necessary to induce pseudohyphal growth. In previous studies, it was reported that Mep2-dependent pseudohyphal growth occurs only with limiting ammonium as a nitrogen source (Lorenz and Heitman, 1998a). This suggested that ammonium binding/transport via Mep2 is important for its regulatory function. Contrary to this, studies with *C. albicans* found that Mep2-dependent pseudohyphal growth occurs when this yeast is grown on a variety of nitrogen sources (Biswas and Morschhäuser, 2005). Similarly we find that *S. cerevisiae* also undergoes Mep2-dependent pseudohyphal growth in response to growth on glutamate and proline. In our previous *S. cerevisiae* studies, growth and filamentation assays were conducted on noble agar or agarose (Lorenz and

Heitman, 1998a). Under these conditions, pseudohyphal growth is more limited, and even more so with glutamine or proline as the nitrogen source in which there was no clear obligate role for Mep2 in pseudohyphal growth. When growth assays are conducted on standard SLAD medium containing agar (including contaminating minor nitrogen sources), more robust pseudohyphal growth occurs and under these conditions Mep2 plays a clearly demonstrable role in promoting pseudohyphal differentiation, even with glutamine and proline as nitrogen source. During the course of this work, Marini and colleagues published similar findings implicating Mep2 in physiological roles during growth on nitrogen sources other than ammonium (Boeckstaens *et al.*, 2007). They found that cells leak ammonium when grown on a variety of nitrogen sources, and they advanced the hypothesis that one role for Mep2 is to reimport ammonium that exits the cell during growth on alternative nitrogen sources. In the context of this model, pseudohyphal growth on nitrogen sources such as glutamine and proline still requires the ability of Mep2 to transport and sense ammonia, in this case involving ammonia that exits the cell from internal sources.

Mutational analysis of Mep2 supports the hypothesis that ammonium transport through Mep2 is required for the induction of pseudohyphal growth. A $Mep2^{D186E}$ variant that is correctly expressed and localized to the plasma membrane fails to transport ammonium and does not induce pseudohyphal growth (Marini *et al.*, 2006). Our present study establishes that residues H194 and H348, which are conserved residues lining the pore of Mep2, are important in the initiation of pseudohyphal growth. The conservation of these residues throughout the AmtB/Mep/Rh family, and their position within the hydrophobic pore, suggest that their function is to bind ammonium as it translocates through the protein (Khademi *et al.*, 2004). The importance of these residues for ammonium transport has been underscored by mutational analysis of the equivalent residues in AmtB from *E. coli* (Javelle *et al.*, 2006). In *S. cerevisiae*, the $Mep2^{H194A}$ and $Mep2^{H348A}$ variants are stably expressed and localized to the cell membrane. The $Mep2^{H194A}$ protein has a significantly reduced ability to transport ammonium and does not induce pseudohyphal growth. The $Mep2^{H348A}$ protein transports ammonium but does not signal pseudohyphal growth. Somewhat unexpectedly, the ability of $Mep2^{H348A}$ to support growth on low ammonium contrasts to the lack of transport activity resulting from the equivalent mutation in AmtB from *E. coli*. Together, these data suggest ammonium translocation through Mep2 is required to initiate pseudohyphal growth and that mutation of residues D186 and H194 prevents this signaling process. The phenotype of the $Mep2^{H348A}$ protein suggests that the binding of ammonium ions to this residue could cause a conformational change in Mep2 that initiates pseudohyphal growth. Consistent with this, a Mep2 mutant that is hyperactive for both ammonium transport and pseudohyphal growth contains a mutation in the adjacent residue, G349 (Boeckstaens *et al.*, 2007).

The requirement for Mep2 transport activity may explain the inability of mutants lacking the Npr1 kinase to undergo pseudohyphal growth (Lorenz and Heitman, 1998a). Our data establish that Mep2 is clearly localized to the plasma membrane and highly expressed in mutants lacking the Npr1 kinase. However, in the absence of Npr1, Mep2 does not transport ammonium (Boeckstaens *et al.*, 2007). The $Mep2^{G349C}$ variant has increased transport activity and restores pseudohyphal growth in an *npr1*Δ strain (Boeckstaens *et al.*, 2007). This is consistent with Npr1 being required to activate Mep2-dependent ammonium transport, but not expression or localization, which then enables a Mep2-dependent induction of pseudohyphal growth. Interestingly, Mep2 is also correctly localized in a mutant lacking the Ure2 transcriptional repressor. Further studies will be required to determine whether the inability of a *ure2*Δ mutant to initiate dimorphic growth is a result of a loss of Mep2 transport function or some other regulatory process in which constitutive induction of the nitrogen catabolite repression response blocks pseudohyphal growth.

We have established a correlation between the level of Mep2 expression and the degree of pseudohyphal growth in *S. cerevisiae*. Increased expression of Mep2 results in greater pseudohyphal growth and a modest increase in Mep2 expression can compensate for the pseudohyphal growth induction defect in cells expressing the $Mep2^{T288A}$ protein. In *C. albicans*, high expression levels of Mep2 are required for its ability to induce hyphal growth (Biswas and Morschhäuser, 2005). It is interesting to note that in each yeast that undergoes ammonium-dependent development, the relevant inducing permease is the most highly expressed of the family of ammonium permeases (Marini *et al.*, 1997; Smith *et al.*, 2003; Biswas and Morschhäuser, 2005; Rutherford *et al.*, 2008). Mep2 is required for the induction of haploid invasive growth in response to low-ammonium growth, similar to other haploid yeasts. This takes place under conditions that are distinct from the invasive growth that occurs in response to carbon source availability and the presence of fusel alcohols (Lorenz *et al.*, 2000a), which probably accounts for the novel finding of the involvement of Mep2 in this process. Similar to the diploid Mep2 pseudohyphal pathway, the Tpk2 catalytic subunit of PKA, the Npr1 kinase, and the Ste12 and Tec1 transcription factors are required for haploid invasive growth. The Tpk1/Tpk3 catalytic subunits of PKA repress ammonium-responsive invasive growth and Mep2 mutants altered in the conserved H194 and H348 residues do not undergo invasive growth. Cells that have undergone invasive growth in response to ammonium limitation can adopt an elongated morphology similar to that observed during diploid pseudohyphal growth. Together, these data support the view that the Mep2-dependent signaling processes that occur during haploid invasive growth are similar to those occurring during pseudohyphal growth. Our data contradict a previous study that reported that Mep2 is not required for haploid invasive growth when cells are grown on medium lacking or containing minimal (100 μM) ammonium (Van Nuland *et al.*, 2006). The complementation of the *mep2*Δ strain with *MEP2* expressed from a plasmid confirms that under these conditions, Mep2 is required for ammonium induced haploid invasive growth. Ammonium permease haploid invasive growth may be widely conserved within yeast, because this conservation has now been observed in haploid *S. pombe*, *C. neoformans*, and *S. cerevisiae*.

The expression of Mep2 under conditions that do not normally induce pseudohyphal growth generates a transcriptional profile that includes genes that are involved in cellular processes that are likely to be differentially regulated during pseudohyphal growth. Of particular interest is a group of genes controlled by Ste12 involved in the cell wall (*AGA1*, *SED1*, and *CWP2*), cell cycle (*CLB1* and *SCH9*), MAP kinase pathway (*GIC2*), PKA pathway (*SCH9*), and pseudohyphal growth (*STE12*, *FLO11*, and *HMS1*). Also of interest is the induction of genes involved in the activity of Cdc42, a GTPase that establishes cell polarity and is also a component of the MAP kinase pathway (*CDC25*, *SDC25*, *RGA1*, and *GIC2*). Therefore, Mep2 expression results in the induction of a subset of Ste12-regulated genes and genes involved in the

regulation of the MAP kinase pathway, indicative of Mep2-dependent differential activation of the pathway.

Consistent with a link between Ste12 and Mep2, activation of the MAP kinase pathway, through either overexpression of Ste12 or the hyperactive *STE11-4* allele restored pseudohyphal growth in a diploid strain lacking Mep2, in contrast to a previous report (Lorenz and Heitman, 1998a). In addition, overexpression of Mep2 from the *GAL* promoter restored pseudohyphal growth in mutants lacking elements of the RAS–cAMP pathway but not in a mutant that lacks Ste12. This evidence strongly supports a link between Ste12 activity and the putative transceptor role of Mep2 during pseudohyphal growth. This, together with previous data that pseudohyphal growth in a *S. cerevisiae* strain lacking Mep2 can be restored by the exogenous addition of cAMP to cells (Lorenz and Heitman, 1998a), is similar to the epistatic relationship of *C. albicans* Mep2 and the PKA and MAPK AQ:8 kinase pathways during filamentous growth. This mechanistic conservation in different fungi is consistent with the finding that the expression of certain Mep2 fungal homologues restores pseudohyphal growth in an *S. cerevisiae* strain lacking the endogenous Mep2, suggesting that significant aspects of the signaling role of these homologues is conserved in some fungal species (Montanini *et al.*, 2002; Javelle *et al.*, 2003; Smith *et al.*, 2003).

Although the constitutive expression of Mep2 induces pseudohyphal growth under normally repressing conditions, overexpression of Ste12 under the same conditions does not (Borneman *et al.*, 2007). This may be due to the increased turnover of Ste12 in nitrogen-sufficient conditions, a process regulated by the Srb10 cyclin-dependent kinase, which itself becomes depleted during nitrogen limitation (Nelson *et al.*, 2003). This therefore argues against a simple model whereby Mep2 only activates the MAP kinase pathway. Mep2 could influence the turnover of Ste12 and/or regulate pathways that influence Ste12 activity. It is possible that mechanisms that regulate the differential output of the MAP kinase in haploid and diploid cells are responsible for the transcriptional profiles that we have identified. Interestingly, we have shown here and in previous work that Mcm1 and Tec1, two transcription factors that interact with Ste12 to modulate its activity, suppress the loss of pseudohyphal growth in cells lacking Mep2 (Lorenz and Heitman, 1998a). Additional candidates for signaling pathways that Mep2 might interact with were also identified in microarray experiments including PP2A and the Tor kinases.

Together, our data suggest a novel model of Mep2 function (Figure 9). The requirement for ammonium transport by Mep2 suggests that the lack of ammonium in the environment is not the initiating signal for pseudohyphal growth as has been proposed. This is supported by the Mep2 dependent induction of pseudohyphal growth under ammonium-sufficient growth because presumably, under these conditions, Mep2 is transporting ammonium into the cell. This strongly suggests that the importance of Mep2 does not relate to its influence on the internal levels of nitrogen, because it will induce pseudohyphal growth irrespective of ammonium levels when expressed, further supporting the designation of Mep2 as a transceptor. We propose that when ammonium is absent from the external environment, Mep2 is expressed and localized on the plasma membrane (Figure 9). Under these conditions, Mep2 does not transport ammonium and the lowering of internal nitrogen levels prevents growth. When low levels of ammonium become available, the transport of ammonium through Mep2 triggers conformational changes that most likely involve the C-terminal domains, which signal to the cell that there is sufficient ammonium for growth. Support for the conformational fluidity of Mep2 comes from the finding that the C-terminal domain of each monomer of the *Arabidopsis thaliana* Mep2 homologue Amt1;1 interacts with the adjacent monomer to confer allosteric regulation (Loqué *et al.*, 2007). The physical act of transport through Mep2 enables the permease to engage signaling components that result in Ste12 activation and the possible regulation of the Tor and PP2A pathways. Together, these result in the induction of pseudohyphal growth. If increased levels of ammonium become available, the transcription of the *MEP2* gene is repressed via catabolite repression (Marini *et al.*, 1997), and Mep2 is internalized, localized to the vacuole, and degraded (Zurita-Martinez *et al.*, 2007). Under these conditions, ammonium is able to diffuse through the plasma membrane, and the loss of the pseudohyphal-inducing signal from Mep2 results in the repression of pseudohyphal growth.

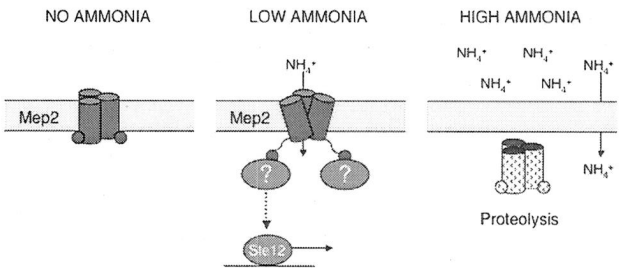


**Figure 9.** Model of Mep2 signaling during pseudohyphal growth. Mep2 forms a trimer within the membrane and acts as a sensor of ammonium availability. When no ammonium is present in the environment the signaling function of Mep2 is repressed. When limiting ammonium becomes available, its transport causes a conformational change in Mep2, which enables the permease to engage signaling partners that initiate pseudohyphal growth. High levels of ammonium result in the loss of Mep2 signaling because Mep2 is removed from the membrane and *MEP2* transcription is repressed.

Ammonium permeases have been implicated in regulating haploid invasive growth, diploid pseudohyphal growth, and mating in different model fungal systems. Members of the Amt/Mep/Rh family are also required for certain aspects of the development of *Dictyostelium discoideum* (Kirsten *et al.*, 2005; Singleton *et al.*, 2006). Together, these systems suggest that ammonium permease-mediated control of development may be widespread throughout unicellular, and possibly also multicellular, eukaryotic organisms. The molecular mechanisms that link Mep2 to pseudohyphal differentiation may therefore be conserved and relevant for studies in other model developmental systems. The present study establishes for the first time, Mep2-dependent regulation of gene expression that likely involves, at least in part, the transcription factor Ste12. The challenge now is to identify the putative regulatory proteins that physically interact with Mep2 to govern transcriptional cascades that evoke novel cellular fates in response to external nutrient sources.

## ACKNOWLEDGMENTS

We thank Mike Perlin and Ralf-Peter Jansen for useful discussions and Mike Perlin for the gift of pYES2.1-MEP2. This research was funded by a National Institutes of Health/National Institute of Allergy and Infectious Diseases grant AI39115 and Department of Defense award W81xwh-04-01-0208 (to J.H.). Support was also provided in part by grant CA94925-03 from the National Cancer Institute (to M.E.C.) and by a grant from Genome Canada and the Natural Sciences and Engineering Research Council (to T.H.). G.C. was supported by a Charles H. Best postdoctoral fellowship, and J.C.R. is supported by a Research Councils (United Kingdom) Academic Fellowship.

## REFERENCES

Andrade, S. L., and Einsle, O. (2007). The Amt/Mep/Rh family of ammonium transport proteins. Mol. Membr. Biol. *24*, 357–365.

Andrade, S. L., Dickmanns, A., Ficner, R., and Einsle, O. (2005). Crystal structure of the archaeal ammonium transporter Amt-1 from *Archaeoglobus fulgidus*. Proc. Natl. Acad. Sci. USA *102*, 14994–14999.

Bagnat, M., and Simons, K. (2002). Cell surface polarization during yeast mating. Proc. Natl. Acad. Sci. USA *99*, 14183–14188.

Barbet, N. C., Schneider, U., Helliwell, S. B., Stansfield, I., Tuite, M. F., and Hall, M. N. (1996). TOR controls translation initiation and early G1 progression in yeast. Mol. Biol. Cell *7*, 25–42.

Biswas, K., and Morschhäuser, J. (2005). The Mep2 ammonium permease controls nitrogen starvation-induced filamentous growth in *Candida albicans*. Mol. Microbiol. *56*, 649–669.

Blinder, D., Coschigano, P. W., and Magasanik, B. (1996). Interaction of the GATA factor Gln3p with the nitrogen regulator Ure2p in *Saccharomyces cerevisiae*. J. Bacteriol. *178*, 4734–4736.

Boeckstaens, M., André, B., and Marini, A. M. (2007). The yeast ammonium transport protein Mep2 and its positive regulator, the Npr1 kinase, play an important role in normal and pseudohyphal growth on various nitrogen media through retrieval of excreted ammonium. Mol. Microbiol. *64*, 534–546.

Borneman, A. R., Gianoulis, T. A., Zhang, Z. D., Yu, H., Rozowsky, J., Seringhaus, M. R., Wang, L. Y., Gerstein, M., and Snyder, M. (2007). Divergence of transcription factor binding sites across related yeast species. Science *317*, 815–819.

Borneman, A. R., Leigh-Bell, J. A., Yu, H., Bertone, P., Gerstein, M., and Snyder, M. (2006). Target hub proteins serve as master regulators of development in yeast. Genes Dev. *20*, 435–448.

Cardenas, M. E., Laroche, T., and Gasser, S. M. (1990). The composition and morphology of yeast nuclear scaffolds. J. Cell Sci. *96*, 439–450.

Ciriacy, M., Freidel, K., and Löhning, C. (1991). Characterization of trans-acting mutations affecting Ty and Ty-mediated transcription in *Saccharomyces cerevisiae*. Curr. Genet. *20*, 441–448.

Conroy, M. J., Jamieson, S. J., Blakey, D., Kaufmann, T., Engel, A., Fotiadis, D., Merrick, M., and Bullough, P. A. (2004). Electron and atomic force microscopy of the trimeric ammonium transporter AmtB. EMBO Rep. *5*, 1153–1158.

Conte, D Jr., Barber, E., Banerjee, M., Garfinkel, D. J., and Curcio, M. J. (1998). Posttranslational regulation of Ty1 retrotransposition by mitogen-activated protein kinase Fus3. Mol. Cell. Biol. *18*, 2502–2513.

Cutler, N. S., Pan, X., Heitman, J., and Cardenas, M. E. (2001). The TOR signal transduction cascade controls cellular differentiation in response to nutrients. Mol. Biol. Cell *12*, 4103–4113.

De Craene, J. O., Soetens, O., and André, B. (2001). The Npr1 kinase controls biosynthetic and endocytic sorting of the yeast Gap1 permease. J. Biol. Chem. *276*, 43939–43948.

Dudley, A. M., Gansheroff, L. J., and Winston, F. (1999). Specific components of the SAGA complex are required for Gcn4- and Gcr1-mediated activation of the *his4-912Δ* promoter in *Saccharomyces cerevisiae*. Genetics *151*, 1365–1378.

Errede, B. (1993). MCM1 binds to a transcriptional control element in Ty1. Mol. Cell. Biol. *13*, 57–62.

Fields, S., and Herskowitz, I. (1987). Regulation by the yeast mating-type locus of STE12, a gene required for cell-type-specific expression. Mol. Cell. Biol. *7*, 3818–3821.

Galan, J. M., Moreau, V., André, B., Volland, C., and Haguenauer-Tsapis, R. (1996). Ubiquitination mediated by the Npi1p/Rsp5p ubiquitin-protein ligase is required for endocytosis of the yeast uracil permease. J. Biol. Chem. *271*, 10946–10952.

Gavin, A. C. *et al.* (2006). Proteome survey reveals modularity of the yeast cell machinery. Nature *440*, 631–636.

Grant, P. A., *et al.* (1997). Yeast Gcn5 functions in two multisubunit complexes to acetylate nucleosomal histones: characterization of an Ada complex and the SAGA (Spt/Ada) complex. Genes Dev. *11*, 1640–1650.

Gray, W. M., and Fassler, J. S. (1993). Role of *Saccharomyces cerevisiae* Rap1 protein in Ty1 and Ty1-mediated transcription. Gene Expr. *3*, 237–251.

Grigull, J., Mnaimneh, S., Pootoolal, J., Robinson, M. D., and Hughes, T. R. (2004). Genome-wide analysis of mRNA stability using transcription inhibitors and microarrays reveals posttranscriptional control of ribosome biogenesis factors. Mol. Cell. Biol. *24*, 5534–5547.

Happel, A. M., Swanson, M. S., and Winston, F. (1991). The *SNF2*, SNF5 and SNF6 genes are required for Ty transcription in *Saccharomyces cerevisiae*. Genetics *128*, 69–77.

Harashima, T., and Heitman, J. (2002). The Galpha protein Gpa2 controls yeast differentiation by interacting with kelch repeat proteins that mimic Gbeta subunits. Mol. Cell *10*, 163–173.

Harashima, T., Anderson, S., Yates, J. R., 3rd., and Heitman, J. (2006). The kelch proteins Gpb1 and Gpb2 inhibit Ras activity via association with the yeast RasGAP neurofibromin homologs Ira1 and Ira2. Mol. Cell *22*, 819–830.

Ho, Y. *et al.* (2002). Systematic identification of protein complexes in *Saccharomyces cerevisiae* by mass spectrometry. Nature *415*, 180–183.

Holsbeeks, I., Lagatie, O., Van Nuland, A., Van de Velde, S., and Thevelein, J. M. (2004). The eukaryotic plasma membrane as a nutrient-sensing device. Trends Biochem. Sci. *29*, 556–564.

Huh, W. K., Falvo, J. V., Gerke, L. C., Carroll, A. S., Howson, R. W., Weissman, J. S., and O'Shea, E. K. (2003). Global analysis of protein localization in budding yeast. Nature *425*, 686–691.

Ishikita, H., and Knapp, E. W. (2007). Protonation states of ammonia/ammonium in the hydrophobic pore of ammonia transporter protein AmtB. J. Am. Chem. Soc. *129*, 1210–1215.

Jackson, C. L., and Hartwell, L. H. (1990). Courtship in *S. cerevisiae*: both cell types choose mating partners by responding to the strongest pheromone signal. Cell *63*, 1039–1051.

Javelle, A., Morel, M., Rodríguez-Pastrana, B. R., Botton, B., André, B., Marini, A. M., Brun, A., and Chalot, M. (2003). Molecular characterization, function and regulation of ammonium transporters (Amt) and ammonium-metabolizing enzymes (GS, NADP-GDH) in the ectomycorrhizal fungus *Hebeloma cylindrosporum*. Mol. Microbiol. *47*, 411–430.

Javelle, A., Severi, E., Thornton, J., and Merrick, M. (2004). Ammonium sensing in *Escherichia coli*. Role of the ammonium transporter AmtB and AmtB-GlnK complex formation. J. Biol. Chem. *279*, 8530–8538.

Javelle, A., Lupo, D., Zheng, L., Li, X. D., Winkler, F. K., and Merrick, M. (2006). An unusual twin-his arrangement in the pore of ammonia channels is essential for substrate conductance. J. Biol. Chem. *281*, 39492–39498.

Karpova, T. S., Reck-Peterson, S. L., Elkind, N. B., Mooseker, M. S., Novick, P. J., and Cooper, J. A. (2000). Role of actin and Myo2p in polarized secretion and growth of *Saccharomyces cerevisiae*. Mol. Biol. Cell *11*, 1727–1737.

Keleher, C. A., Passmore, S., and Johnson, A. D. (1989). Yeast repressor alpha 2 binds to its operator cooperatively with yeast protein Mcm1. Mol. Cell. Biol. *9*, 5228–5230.

Kent, N. A., Karabetsou, N., Politis, P. K., and Mellor, J. (2001). In vivo chromatin remodeling by yeast ISWI homologs Isw1p and Isw2p. Genes Dev. *15*, 619–626.

Khademi, S., O'Connell, J. 3rd, Remis, J., Robles-Colmenares, Y., Miercke, L. J., and Stroud, R. M. (2004). Mechanism of ammonia transport by Amt/MEP/Rh: structure of AmtB at 1.35 A. Science *305*, 1587–1594.

Kirsten, J. H., Xiong, Y., Dunbar, A. J., Rai, M., and Singleton, C. K. (2005). Ammonium transporter C of *Dictyostelium discoideum* is required for correct prestalk gene expression and for regulating the choice between slug migration and culmination. Dev. Biol. *287*, 146–156.

Kuo, M. H., and Grayhack, E. (1994). A library of yeast genomic MCM1 binding sites contains genes involved in cell cycle control, cell wall and membrane structure, and metabolism. Mol. Cell. Biol. *14*, 348–359.

Laloux, I., Dubois, E., Dewerchin, M., and Jacobs, E. (1990). TEC1, a gene involved in the activation of Ty1 and Ty1-mediated gene expression in *Saccharomyces cerevisiae*: cloning and molecular analysis. Mol. Cell. Biol. *10*, 3541–3550.

Liu, H., Styles, C. A., and Fink, G. R. (1993). Elements of the yeast pheromone response pathway required for filamentous growth of diploids. Science *262*, 1741–1744.

Long, R. M., Gu, W., Lorimer, E., Singer, R. H., and Chartrand, P. (2000). She2p is a novel RNA-binding protein that recruits the Myo4p-She3p complex to *ASH1* mRNA. EMBO J. *19*, 6592–6601.

Lorenz, M. C., and Heitman, J. (1997). Yeast pseudohyphal growth is regulated by GPA2, a G protein alpha homolog. EMBO J. *16*, 7008–7018.

Lorenz, M. C., and Heitman, J. (1998a). The MEP2 ammonium permease regulates pseudohyphal differentiation in *Saccharomyces cerevisiae*. EMBO J. *17*, 1236–1247.

Lorenz, M. C., and Heitman, J. (1998b). Regulators of pseudohyphal differentiation in *Saccharomyces cerevisiae* identified through multicopy suppressor analysis in ammonium permease mutant strains. Genetics *150*, 1443–1457.

Lorenz, M. C., Pan, X., Harashima, T., Cardenas, M. E., Xue, Y., Hirsch, J. P., and Heitman, J. (2000a). The G protein-coupled receptor Gpr1 is a nutrient sensor that regulates pseudohyphal differentiation in *Saccharomyces cerevisiae*. Genetics *154*, 609–622.

Lorenz, M. C., Cutler, N. S., and Heitman, J. (2000b). Characterization of alcohol-induced filamentous growth in *Saccharomyces cerevisiae*. Mol. Biol. Cell *11*, 183–199.

Loqué, D., Lalonde, S., Looger, L. L., von Wirén, N., and Frommer, W. B. (2007). A cytosolic trans-activation domain essential for ammonium uptake. Nature *446*, 195–198.

Lydall, D., Ammerer, G., and Nasmyth, K. (1991). A new role for MCM1 in yeast: cell cycle regulation of SW15 transcription. Genes Dev. *5*, 2405–2419.

Ma, H., Kunes, S., Schatz, P. J., and Botstein, D. (1987). Plasmid construction by homologous recombination in yeast. Gene *58*, 201–216.

Madison, J. M., Dudley, A. M., and Winston, F. (1998). Identification and analysis of Mot3, a zinc finger protein that binds to the retrotransposon Ty long terminal repeat (delta) in *Saccharomyces cerevisiae*. Mol. Cell. Biol. *18*, 1879–1890.

Marini, A. M., Boeckstaens, M., Benjelloun, F., Chérif-Zahar, B., and André, B. (2006). Structural involvement in substrate recognition of an essential aspartate residue conserved in Mep/Amt and Rh-type ammonium transporters. Curr. Genet. *49*, 364–374.

Marini, A. M., Soussi-Boudekou, S., Vissers, S., and André, B. (1997). A family of ammonium transporters in *Saccharomyces cerevisiae*. Mol. Biol. Cell *17*, 4282–4293.

Marini, A. M., and André, B. (2000). In vivo N-glycosylation of the Mep2 high-affinity ammonium transporter of *Saccharomyces cerevisiae* reveals an extracytosolic N-terminus. Mol. Microbiol. *38*, 552–564.

Messenguy, F., and Dubois, E. (1993). Genetic evidence for a role for MCM1 in the regulation of arginine metabolism in *Saccharomyces cerevisiae*. Mol. Cell. Biol. *13*, 2586–2592.

Mitsuzawa, H. (2006). Ammonium transporter genes in the fission yeast *Schizosaccharomyces pombe*: role in ammonium uptake and a morphological transition. Genes Cells *11*, 1183–1195.

Montanini, B., Moretto, N., Soragni, E., Percudani, R., and Ottonello, S. (2002). A high-affinity ammonium transporter from the mycorrhizal ascomycete *Tuber borchii*. Fungal Genet. Biol. *36*, 22–34.

Morillon, A., Bénard, L., Springer, M., and Lesage, P. (2002). Differential effects of chromatin and Gcn4 on the 50-fold range of expression among individual yeast Ty1 retrotransposons. Mol. Cell. Biol. *22*, 2078–2088.

Mueller, C. G., and Nordheim, A. (1991). A protein domain conserved between yeast MCM1 and human SRF directs ternary complex formation. EMBO J. *10*, 4219–4229.

Nelson, C., Goto, S., Lund, K., Hung, W., and Sadowski, I. (2003). Srb10/Cdk8 regulates yeast filamentous growth by phosphorylating the transcription factor Ste12. Nature *421*, 187–190.

Novick, P., Field, C., and Schekman, R. (1980). Identification of 23 complementation groups required for post-translational events in the yeast secretory pathway. Cell *21*, 205–215.

Pan, X., and Heitman, J. (1999). Cyclic AMP-dependent protein kinase regulates pseudohyphal differentiation in *Saccharomyces cerevisiae*. Mol. Cell. Biol. *19*, 4874–4887.

Pan, X., and Heitman, J. (2000). Sok2 regulates yeast pseudohyphal differentiation via a transcription factor cascade that regulates cell-cell adhesion. Mol. Cell. Biol. *20*, 8364–8372.

Pan, X., Harashima, T., and Heitman, J. (2000). Signal transduction cascades regulating pseudohyphal differentiation of *Saccharomyces cerevisiae*. Curr. Opin. Microbiol. *3*, 567–572.

Pollard, K. J., and Peterson, C. L. (1997). Role for ADA/GCN5 products in antagonizing chromatin-mediated transcriptional repression. Mol. Cell. Biol. *17*, 6212–6222.

Pruyne, D. W., Schott, D. H., and Bretscher, A. (1998). Tropomyosin-containing actin cables direct the Myo2p-dependent polarized delivery of secretory vesicles in budding yeast. J. Cell Biol. *143*, 1931–1945.

Roberts, R. L., and Fink, G. R. (1994). Elements of a single MAP kinase cascade in *Saccharomyces cerevisiae* mediate two developmental programs in the same cell type: mating and invasive growth. Genes Dev. *15*, 2974–2985.

Rutherford, J. C., Lin, X., Nielsen, K., and Heitman, J. (2008). Amt2 permease is required to induce ammonium responsive invasive growth and mating in *Cryptococcus neoformans*. Eukaryot. Cell *7*, 237–246.

Samanta, M. P., and Liang, S. (2003). Predicting protein functions from redundancies in large-scale protein interaction networks. Proc. Natl. Acad. Sci. USA *100*, 12579–12583.

Sambrook, J., Fritsch, E. F., and Maniatis, T. (1989). Molecular Cloning: A Laboratory Manual, Cold Spring Harbor, NY: Cold Spring Harbor Laboratory Press.

Schiestl, R. H., and Gietz, R. D. (1989). High efficiency transformation of intact yeast cells using single stranded nucleic acids as a carrier. Curr. Genet. *16*, 339–346.

Schmidt, A., Kunz, J., and Hall, M. N. (1996). TOR2 is required for organization of the actin cytoskeleton in yeast. Proc. Natl. Acad. Sci. USA *93*, 13780–13785.

Schmidt, A., Bickle, M., Beck, T., and Hall, M. N. (1997). The yeast phosphatidylinositol kinase homolog TOR2 activates RHO1 and RHO2 via the exchange factor ROM2. Cell *88*, 531–542.

Sengupta, P., and Cochran, B. H. (1990). The PRE and PQ box are functionally distinct yeast pheromone response elements. Mol. Cell. Biol. *10*, 6809–6812.

Singleton, C. K., Kirsten, J. H., and Dinsmore, C. J. (2006). Function of ammonium transporter A in the initiation of culmination of development in *Dictyostelium discoideum*. Eukaryot. Cell *5*, 991–996.

Smith, D. G., Garcia-Pedrajas, M. D., Gold, S. E., and Perlin, M. H. (2003). Isolation and characterization from pathogenic fungi of genes encoding ammonium permeases and their roles in dimorphism. Mol. Microbiol. *50*, 259–275.

Stevenson, B. J., Rhodes, N., Errede, B., and Sprague, G. F. Jr. (1992). Constitutive mutants of the protein kinase *STE11* activate the yeast pheromone response pathway in the absence of the G protein. Genes Dev. *6*, 1293–1304.

Takizawa, P. A., Sil, A., Swedlow, J. R., Herskowitz, I., and Vale, R. D. (1997). Actin-dependent localization of an RNA encoding a cell-fate determinant in yeast. Nature *389*, 90–93.

TerBush, D. R., Maurice, T., Roth, D., and Novick, P. (1996). The Exocyst is a multiprotein complex required for exocytosis in *Saccharomyces cerevisiae*. EMBO J. *15*, 6483–6494.

TerBush, D. R., and Novick, P. (1995). Sec6, Sec8, and Sec15 are components of a multisubunit complex which localizes to small bud tips in *Saccharomyces cerevisiae*. J. Cell Biol. *130*, 299–312.

Türkel, S., Liao, X. B., and Farabaugh, P. J. (1997). GCR1-dependent transcriptional activation of yeast retrotransposon Ty2-917. Yeast *13*, 917–930.

Urban, J. *et al.* (2007). Sch9 is a major target of TORC1 in *Saccharomyces cerevisiae*. Mol. Cell *26*, 663–674.

Van Nuland, A., Vandormael, P., Donaton, M., Alenquer, M., Lourenço, A., Quintino, E., Versele, M., and Thevelein, J. M. (2006). Ammonium permease based sensing mechanism for rapid ammonium activation of the protein kinase A pathway in yeast. Mol. Microbiol. *59*, 1485–1505.

Ward, M. P., Gimeno, C. J., Fink, G. R., and Garrett, S. (1995). SOK2 may regulate cyclic AMP-dependent protein kinase-stimulated growth and pseudohyphal development by repressing transcription. Mol. Cell. Biol. *15*, 6854–6863.

Wedaman, K. P., Reinke, A., Anderson, S., Yates, J., III, McCaffery, J. M., and Powers, T. (2003). Tor kinases are in distinct membrane-associated protein complexes in *Saccharomyces cerevisiae*. Mol. Biol. Cell *14*, 1204–1220.

Zeitlinger, J., Simon, I., Harbison, C. T., Hannett, N. M., Volkert, T. L., Fink, G. R., and Young, R. A. (2003). Program-specific distribution of a transcription factor dependent on partner transcription factor and MAPK signaling. Cell *113*, 395–404.

Zheng, L., Kostrewa, D., Bernèche, S., Winkler, F. K., and Li, X. D. (2004). The mechanism of ammonia transport based on the crystal structure of AmtB of *Escherichia coli*. Proc. Natl. Acad. Sci. USA *101*, 17090–17095.

Zheng, Y., and Jiang, Y. (2005). The yeast phosphotyrosyl phosphatase activator is part of the Tap42-phosphatase complexes. Mol. Biol. Cell *16*, 2119–2127.

Zurita-Martinez, S. A., Puria, R., Pan, X., Boeke, J. D., and Cardenas, M. E. (2007). Efficient Tor signaling requires a functional class C Vps protein complex in *Saccharomyces cerevisiae*. Genetics *176*, 2139–2150.